Generating and Characterizing Phosphospecific Affinity Reagents Using the Forkhead-Associated 1 Domain

BY

Leon A. Venegas
B.S., St. Edward's University, 2010

THESIS

Submitted as partial fulfillment of the requirements for the degree of Doctor of Philosophy in Biological Sciences in the Graduate College of the University of Illinois at Chicago, 2018

Chicago, Illinois

Defense Committee:

Dr. Teresa Orenic, Chair
Dr. Brian Kay, Advisor
Dr. Don Morrison, Biological Sciences
Dr. Alexander (Shura) Mankin, Medicinal Chemistry and Pharmacognosy
Dr. Andrei Karginov, Pharmacology

This thesis is dedicated to my mother, Carmen Venegas, who gave up her world to give me mine.

ACKNOWLEDGEMENTS

I would like to start by thanking my thesis advisor, Dr. Brian Kay. Dr. Kay was instrumental in helping me grow as a scientist and mentor. He taught me proper experimental design and improved my ability to think critically. Dr. Kay's creativity always amazed me as he would devise the most elegant solutions to problems in my experiments. Dr. Kay developed me into a well-rounded graduate student. He provided many opportunities to mentor undergraduates either through the university or through programs the Bachelor's to the Baccalaureate program. Dr. Kay was always supportive when I approached him about going to conferences, forming collaborations, or new ideas for my thesis.

I am very appreciative of all my committee members, Drs. Teresa Orenic, Don Morrison, Shura Mankin, and Andrei Karginov. Their suggestions and expertise brought a lot of value to my research project. Dr. Orenic was always encouraging and there to help me with any aspect of my project. Dr. Morrison was never too busy to provide feedback on my student seminars and writing samples. Dr. Karginov did not hesitate to allow me to work in his lab to develop my technical skills. Dr. Mankin was always the first person to push me to a higher level as a scientist.

I am grateful to have been part of the Molecular, Cell, and Developmental Biology (MCDB) program. I would like to give special thanks to Dr. David Stone. Even though he was not part of my committee, he was there to help teach me as if I was his own student. He would take the time to provide feedback on my project, writing samples, and presentations.

ACKNOWLEDGEMENTS (continued)

The Kay lab was a wonderful place to conduct my thesis work. Every member, both past and present, of the lab contributed in their own way to my project. Dr. Michael Kierny was a tremendous help during my graduate school experience. He selflessly took the time to teach me techniques and experimental design. Even after moving on from the lab, Dr. Kierny continued to help me with anything that I needed. Dr. Kevin Gorman was extremely supportive as he never hesitated to offer advice or share with me anything that would help me in my work.

I want to thank all my friends in the MCDB program and in the department. Special thanks to the “A-squad,” Deanna and Arjun, for listening to all my troubles and sharing in the good times. Sarah Zinn and Dan Applegate were always there for me when I needed it. I want to thank both the Stone and Orenic groups for making me an honorary member of their labs.

Most importantly, I want to thank my family. My family made great sacrifices to give me the best education. Whatever I needed, they figured out a way to provided it to me. The most important person that got me where I am is my mother, Carmen Venegas. Words cannot describe how grateful I am for everything that she has done for me. In many ways, this degree is as much hers as it is mine.

LAV

CONTRIBUTIONS OF AUTHORS

I would like to acknowledge the contributions of the authors for each of my manuscripts. Each manuscript was used, either partially or fully as noted, to write chapters 1, 2, and 3.

Chapter 1 Introduction

Reference: Venegas LA, Zhao Q, Weiner MP, Kay BK (2017). *Reagents for Detecting Phosphosites within Proteins*. *J Bioinform, Genomics, Proteomics* 2(3): 1022

Leon A. Venegas- Wrote, generated figures, and edited all sections of the review article with the following exceptions: paragraphs 2-4 of the "Detection with recombinant affinity reagents" section and Figure 3 "Structural model of an scFV in complex with a phosphopeptide."

Dr. Qi Zhao- Wrote paragraphs 2-4 of the "Detection with recombinant affinity reagents" section and generated Figure 3 "Structural model of an scFV in complex with a phosphopeptide."

Dr. Michael Weiner- Wrote and edited paragraphs 2-4 of the "Detection with recombinant affinity reagents" section.

Dr. Brian K. Kay- Edited the entire review article.

Chapter 2 A comparison of phosphospecific affinity reagents reveals the utility of recombinant Forkhead-associated 1 domains in recognizing phosphothreonine-containing peptides

Reference: Venegas LA, Pershad K, Bankole O, Shah N, Kay BK. A comparison of phosphospecific affinity reagents reveals the utility of recombinant Forkhead-associated 1 domains in recognizing phosphothreonine-containing peptides. *New Biotechnology*. doi:10.1016/j.nbt.2015.12.006, 2016.

Leon A. Venegas- Wrote, generated figures, and edited all sections of the research article.

Dr. Kritika Pershad- Isolated the following FHA reagents that are listed in Table 1: FHAαCaMKII, FHAαMAPK3, FHAαMAPK1, FHAαSch-1, FHAαJunB, FHAαJunD, and FHAαMyc.

Oluwadamilola Bankole- Subcloned the different FHA coding regions into the protein expression vectors. Generated preliminary data for Figure 2 "FHA variants are phosphorylation-dependent."

CONTRIBUTIONS OF AUTHORS (continued)

Noman Shah- Subcloned the different FHA coding regions into the protein expression vectors. Generated preliminary data for Figure 5 “Comparison of phosphospecificαERK1/2 reagents.”

Dr. Brian K. Kay- Edited the entire research article

Chapter 3 Generating a recombinant phosphothreonine-binding domain for a phosphopeptide of the human transcription factor, c-Myc

Reference: Venegas LA, Kall SL, Bankole O, Lavie A, Kay BK. Generating a recombinant phosphothreonine-binding domain for a phosphopeptide of the human transcription factor, c-Myc. N. Biotechnol, 2018. pii:S1871-6784(18)30120-1.

Leon A. Venegas- Wrote, generated figures, and edited all sections of the research article with the following exceptions: paragraph 2 of the “Protein purification” section, “Crystallization of Myc-pTBD with Myc-pT58,” “Data Collection and Structure determination of Myc-pTBD with Myc-pT58,” Table 1, and Figure 3 “Structural model of an scFv in complex with a phosphopeptide,” paragraphs 1-3 of “The Myc-pTBD builds a network of interactions with the pThr moiety” section, Figure 3 “The engineered Myc-pTBD strongly resembles the structure of the yeast FHA1 domain and how it interacts with a phosphopeptide,” Figure 4 “The Myc-pTBD creates a large electrostatic pocket for the binding of pThr,” paragraph 1 of “The Myc-pTBD interacts with the Leu at the pT+3 position through a hydrophobic network” section, Figure 5a “The +3 position is the major determinant of specificity.”

Dr. Stefanie L. Kall- Wrote and edited the following portions of the research article: paragraph 2 of the “Protein purification” section, “Crystallization of Myc-pTBD with Myc-pT58,” “Data Collection and Structure determination of Myc-pTBD with Myc-pT58,” Table 1, and Figure 3 “Structural model of an scFV in complex with a phosphopeptide,” paragraphs 1-3 of “The Myc-pTBD builds a network of interactions with the pThr moiety” section, Figure 3 “The engineered Myc-pTBD strongly resembles the structure of the yeast FHA1 domain and how it interacts with a phosphopeptide,” Figure 4 “The Myc-pTBD creates a large electrostatic pocket for the binding of pThr,” paragraph 1 of “The Myc-pTBD interacts with the Leu at the pT+3 position through a hydrophobic network” section, Figure 5A “The +3 position is the major determinant of specificity.”

Oluwadamilola Bankole- Generated data for Figure 5B “The +3 position is the major determinant of specificity.”

Dr. Arnon Lavie- Edited the research article and analyzed the structural data.

Dr. Brian K. Kay- Edited the entire research article

TABLE OF CONTENTS

Chapter **Page**

LIST OF TABLES

TABLE **PAGE**

LIST OF FIGURES

FIGURE **PAGE**

LIST OF ABBREVIATIONS

10FnIII	10th fibronectin type III domain
β-elimination	β-elimination/Michael addition
Ab	antibody
Akt1	Protein kinase B
ATF2	Activating transcription factor 2
bHLH	Basic helix-loop-helix
BRCT	BRCA1 COOH-terminal
CaMKII	Ca^{2+}/calmodulin kinase II
CDK	Cyclin-dependent kinase
CDR	Complementarity-determining region
cFHA	Chimeric forkhead-associated
Chk2	Checkpoint kinase 2
DARPin	Designed ankyrin repeat proteins
EC_{50}	Concentration that gives the half maximal response
EGFR	Isoform 1 of epidermal growth factor receptor precursor
ELISA	Enzyme-linked immunosorbent assay
epPCR	Error-prone polymerase chain reaction
ERK	Extracellular-regulated kinase
FAM38A	Family with Sequence Similarity 38, Member A
FHA	Forkhead-associated
FHA1	Forkhead-associated 1
FHA2	Forkhead-associated 2

FN3	Fibronectin type III monobody
FRET	Fluorescence resonance energy transfer
GSK3β	Glycogen synthase kinase-3β
HPLC	High performance liquid chromatography
HRP	Horseradish peroxidase
IκBα	Kappa light polypeptide gene enhancer in B-cells inhibitor, alpha
IMAC	Immobilized metal affinity chromatography
IP	Immunoprecipitation
IR	Infrared fluorescence
JunB	Transcription factor jun-B
JunD	Transcription factor jun-D
LiCl	Lithium chloride
lysC	Lysyl endopeptidase
LZ	Leucine zipper
m/z	Mass to charge ratio
mAb	Monoclonal antibody
MALDI-TOF MS	Matrix-assisted laser desorption/ionization time-of-flight mass spectrometry
MAPK1	Mitogen-activated protein kinase 1
MAPK3	Mitogen-activated protein kinase 3
MAP2K2	Mitogen-activated protein kinase kinase 2
MAP4K4	Mitogen-activated protein kinase kinase kinase kinase 4

MegaSTAR	Megaprimer Shuffling for Tandem Affinity Reagents
Mrc1	Mediator of replication checkpoint 1
MS	Mass spectrometry
MS/MS	Tandem mass spectrometry
Myc	Transcription factor c-Myc
NA	Neutravidin
Nbs1	Nibrin
NCL	Nucleolin
ORF	Open reading frame
P3	Minor coat protein III
pAb	Polyclonal antibody
PCR	Polymerase chain reaction
PP2A	Protein phosphatase 2A
pSer	Phosphoserine
pTBD	Phosphothreonine-binding domain
pTyr	Phosphotyrosine
PIKK	Phosphoinositide 3’-kinase-like kinase
Pkn	Serine/threonine-protein kinase N
PLK	Polo-like kinase 1
PNK	Polynucleotide kinase
PTB	Phosphotyrosine-binding domains
PTM	Post-translational modification
pThr	Phosphothreonine

Phosphosite	Phosphorylatable site
Raf1	RAF proto-oncogene serine/threonine protein kinase
rtTA	Reverse tetracycline-controlled transactivator
SA	Streptavidin
scFv	Single-chain fragment of variable regions
SDS-PAGE	Sodium dodecyl sulfate polyacrylamide gel electrophoresis
SEC	Size-exclusion chromatography
SH2	Src-homology 2
Shc-1	Src homology 2 domain containing transforming protein 1
SPR	Surface plasmon resonance
Ser	Serine
TIFA	TRAF-interacting protein with an FHA domain
Thr	Threonine
TR	Tandem repeat
tRE	Tetracycline response element
Tyr	Tyrosine

SUMMARY

Cell signaling is a complex network of communication within the cell that is initiated upon environmental stimulation. A common outcome of cell signaling is phosphorylation which is a major regulator of signaling events that impacts important biological processes such as metabolism, growth, and proliferation. Phosphorylation is such a heavily used post-translational modification that an estimated 30% of proteins within the cell are phosphorylated at any given time. Phosphorylation primarily occurs on either Serine (88%), Threonine (11%), or Tyrosine (<1%). Mutations in either the kinase or substrate results in a state of either a hyper- or hypo-state of phosphorylation. Either of these phosphorylation states is a cause for diseases such as cancer or neurodegeneration.

Monitoring phosphorylation events, which has traditionally been accomplished using immunoglobulin Gs (IgGs), allows for the study of cell signaling and for disease detection. IgG technology has allowed elucidation of the biological consequences of phosphorylated residues in different signaling pathways. Furthermore, IgGs have also been used to detect phosphorylated markers of disease through biochemical assays such as immunohistochemistry or western blot. While IgGs have proven to be effective tools for monitoring phosphorylation, they are limited in their renewability and are not amenable to improvements in specificity or affinity. Most importantly, many commercially available IgGs have been demonstrated to be cross-reactive with similar phosphorylated sites (phosphosites).

Recombinant affinity reagent technology was developed to overcome IgG limitations. Affinity reagents are engineered proteins that are created using techniques in

molecular biology. Affinity reagent production does not involve animals, reagents are renewable, and their affinities can be improved. Dr. Kritika Pershad engineered a naturally occurring phosphothreonine (pThr)-recognizing domain of *Saccharomyces cerevisiae* from the Rad53 protein, namely the Forkhead-associated 1 (FHA1) domain, for use as a phosphorylation-specific affinity reagent. An FHA1 phage library of variants was generated and used in phage display affinity selection to isolate engineered FHA variants that bind pThr-containing peptides from various kinases and transcription factors. These engineered domains will be referred to as phosphothreonine-binding domains (pTBDs).

A total of 17 different pThr-containing peptides served as targets in phage display affinity selection. pTBDs were isolated against 14 of the targets, five of which I isolated, reflecting an 82% success rate. I found that the major determinant of success is the amino acid three residues C-terminal to the pThr moiety, the pT+3 position. I showed that FHA1 library does not contain variants that are able to bind to either phosphoserine (pSer)- or phosphotyrosine (pTyr)-containing peptides or peptides containing a positively charged residue at the pT+3 position. I further demonstrated that all isolated pTBDs from the library are both phosphorylation-dependent and pThr-specific. These results were reported in Venegas *et al.*, 2016.

I continued to use the FHA technology to isolate an FHA variant against a pThr-containing peptide from transcription factor c-Myc (Myc). In collaboration with Dr. Arnon Lavie’s group, I isolated and solved the crystal structure of

the Myc-recognizing, engineered FHA-pThr binding domain (Myc-pTBD). Using a biochemical and structural approach, I identified the Myc-pTBD's molecular determinants of specificity and identified the molecular interactions between the domain and its peptide target. I then compared the Myc-pTBD's specificity to commercially available antibodies. These results were submitted to *New Biotechnology* and are currently under review.

Finally, I devised a way for improving the affinity of the pTBDs through multimerization. I generated homodimers using the Myc-pTBD, Extracellular-regulating kinase1/2-recognizing pTBD (ERK-pTBD), and Ca^{2+}/calmodulin kinase II-recognizing pTBD (CaMKII-pTBD). I measured and observed a 10-100x-fold improvement in their apparent affinities. I then chose the Myc-pTBD homodimer to probe for phosphorylated Myc in whole cell lysates by western blot. While the Myc-pTBD homodimer did not recognize its cognate target, it was able to recognize other proteins within the lysate suggesting that the reagent may be better used as a probe for other targets. This was the first time that a pTBD could recognize any targets in a lysate by western blot.

Chapter 1

Introduction

Part of this research has been published in

Venegas LA, Zhao Q, Weiner MP, Kay BK. Reagents for detecting phosphosites within proteins. *J Bioinform, Genomics, Proteomics* 2(3): 1022.

1 Introduction

1.1 Protein phosphorylation

Protein phosphorylation is an important post-translational modification (PTM) implicated in regulating cellular activities [1]. The human genome encodes ~ 560 protein kinases [2] and ~ 200 protein phosphatases [3] that coordinate signaling events through the phosphorylation and dephosphorylation of proteins, respectively. With 30% of a eukaryotic cell's proteins estimated to be phosphorylated at any given time [4], this PTM is utilized in diverse ways to regulate protein function. Examples include providing docking sites for protein-protein interactions [5], coordinating activity and subcellular localization [6], marking proteins for degradation [7], and activating or inactivating proteins in cell signaling pathways [4].

Most eukaryotic proteins contain more than one phosphorylatable site (phosphosite), which primarily occurs on serine (89%), threonine (10%), and tyrosine (<1%) residues [8-11]. Elucidating the functional role of phosphosites is an important task, as altered expression or activity of protein kinases [12] and phosphatases [13] or mutation of the site of phosphorylation [14] are linked to a variety of diseases, including cancer [15]. With over 100,000 phosphosites reported to date [16], there is a substantial need for techniques and tools for quantitative and qualitative studies of phosphorylation events.

1.2 Phosphosite-interacting domains

In eukaryotic cells, signal transduction events include the reversible assembly of multiprotein complexes. Construction and deconstruction of these complexes is regulated

by protein phosphorylation via shifts in the concentration of kinases and phosphatases, respectively [17]. Phosphorylation of serine (Ser), threonine (Thr), and tyrosine (Tyr) create binding sites for phosphoprotein-binding domains that allow protein-protein interactions between the upstream kinase and the downstream substrate [17, 18]. Phosphoprotein-binding domains are modular domains that recognize distinct phosphorylated sequence motifs. Examples of phosphoserine/phosphothreonine (pSer/pThr)-binding domains (Fig. 1) include the BRCA1 COOH-terminal (BRCT) domain from the breast cancer 1 BRCA1 protein [19, 20], the 14-3-3 family of proteins [21, 22], the WD40 repeat domain [23], and the Forkhead-associated (FHA) domains [24-29] [17, 18, 30, 31]. The Src-homology 2 (SH2) domain and phosphotyrosine (pTyr)-binding domains (PTBs) recognize pTyr-containing motifs [17].

1.3 Forkhead-associated (FHA) domains

FHA domains, first identified in Forkhead-type transcription factors, are 80-100 amino acid long, modular phosphoprotein-binding domains that specifically recognize pThr-containing peptides [24, 25]. These domains, present in both eukaryotes and prokaryotes, have been identified in over 2000 different proteins [32, 33], including regulatory proteins, kinases, phosphatases, and transcription factors [24, 33], which are involved in diverse cellular activities including transcriptional regulation [34], DNA damage response [35], cell cycle progression [36], apoptosis [37], protein trafficking, and protein degradation [26, 29, 38]. According to the Simple Modular Architecture Research Tool (SMART; http://smart.embl-heidelberg.de/), FHA domains occur in 83 and 14 proteins in the human and yeast genomes, respectively. While there is much speculation on the functional role

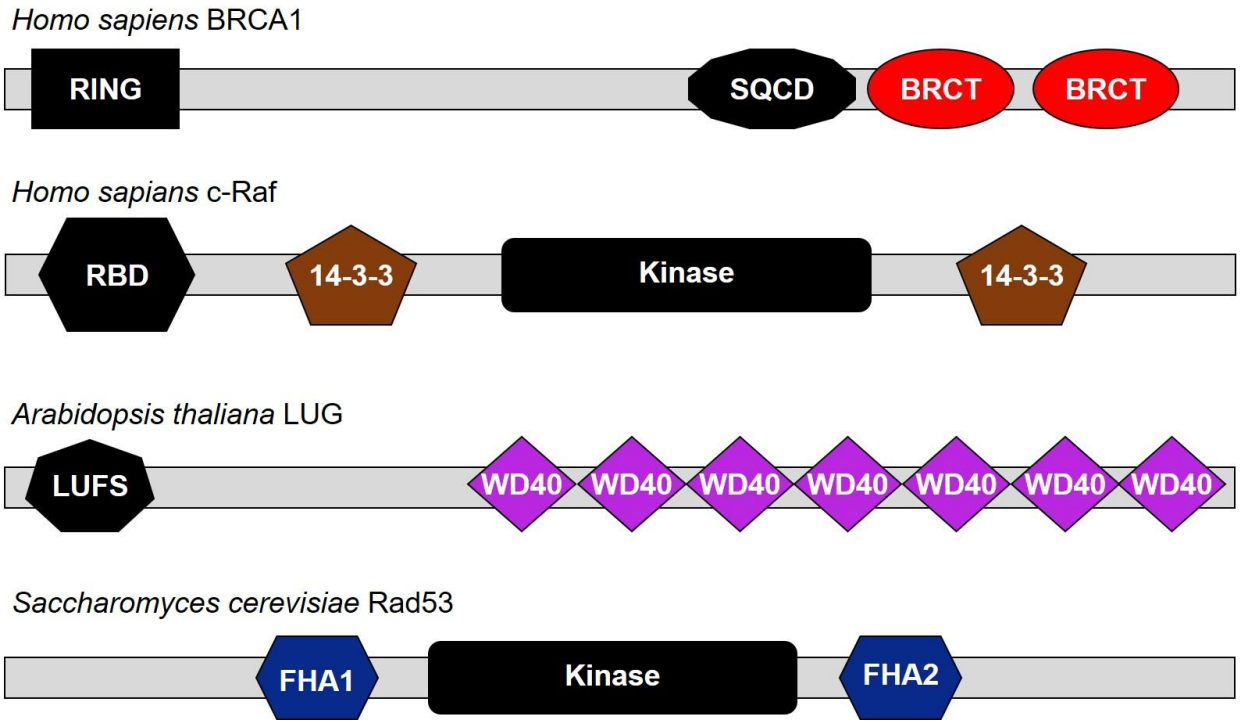

Figure 1. Domain structures of phosphoserine- and phosphothreonine-binding domain proteins. Shown here are four examples of proteins that contain phosphoserine- and phosphothreonine-binding domains (color), along with other functional domains (black). Domains are not drawn to scale.

of FHAs in prokaryotes, their role in eukaryotes is well understood. In humans, the FHA domains from Checkpoint kinase 2 (Chk2) and Nibrin (Nbs1), are essential for the DNA damage response and tumor suppression pathways [39-42]. In *Drosophila melanogaster* and *Caenorhabditis elegans,* kinesins with FHA domains function in vesicular transport [43].

FHA domains share ~ 20-30% sequence similarity, with only six conserved residues (Fig. 2) that are critical for either structural stability or for the protein-peptide interaction. For example, Gly69, Arg70, Ser85, His88 [26] of the FHA1 domain of Rad53 line up with residues Gly116, Arg117, Ser140, and His143 of the FHA domain of the Chk2 protein. [28]. Despite a low-level sequence similarity, the three-dimensional structure of FHA domains remains highly conserved: all FHA domains have 11 or 12 β-sheets that fold into a β-sandwich, with loops between the β-strands [33]. The major structural differences between FHA domains are loop lengths and the presence of alpha helices in various loops [38].

Although structurally similar, FHA domains vary in how they interact with their cognate ligand; furthermore, FHA cognate ligands can range in amino acid composition (Table I). Combinatorial peptide libraries were first employed to identify the major determinants of specificity [33, 38, 44]; they revealed that FHA domains recognize the pThr residue and the amino acid three positions C-terminal to the pThr moiety (pT+3 position). As new FHA domains were discovered, and their molecular determinants of specificity studied, five distinct recognition classes emerged (Table I). Members of the first recognition class interact with their phosphoepitope targets through the pThr and the pT+3 position (Fig. 3). Most FHA domains fall into this recognition class [29]. The second recognition class

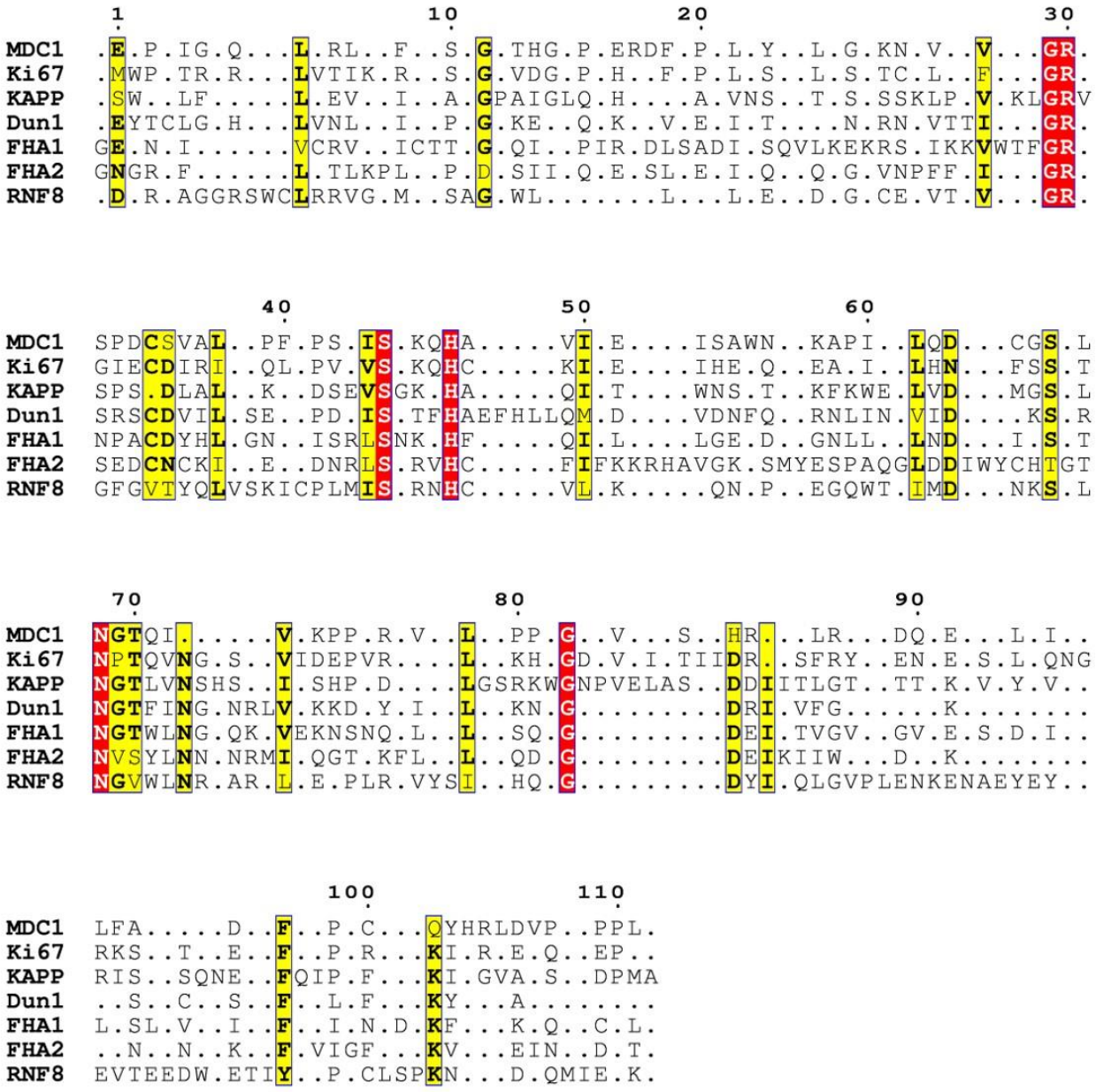

Figure 2. Sequence alignment of naturally occurring FHA domains. Conserved residues are highlighted in red and semi-conserved (≥50% similarity) residues are highlighted in yellow. Dots represent residue gaps between the different FHA domains.

FHA domain-containing protein	Species	Interacting partner	Epitope	Interaction rule	References
Rad53 (FHA1)	*S. cerevisiae*	Rad9	SLEV**pT**EAD	pT+3	[38]
Ki-67	*H. sapiens*	hNIFK	KTVD**pS**QGP**pT**PV C**pT**PTFL ERRKSQVAELN DDDKDDEIVFKQPISC	pT+ extended binding surface	[45]
Dun1	*S. cerevisiae*	Rad53	NI**pT**QP**pT**QQST	pT-pT+3	[46]
Polynucleotide kinase (PNK)	*M. musculus*	XRCC4	YDES**pT**DEESEKK	N and C termini to pT	[47]
Tumor necrosis factor-associated factor-interacting protein with a forkhead-associated domain (TIFA)	*H. sapiens*	TIFA	MTSFEDADp**T**EETVTC	N-terminal to pT	[48]

Table I. Representative members of the five recognition classes of FHA domains and their ligands.

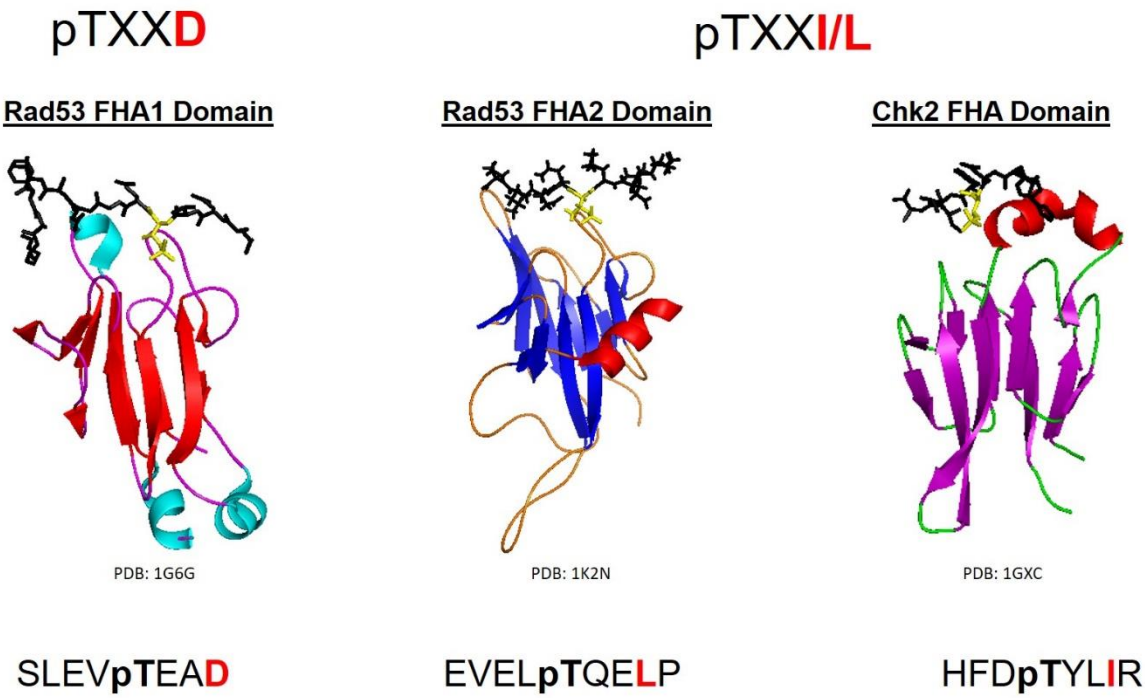

Figure 3. Examples of the first recognition class of FHAs interacting with their ligand. Each FHA domain recognizes their target based on the reside at the pT+3 position. The FHA1 from the Rad53 protein recognizes Asp (D) at the pT+3 position. The FHA2 from Rad53 recognizes Leu (L) at the pT+3 position. The Chk2-FHA recognizes any hydrophobic residue at the pT+3 position, but its native target contains an Ile (I) at the pT+3 position.

recognizes the pTxxpTxx(A/S) motif. This class was identified when the crystal structure of Dun1-FHA domain revealed that its FHA domain interacts with two pThr residues, as well as the residue at the pT+3 position relative to the second pThr residue [46]. The third recognition class was discovered when an oriented peptide array library revealed that the FHA domain of the Serine/threonine-protein kinase N (PKN) protein interacts with residues on both N- and C-terminal sides of the pThr moiety [47, 49]. The fourth recognition class was found through studies on the FHA domain of the Ki-67 protein. The FHA domain of this protein only interacts with a pThr-containing peptide that is composed of 44 residues from the human nucleolar protein interacting with the FHA domain of pKi-67 (hNIFK) protein [50, 51]. This was surprising as all FHA domains characterized to date bind phosphopeptides that are 8-12 amino acids in length [33]; presumably the Ki-67 FHA domain recognizes a secondary structure in the hNIFK protein. Finally, a fifth recognition class was revealed through the structural analysis of the TRAF-interacting protein with an FHA domain (TIFA) in complex with its peptide ligand; this FHA domain interacts with residues N-terminal to the pThr site [48].

1.4 The FHA1 domain of the *Saccharomyces cerevisiae* Rad53 protein

In the budding yeast, *S. cerevisiae*, DNA damage activates a signaling cascade that arrests cell cycle progression [36]. The phosphoinositide 3'-kinase-like kinase (PIKK), Mec1, phosphorylates Rad9 (pRad9), which then forms a complex with Rad53 protein [52, 53]. Subsequently, the Rad53 component of the pRad9-Rad53 complex is phosphorylated by both PIKK and mediator of replication checkpoint 1 (Mrc1) [53], which activates the kinase activity of pRad53, allowing it to phosphorylate and activate Dun1

kinase. This phosphorylation cascade eventually leads to inactivation of cell cycle control genes [54]. While the signaling cascade was a well-studied event, it was not clear how pRad9 was interacting with Rad53.

Rad53 is a calcium/calmodulin-dependent protein kinase that contains two FHA domains, FHA1 and FHA2 domains, at the N- and C-termini, respectively [26]. Rad53 was observed to interact with Rad9 in a phosphorylation-dependent manner [36, 55, 56]. Sun *et al.*, [36] demonstrated that the purified Rad53 FHA2 domain interacts with phosphorylated Rad9, but not un-phosphorylated Rad9 protein *in vitro*, indicating that binding of the FHA2 domain and pRad9 was dependent on Rad9 being phosphorylated. These data corroborated the observation that the FHA-containing KAPP protein of *Arabidopsis* was only capable of interacting with its target, RLK5, when it was phosphorylated [57].

These observations led to the question if the FHA domains of Rad53 played a role in protein-protein interactions. Durocher *et al.,* [26] addressed this through immunoprecipitation of proteins with Rad53's two FHA domains; both the FHA1 and the FHA2 domains pull-downed Rad9 only when it is phosphorylated. The interaction between the FHA1-pRad9 was later observed to be inhibited when incubated with a pThr-containing peptide (188-SLEV**pT**EADATFVQ-200) [58]. To characterize the interaction of the FHA1 domain and the pThr-containing peptide, alanine-scanning indicated that the residue three positions C-terminal to the pThr-moiety (pT+3 position) was critical for the interaction between the FHA1 and the phosphopeptide.

These early studies identified two attributes shared by FHA domains [26]. The first is that the FHA1 domain is both pThr-dependent and specific as binding did not occur when

phosphothreonine was substituted by pSer or Aspartic acid (Asp), a mimetic of the phosphate's negative charge, in the peptide ligand. Second, it also established the importance of the residue at the pT+3 position in the peptide ligand for binding. When residues N-terminal to the pThr-moiety were substituted with Ala in the peptide there was no significant loss of binding, whereas substitution of Asp at the pT+3 with Ala resulted in loss of binding. It was concluded that a major recognition element of the yeast FHA1 domain is the pT+3 position.

1.5 Mass Spectrometry

Mass spectrometry (MS) is a method that has provided a deep understanding of cell signaling events through the identification of phosphosites on proteins. Quantitative mass spectrometry has allowed for the observation of the temporal dynamics of the phosphoproteome in growth factor signaling [59-61], identification of novel phosphosites in T-cell receptor signaling [61], cell cycle dependent changes in phosphorylation [60], and identification of novel kinase substrates [62-64].

A general workflow is shown in Figure 4. Mapping phosphosites begins with the fragmentation of proteins using proteases, such as trypsin or lysyl endopeptidase (lysC) [65, 66]. The resulting peptides are then separated by reverse-phase high performance liquid chromatography (HPLC), eluted, and introduced in an ionized form into the mass spectrometer. The mass spectrometer separates the ions based on their mass-to-charge ratio *(m/z)* [67] and generates a mass spectrum. The spectral data is then processed by computer algorithms (e.g., SEQUEST, MASCOT, X!TANDEM) [68] that identify peptides by matching the experimental data to the theoretical spectrum of the sequenced genome

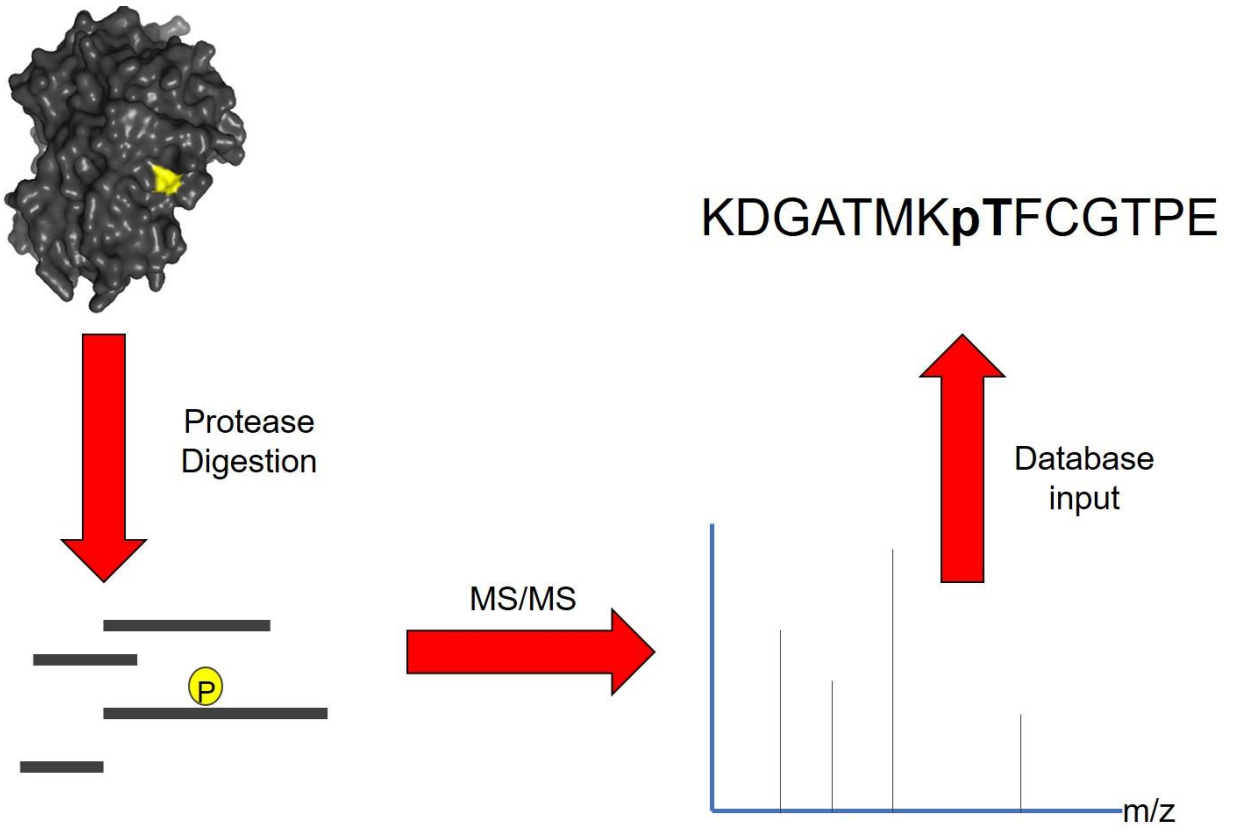

Figure 4. A standard workflow for identifying new phosphosites by tandem mass spectrometry. The protein of interest containing a phosphoresidue (yellow) is enzymatically digested to produce peptide fragments. The fragments are ionized and analyzed by tandem mass spectrometry to produce a peptide mass spectrum. The m/z values of the resulting peptide fragments are then input into databases to identify the the phosphosite.

[66]. Individual peptides can be subsequently fragmented and sequenced in a tandem mass spectrometer (MS/MS). Phosphopeptide mapping is accomplished by matching fragment ion spectra with all possible phosphorylated versions of each peptide [65, 66]. Improvements in statistical analysis have led to the development of programs such as the A-score [69], PTM score [59], the Mascot Delta Score [70], and the SLIP score [71] that estimate the position of the phosphosite within the peptide.

Compared to unphosphorylated proteins, phosphorylated proteins are present at low levels in the cell. Enriching for phosphopeptides thus minimizes the complexity of the sample for mass spectrometric analysis [72]. Three enrichment strategies are commonly used: 1) immunoprecipitation (IP), 2) immobilized metal affinity chromatography (IMAC), and 3) β-elimination/Michael addition (β-elimination) with the addition of an affinity tag [65, 66, 68, 72]. In immunoprecipitation experiments [65, 73], individual proteins are affinity purified with antibodies, fragmented with trypsin, and ionized peptides introduced into the mass spectrometer. In IMAC, chelates of Fe(III), Ge (III) or titanium ions [74] are used to affinity purify phosphate-containing peptides from a trypsinized cell lysate. [65]. In β-elimination, the phosphate group is replaced with an affinity tag such as biotin [75].

While enrichment strategies have proven effective for identifying novel phosphosites within a protein, there are several limitations to each approach. Enriching with antibodies may not be possible if the target of interest does not contain a ligand tag or no antibodies are available to IP the protein. One concern with IMAC is that the chelated metal ions will also purify peptides with acidic residues. Lastly, with β-elimination, O-linked sugars undergo the same elimination chemistry, which causes glycosylation sites to be mistaken

for phosphorylation sites. Furthermore, the reaction requires large amounts of sample that may be difficult to obtain [65].

1.6 Phosphospecific antibodies for monitoring phosphorylation events

Antibodies are commonly used tools for probing proteins in complex mixtures and cells. Antibody production and validation is a long (i.e., 3-12 months) and rigorous process (Fig. 5). To produce an antibody, a purified or recombinant target protein is injected into an animal host, which triggers an immune response and subsequent production of antibodies. Polyclonal antibodies (pAbs) are purified from the serum of the immunized animal, whereas monoclonal antibodies (mAbs) are secreted from an immortalized B cell of the immunized animal. pAbs and mAbs can also be generated to synthetic peptides corresponding to peptide segments of a protein that incorporate a phosphorylated residue. For example, to produce an antibody against phosphorylated human Akt1, which carries a phosphothreonine at position 308 (i.e., pT308), a 15-mer peptide (KDGATMK**pT**FCGTPE) would be synthesized and used as the immunogen (with adjuvant). Serum from the immunized animal can be chromatographed over a column containing the immobilized phosphopeptide, and antibodies that recognize the peptide are then affinity purified. If desired, a subsequent subtraction step can be used to eliminate antibodies from serum that cross-react with the non-phosphorylated form of the peptide; the affinity purified antibodies can be chromatographed over a column containing the non-phosphorylated form of the peptide attached to resin, yielding antibodies (in the flow-through) that recognize the peptide sequence only when phosphorylated. To generate mAbs, an animal host is injected with the phosphopeptide of interest, and after

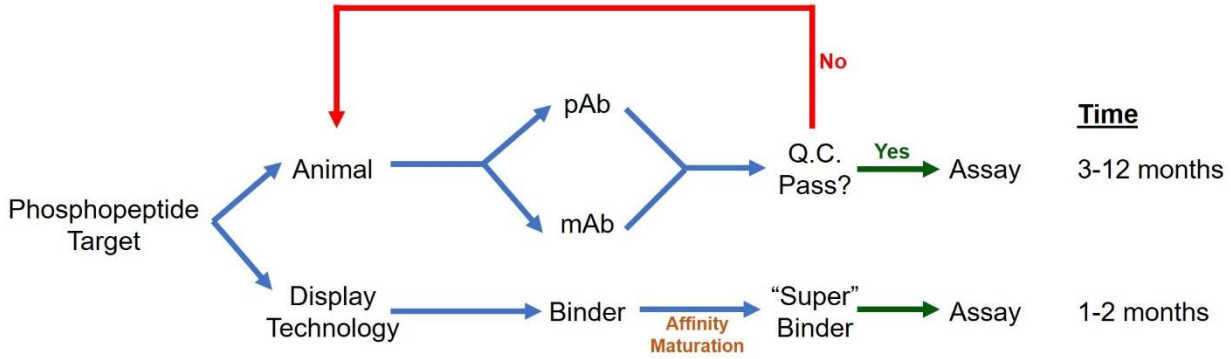

Figure 5. A pipeline to produce phosphospecific reagents. There are two approaches for generating phosphospecific reagents. The first is that an animal is injected with a phosphopeptide to produce antibodies (i.e., mAb, pAb). The reagents then undergo a series of quality control (QC) checks before they are tested in assays. Failure to pass QC checkpoints results in the process having to be repeated. Alternatively, in display technologies, a phosphopeptide is used as a target in affinity selection, binding variants are isolated, and affinity matured to produce a “super binder," which can be used in assays. Production of an antibody takes between 3 to 12 months, while display technologies are generally faster, often requiring only 1 to 2 months.

several rounds of injections, splenocytes from the host are isolated and B cells fused with immortalized myeloma cells to produce hybridomas. Hybridoma clones are plated into microtiter plate wells, and cells that secrete the desired phosphospecific antibody are then cloned. By either method, it is possible to generate antibodies that bind the peptide sequence only when phosphorylated (i.e., the phosphate is part of the epitope).

While pAbs and mAbs can be very effective in monitoring phosphorylation events by western blot [76-80] and cell staining [81], there are several limitations to this approach. First, when pAbs and mAbs are raised against a phosphopeptide, there is no assurance that such antibodies will recognize the native, folded form of the phosphoprotein. Consequently, they may not be useful for pull-down and cell staining experiments. Second, the quality of pAbs and mAbs is not completely reproducible from lot to lot [82] immune responses vary between animals, which leads to batch-to-batch differences [83], and hybridomas may stop secreting mAbs due to genetic drift [84, 85] or clonal instability [86]. Third, there are many examples of cross-reactivate antibodies [87-91], requiring immunization of additional animals until the desired specificity is attained. Fortunately, advancements in chemical and protein engineering have provided alternative approaches for overcoming the limitations of generating antibodies to phosphoepitopes. These methods provide shorter production times, eliminate the need for animals, ensure renewability, and offer improved specificity.

Advancements in chemical and protein engineering have provided ways to overcome the limitations of generating antibodies to phosphoepitopes. These methods provide shorter production times, eliminate the need for animals, ensure renewability, and offer improved specificity.

1.7 New reagents for detecting protein phosphorylation

Investigators have turned their attention to developing polymers and recombinant affinity reagents for monitoring phosphorylation. These alternative technologies have demonstrated great utility in detecting phosphorylated targets with a high level of accuracy. Both the Phos-tag and pIMAGO systems bind the phosphoryl moiety and can be used to quantify the level of phosphorylation within a protein or cell lysate. Recombinant affinity reagents offer the same advantages of antibodies, but their affinities and specificities can be readily manipulated through molecular biology techniques.

1.7.1 Detection of phosphoepitopes using the Phos-tag system

The Phos-tag (Fig. 6) was developed to identify phosphorylation and monitor kinase activity without the need of phosphospecific antibodies or radiolabeling [92, 93]. The reagent can be used in a variety of experimental formats. The Phos-tag enhances detection of phosphopeptides in matrix-assisted laser desorption/ionization time-of-flight mass spectrometry (MALDI-TOF MS) [94, 95], Phosphorylation of proteins can be also monitored with this reagent in surface plasmon resonance (SPR) [96], SDS-PAGE [97-102], western blots [92], and fluorescence resonance energy transfer (FRET) [103] experiments. Finally, the Phos-tag can be used in affinity chromatography [104, 105] to purify phosphopeptides in bulk from a trypsin-digested cell lysate for biochemical analysis. However, one limitation to note about the Phos-tag is the inability of this reagent to differentiate between distinct phosphosites within a protein.

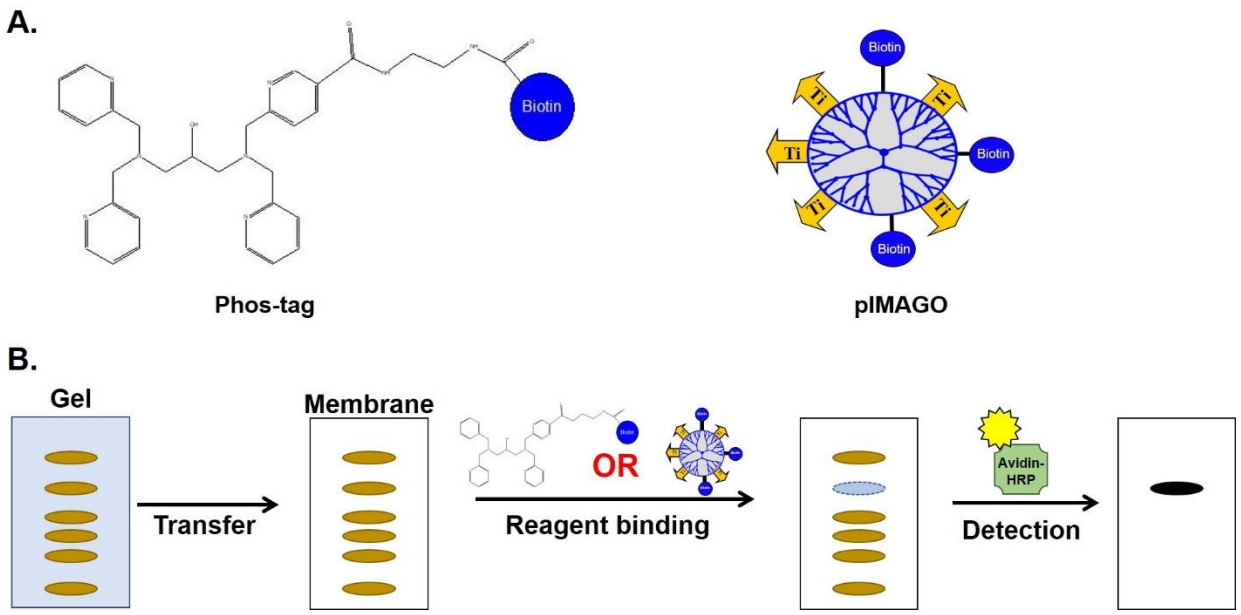

Figure 6. Phosphoprotein detection by antibody alternatives. A. Phos-tag (left) is a binuclear metal (II) complex of 1,3-bis[bis(pyridine-2-ylmethyl)amino]propan-2-olate that interacts with the phosphoryl moiety. The Phos-tag has a vacancy on two metal ions that is suitable for accessing the monoester dianion as a bridging ligand. pIMAGO (right) is a dendrimer conjugated to titanium ions (yellow arrows) that bind the phosphoryl moiety. Each molecule can be tagged with biotin (blue circle). B. Detection of the phosphoprotein can be achieved by following the binding of biotinylated Phos-tag or pIMAGO to a protein species, followed by detection with horseradish peroxidase (HRP) conjugated to avidin. Not to scale.

1.7.2 Detection with novel polymers

The pIMAGO system (Fig. 6) is a water-soluble nanopolymer conjugated to titanium ions that can bind phosphate [106-109]. pIMAGO reagents can be tagged with an infrared fluorescence (IR) dye or biotin for detection of phosphoproteins in dot blots [110], western blots [111], or ELISAs [108]. The small size of the polymer is one of its main strengths; it is small enough to be used simultaneously in a western or dot blot with an antibody that recognizes a different epitope in the same protein. This is advantageous because steric hindrance can decrease simultaneous binding by two different immunoglobulins, which are 150 kDa in size. Simultaneous binding of the pIMAGO reagent and an antibody allows one to quantify the amount of phosphorylated protein relative to the total amount of the target. However, as the pIMAGO reagent binds equally well to different phosphorylated amino acids, the reagent cannot be used to identify the actual phosphosite.

1.8 Detection with recombinant affinity reagents

Recombinant affinity reagents offer many distinct advantages over animal produced antibodies. Since recombinant affinity reagents are generated in bacteria or through *in vitro* methods [112], there is no need for animals. Plus, their DNA sequence is known, allowing them to be shared electronically between research groups and easily ordered as synthetic DNA for insertion into a suitable expression vector [113]. Other advantages include their ability to be tagged through molecular biology techniques with different epitope sequences or fusion partners, without interfering with their binding properties [114], and their ability to yield tight, specific binders through directed evolution

approaches [115]. Finally, *in vitro* subtraction of epitopes permits generation of recombinant affinity reagents that are specific for protein conformations, individual members of a protein family, or PTMs [113, 116]. Large (i.e., $>10^8$) libraries of recombinant affinity reagents can be screened against targets of interest using display technologies such as phage-, yeast-, ribosome-, mRNA-, and bacterial-display [117]. Two common types of recombinant affinity reagents, antibody fragments and non-antibody scaffold proteins, are described below.

Antibody fragments, such as human single-chain Fragments of variable regions (scFv) can be displayed on the minor coat protein III (P3) of the M13 bacteriophage and used in phage display affinity selection experiments to isolate phosphospecific binders. For example, a 15-mer peptide is chemically synthesized with a phosphoresidue at its center, and then used in affinity selection experiments. Typically, three rounds of affinity selection are sufficient to recover binding clones from a display library, and their binding properties (i.e., affinity, specificity) can be improved through mutagenesis, if necessary. The final set of binders are often converted to immunoglobulins for stability and avidity. Phosphospecific-scFvs have been isolated by phage display against a panel phosphopeptide targets [118], including a phosphohistidine-containing target [119].

Phosphate binding sites in scFvs can be designed as a localized module. Research published by both Koerber [120] and Shih [118], and work by Dr. Michael Weiner's laboratory, suggest that the ability of an Ab to bind phosphorylated amino acids is dependent on the complementarity-determining region (CDR) 2 of the heavy and/or light chains. CDR2 makes direct contacts with the phosphorylated-amino acid, with CDR2 of the light or heavy chains playing a role in the directionality of the phosphopeptide as it fits

in the scFv's groove. Thus, instead of random mutagenesis of all six CDR residues, prior knowledge of phosphoamino acid binding can be incorporated into the phage display library design to produce a library with a higher frequency of modification-specific relevant binders. Such a phospho-focused library for binding phosphorylated targets using three constrained phosphorylated amino acid positions will be effectively 8,000 (i.e., 20^3) fold more efficient, valuable and practical over randomized libraries. Phosphospecific Abs generally recognize both the phosphorylated amino acid and the surrounding context sequence. The successful phosphorylated peptide Abs usually recognize 4-5 extra residues upstream or downstream of the phosphorylated residue [118, 120], suggesting excess binding to context sequence might be used to offset the contribution of the phosphorylated amino acid and consequently enable phospho-independent peptide binding in a subsequent variant of a recombinant scFv.

Based on alanine scanning results (Fig. 7) and the Weiner lab's and Koerber's findings that H2 is the phosphate-binding center [120], the Ab structure of AxioMx's antibody, AXM1293, was modeled and its complex with its cognate phosphorylated peptide in collaboration with Prof. Jeffrey Gray (Johns Hopkins University) [121, 122]. Through comparison with published structures, we noticed that L2 and H2 can be utilized to target phosphopeptides with C-terminal or N-terminal context sequences, respectively.

The uniform structure, the likely defined context length, as well as the proven design of phosphate binding sites altogether make a highly focused, knowledge-based phospho-status binding library of scFvs possible. Using a combination of functional mutagenesis and structural modeling as well as a comparison with existing structures of phospho-

Alanine Scanning of CDR-H2

Clone	CDR H2 sequence	% activity
W.T.	**AISGSGGSTYYADSVKG**	100
2	A**A**SGSGGSTYYADSVKG	92
3	AI**A**GSGGSTYYADSVKG	44
4	AIS**A**SGGSTYYADSVKG	67
5	AISG**A**GGSTYYADSVKG	72
6	AISGS**A**GSTYYADSVKG	75
7	AISGSG**A**STYYADSVKG	100
8	AISGSGG**A**TYYADSVKG	22
9	AISGSGGS**A**YYADSVKG	100
10	AISGSGGST**A**YADSVKG	25
11	AISGSGGSTY**A**ADSVKG	67
12	AISGSGGSTYYA**A**SVKG	100
13	AISGSGGSTYYAD**A**VKG	100
14	AISGSGGSTYYADS**A**KG	82
15	AISGSGGSTYYADSV**A**G	100
16	AISGSGGSTYYADSVK**A**	67

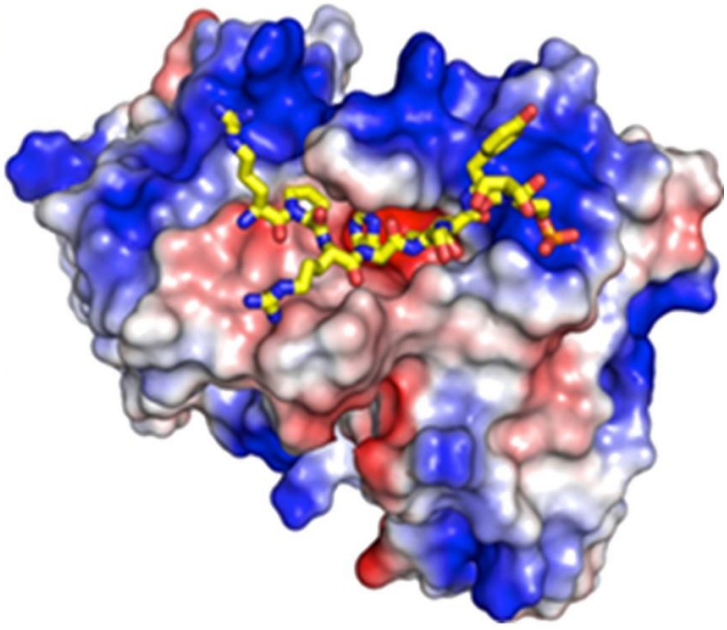

Figure 7. Structural model of an scFv in complex with a phosphopeptide. **Left.** Alanine scanning of CDR H2 and % peptide-binding activity as normalized to the wild type antibody. **Right.** The electrostatic contour of the scFv surface displays a deep negative charged groove connecting to H2; blue, grey, and red surfaces represent, positive, neutral, and negative residues, respectively. The positive charged half of the phosphopeptide (MARRPRHSIY**pS**SDEDDEDFE, where **pS** is phosphoserine) is shown in stick form bound in the scFv's groove; blue, orange, red, and yellow represent nitrogen, phosphorus, oxygen, and carbon, respectively. The peptide was manually modelled in the groove and refined using Rosetta FlexiPepDock software.

peptide Ab complexes, we have identified a shared peptide binding groove holstered by several restricted regions of CDR L3 and H3, which can serve as a suitable candidate for a focused phosphopeptide library design.

1.9 Selecting phosphospecific reagents through phage display

In vitro display systems are powerful high throughput methods for quickly generating large quantities of renewable affinity reagents against predefined antigen targets such as proteins and peptides. In each system, the selection conditions can easily be changed, the selected affinity reagents can be improved, and the genes of each of the reagents become immediately available [82]. There are five types of display methods that include phage display [123], yeast display [124], ribosome display [125], mRNA display [126], and bacterial display [127]. Each of the display methods has its own unique advantages and limitations (Table II) and has provided insight into epitope identification [128], discovery of novel protein-protein interactions [129], and therapeutics [130].

Phage display is the most widely and effective techniques used of all the display systems [131, 132] in which the peptide or protein displayed and its gene sequence is linked to an *Escherichia coli* filamentous bacteriophage [133-135]. The phage's coat protein, pVIII, encapsulates its genetic material (i.e., DNA). There are four other proteins that comprise the coat that include minor coat protein pIII, pVI, pVII, and pIX. pIII consists of 406 amino acids and is present on the tip of the phage in 3-5 copies (Fig. 8) [123]. Recombinant proteins or peptides are commonly displayed as fusions to the pIII coat protein [136]. The major coat protein pVIII is present in 3000 copies and has been used

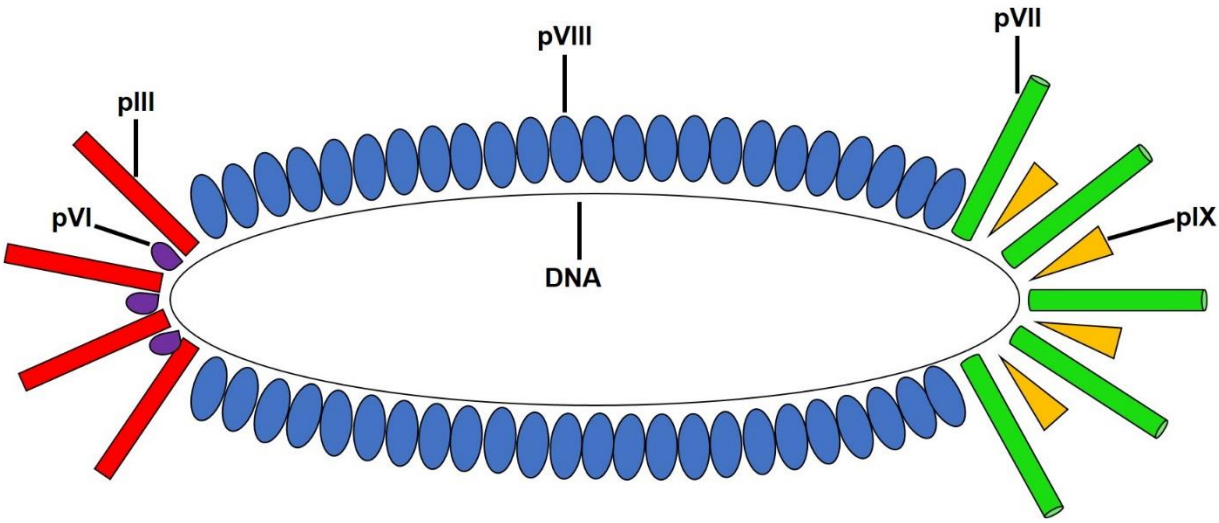

Figure 8. The structure of M13 bacteriophage. The M13 bacteriophage is a virus that infects *E. coli*. Single-stranded DNA is encapsulated by the capsid proteins pIII, pVI, pVII, pVIII, and pIX. Not drawn to scale.

Display technology	Advantages	Disadvantages
Bacterial display	Library size: ≥10^{11} variants [137]. Quantitative screening of selections performed using fluorescence-activated cell sorting [138, 139].	Multivalent display of proteins and peptides is the only available format [139].
mRNA display	Library size: ≥10^{12} variants [140]. Construction of library is not limited by transformation efficiency [141].	Monovalent display is the only available format.
Phage display	Library size: ≥10^{10} variants [123]. *E. coli* cells are easy to handle and manipulate [142]. Availability of monovalent and multivalent display formats [143].	Size of library is limited by the bacterial transformation efficiency [144]. Secondary libraries must be constructed separately for affinity maturation [145].
Ribosome display	Library size: ≥10^{14} variants [146]. Diversity of library is not limited by the transformation efficiency of bacterial cells [144]. Random mutations can be introduced after each step of selection [144].	Monovalent display is the only available format.
Yeast display	Quantitative screening of selections performed using fluorescence-activated cell sorting [142]. Use of an eukaryotic expression system [124]. Ability to incorporate post-translational modification to recombinant protein [124].	Library size is limited by the transformation efficiency of yeast [124]. Library size: ≥10^{9} variants [124, 147].

Table II. Comparison of different display technologies.

for fusion of short (6-7 amino acids) [148, 149] peptides, but is usually left unmodified to serve as an epitope for antibody detection to increase the signal [123].

Phage display affinity selection has been used to select for both recombinant antibody and non-antibody scaffold proteins [113, 150]. This technique has specifically been applied to screen for reagents using phosphorylated peptides from targets of interest. To select for phosphospecific clones using phage display, a biotinylated phosphopeptide target is captured by streptavidin and immobilized on a surface. A phage library of variants (10^8-10^{10} diversity) is incubated with the target peptide to allow for variants to bind the target. A series of washes is performed to remove non-binding variants or those with weak affinity. The remaining variants are then eluted, recovered, and allowed to infect *E. coli* cells. In phagemid systems, a M13KO7 helper phage is then used to infect the cells containing the phagemid from the previous day's screen and amplified. The cycle is repeated with each round of selection using stronger selection pressures (e.g. a decrease in target quantity).

Phagemid systems use a phagemid which is a vector that contains properties of both a bacteriophage and plasmid. Phagemids contain the replication origins of a plasmid (ColE1) and virus (f1) to allow single stranded replication and packing into phage particles. Phagemid genomes also contain an antibiotic resistance marker, a bacteriophage packaging sequence, a gene for a phage coat fusion protein, promoter and terminator sequences, and DNA segment for encoding the recombinant protein [151]. When using a phagemid system for phage display, an M13 helper virus is required for proper bacteriophage production as a phagemid lacks the complete genes required for phage production [152]. The phagemid system is excellent for constructing naïve libraries

[143] for four reasons: 1. The small size of the vector (5-6kb) can accommodate large foreign DNA for encoding the recombinant protein. 2. Phagemids can be efficiently transformed into *E. coli.* either through electroporation or chemical transformation. 3. The expression levels of the fusion protein can be easily manipulated [151]. 4. The recombinant protein is display in a monovalent fashion [143].

1.10 Non-antibody scaffold proteins

Scaffold proteins are good alternatives to recombinant antibodies as they can imitate antibody binding to their target. Scaffold proteins are typically small, well expressed in bacterial and other hosts, lack disulfide bonds, thermal stable, and highly soluble. Three types of scaffolds have been successfully engineered to recognize phosphoepitopes: the fibronectin type III (FN3) monobodies, designed ankyrin repeat proteins (DARPins), and the Forkhead Associated (FHA) domain.

The FN3 scaffold has been used to isolate variants that can bind a phosphopeptide from nuclear factor of kappa light polypeptide gene enhancer in B-cells inhibitor, alpha (IκBα). A library of the FN3 monobodies was mRNA displayed and affinity selected against a phosphorylated peptide target from IκBα. The resulting FN3 domain was shown to be specific for the phosphorylated peptide, had a K_d of 18 nM, and was shown to recognize endogenous IκBα by western blot and detected the products of IκB kinase *in vitro* [153]. A library of designed ankyrin repeat proteins (DARPins) was ribosome displayed and affinity selected against fully folded ERK1/2 protein that were either phosphorylated (ERK1/2-pTpY) or non-phosphorylated. The selected reagents could distinguish between the states of the kinase through ELISA. To test the functional utility

of the ERK panel of DARPins, the reagents were used in immunoprecipitation and bioluminescence resonance energy transfer experiments to showcase the level of specificity for the reagents [154] The ERK1/2-pTpY specific DARPins could be converted into biosensors and were able to detect the subcellular site of ERK1/2 phosphorylation in living cells [155].

1.11 The FHA domain as a scaffold

Alternatively, one can use a scaffold that naturally recognizes a phosphopeptide residue. For example, the FHA1 domain (Fig. 9) naturally recognizes a phosphothreonine site on its target protein, pRad9. There are four major loops are involved in the interaction between the domain and the phosphopeptide ligand (Fig. 10): 1) β3-β4, 2) β4-β5 3) β6-β7 4) β10-β11. Both the β3-β4 and β6-β7 loops create binding pockets for the phosphopeptide. The β4-β5 and β10-β11 loops are involved in interacting with the phosphopeptide ligand. The FHAs can distinguish between pThr and pSer residues due to the interaction of the β4-β5 and β6-β7 loops to create a structural pocket for the γ-methyl of the pThr to fill in. Each FHA domain has its own way of interacting with the ligand. For the sake of clarity, this portion of the text will focus on the structural characteristics of the FHA1 domain. In the FHA1, residues in the β4-β5 and β10-β11 create interactions with the pThr and the pT+3 residue, respectively. Histidine at position 88 (His88), from the β4-β5 loop, interacts with Ser85 (β4-β5), Thr106 (β6-β7), Ile104 (β6-β7), and Gly108 (β6-β7) create a pocket for the γ-methyl group of the phosphothreonine in the peptide ligand [156].

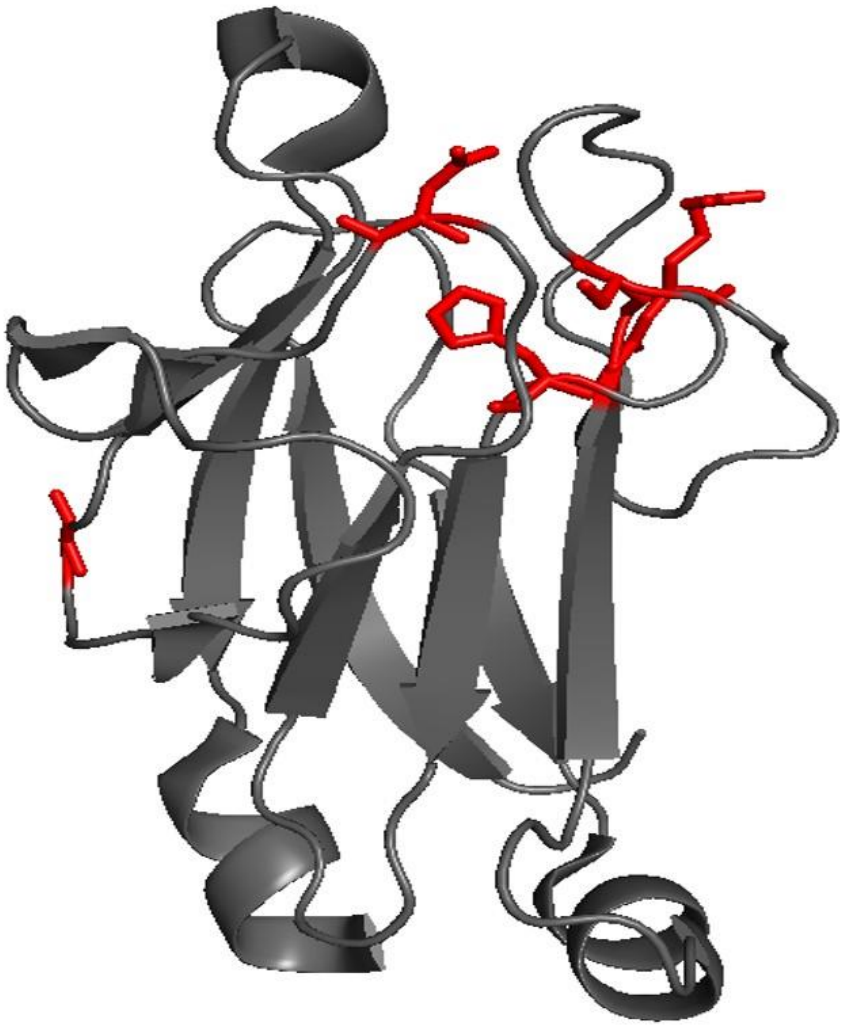

Figure 9. Three-dimensional structure of the FHA1 domain of Rad53 from Saccharomyces cerevisiae. The FHA1 domain is represented in gray as a cartoon (beta sheets, loops, alpha helices). Structurally conserved residues are colored red and shown as sticks.

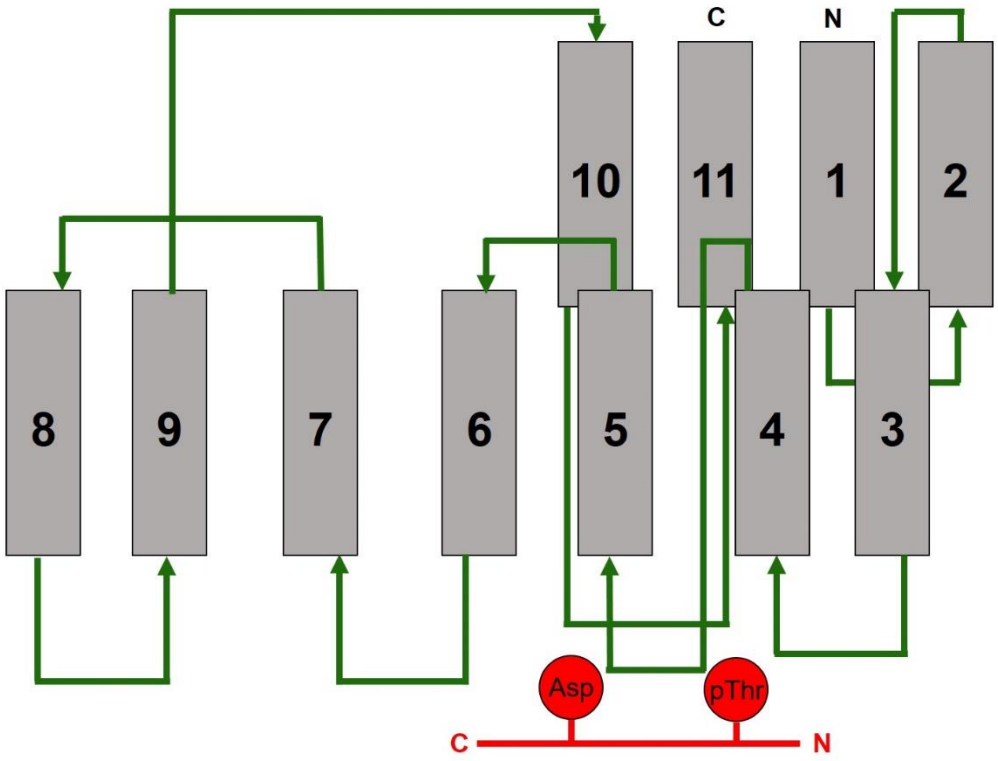

Figure 10. Topology of the FHA1 domain. The FHA1 is comprised of 11 β-sheets (gray) connected by loops (green). All β-sheets are numbered. The pRad9 ligand is represented in red. β-sheets and loop lengths are not drawn to scale.

The specificity of the FHA1 was altered for use as a scaffold in phage display experiments [157]. Through directed evolution, a phage library of the thermal stable FHA1 variants was generated by randomizing residues at positions 82-84 and 133-139 in the β4-β5 and β10-β11 loops, respectively [157, 158]. The phage library was used in phage display selection using either mono-phosphorylated or dual-phosphorylated phosphothreonine-containing peptide targets [157, 159, 160]. Reagents were successfully isolated against 14 out of 17 targets, reflecting an 82% rate of success. All isolated reagents were shown to be both phosphothreonine-dependent and specific, as compared to commercial IgGs raised against the same phosphopeptide [159].

Like all technologies, the use of scaffold proteins to monitor protein phosphorylation have advantages and disadvantages. As a recombinant protein, the DNA of the scaffold is known, and mutations can be introduced to enhance binding strength or specificity. Additionally, point mutations of the scaffold can be created that destroy binding; such variants make excellent negative controls in experiments. Finally, the recombinant scaffolds can be expressed inside cells where they can interfere the phosphorylated form of the target. One major drawback is that there is no guarantee that an isolated binder will be able to the phosphorylated target is in its native, folded state. However, one can screen many clones and identify those that recognize the target in the native state.

1.12 Thesis goals and organization

The overall goals of this thesis were to 1) utilize phage library displaying billions of FHA domain variants as a source of recombinant affinity reagents to phosphothreonine-containing peptides of interest, and 2) investigate the molecular recognition properties of

a set of binders to the pThr38 sequence of the human transcription factor and oncogene, cellular Myc (c-Myc).

In Chapter 2, I characterized three previously isolated FHA domains that were selected against either mono-phosphorylated or dual-phosphorylated peptide targets. I demonstrated that the engineered FHA domains are all pThr-specific and dependent. Furthermore, I established that these reagents are comparable in specificity to commercially available antibodies that were raised against the some phosphopeptides. The content of this chapter has been published in *New Biotechnology* (doi: 10.1016/j.nbt.2015.12.006).

In Chapter 3, I screened the phage-display FHA domain library to isolate phosphothreonine-binding domains (pTBDs) that bind a pThr-containing peptide from human transcription factor c-Myc. I solved the crystal structure of the Myc-recognizing-pTBD (Myc-pTBD) and compared the structure and binding properties of the engineered domain to the FHA1 domain. The molecular determinants of specificity were investigated through biochemical and biophysical analyses for the Myc-pTBD. The residue at the pT+3 position on the phosphopeptide ligand was a major contributor of specificity. A panel of phosphopeptides from c-Myc was used to test the pTBD's specificity against three commercially available antibodies. The content of this chapter has been published in *New Biotechnology* (doi: 10.1016/j.nbt.2018.05.001).

In Chapter 4, I used two designs to generate homodimers of three pTBDs: the Myc-pTBD, Extracellular-regulating kinase1/2-recognizing pTBD (ERK-pTBD), and Ca^{2+}/calmodulin kinase II-recognizing pTBD (CaMKII-pTBD). I measured and observed a

10-100x-fold improvement in apparent affinities of all homodimers. I then chose the Myc-pTBD homodimer to probe for phosphorylated Myc in whole cell lysates by western blot.

In the final chapter, I summarize the work described in the previous chapters and discuss the potential of pTBDs as tools for studying signaling events. I propose future experiments and suggest several approaches for improving the pTBD scaffold.

1.13 References

1. Johnson, L.N., *The regulation of protein phosphorylation.* Biochem Soc Trans, 2009. **37**(Pt 4): p. 627-41.

2. Manning, G., et al., *The protein kinase complement of the human genome.* Science, 2002. **298**(5600): p. 1912-34.

3. Sacco, F., et al., *The human phosphatase interactome: An intricate family portrait.* FEBS Lett, 2012. **586**(17): p. 2732-9.

4. Cohen, P., *The regulation of protein function by multisite phosphorylation--a 25 year update.* Trends Biochem Sci, 2000. **25**(12): p. 596-601.

5. Chalhoub, N. and S.J. Baker, *PTEN and the PI3-kinase pathway in cancer.* Annu Rev Pathol, 2009. **4**: p. 127-50.

6. Plotnikov, A., et al., *The MAPK cascades: signaling components, nuclear roles and mechanisms of nuclear translocation.* Biochim Biophys Acta, 2011. **1813**(9): p. 1619-33.

7. Escamilla-Powers, J.R. and R.C. Sears, *A conserved pathway that controls c-Myc protein stability through opposing phosphorylation events occurs in yeast.* J Biol Chem, 2007. **282**(8): p. 5432-42.

8. Lin, J., et al., *Understanding protein phosphorylation on a systems level.* Brief Funct Genomics, 2010. **9**(1): p. 32-42.

9. Ubersax, J.A. and J.E. Ferrell, Jr., *Mechanisms of specificity in protein phosphorylation.* Nat Rev Mol Cell Biol, 2007. **8**(7): p. 530-41.

10. Endicott, J.A., M.E. Noble, and L.N. Johnson, *The structural basis for control of eukaryotic protein kinases.* Annu Rev Biochem, 2012. **81**: p. 587-613.

11. Mann, M., et al., *Analysis of protein phosphorylation using mass spectrometry: deciphering the phosphoproteome.* Trends Biotechnol, 2002. **20**(6): p. 261-8.

12. Fleuren, E.D., et al., *The kinome 'at large' in cancer.* Nat Rev Cancer, 2016. **16**(2): p. 83-98.

13. Stebbing, J., et al., *The regulatory roles of phosphatases in cancer.* Oncogene, 2014. **33**(8): p. 939-53.

14. Cowling, V.H., S.A. Turner, and M.D. Cole, *Burkitt's lymphoma-associated c-Myc mutations converge on a dramatically altered target gene response and implicate Nol5a/Nop56 in oncogenesis.* Oncogene, 2014. **33**(27): p. 3519-27.

15. Cohen, P., *The role of protein phosphorylation in human health and disease. The Sir Hans Krebs Medal Lecture.* Eur J Biochem, 2001. **268**(19): p. 5001-10.

16. Nita-Lazar, A., H. Saito-Benz, and F.M. White, *Quantitative phosphoproteomics by mass spectrometry: past, present, and future.* Proteomics, 2008. **8**(21): p. 4433-43.

17. Yaffe, M.B., *Phosphotyrosine-binding domains in signal transduction.* Nature Reviews Molecular Cell Biology, 2002. **3**(3): p. 177-186.

18. Yaffe, M.B. and A.E. Elia, *Phosphoserine/threonine-binding domains.* Curr Opin Cell Biol, 2001. **13**(2): p. 131-8.

19. Rodriguez, M., et al., *Phosphopeptide binding specificities of BRCA1 COOH-terminal (BRCT) domains.* J Biol Chem, 2003. **278**(52): p. 52914-8.

20. Yu, X., et al., *The BRCT domain is a phospho-protein binding domain.* Science, 2003. **302**(5645): p. 639-42.

21. Morrison, D.K., *The 14-3-3 proteins: integrators of diverse signaling cues that impact cell fate and cancer development.* Trends Cell Biol, 2009. **19**(1): p. 16-23.

22. Fu, H., R.R. Subramanian, and S.C. Masters, *14-3-3 proteins: structure, function, and regulation.* Annu Rev Pharmacol Toxicol, 2000. **40**: p. 617-47.

23. Orlicky, S., et al., *Structural basis for phosphodependent substrate selection and orientation by the SCFCdc4 ubiquitin ligase.* Cell, 2003. **112**(2): p. 243-56.

24. Hofmann, K. and P. Bucher, *The FHA domain: a putative nuclear signalling domain found in protein kinases and transcription factors.* Trends Biochem Sci, 1995. **20**(9): p. 347-9.

25. Pallen, M., R. Chaudhuri, and A. Khan, *Bacterial FHA domains: neglected players in the phospho-threonine signalling game?* Trends Microbiol, 2002. **10**(12): p. 556-63.

26. Durocher, D., et al., *The FHA domain is a modular phosphopeptide recognition motif.* Mol Cell, 1999. **4**(3): p. 387-94.

27. Ho, Y., et al., *Systematic identification of protein complexes in Saccharomyces cerevisiae by mass spectrometry.* Nature, 2002. **415**(6868): p. 180-3.

28. Li, J., et al., *Structural and functional versatility of the FHA domain in DNA-damage signaling by the tumor suppressor kinase Chk2.* Mol Cell, 2002. **9**(5): p. 1045-54.

29. Liang, X. and S.R. Van Doren, *Mechanistic insights into phosphoprotein-binding FHA domains.* Acc Chem Res, 2008. **41**(8): p. 991-9.

30. Yaffe, M.B. and S.J. Smerdon, *PhosphoSerine/threonine binding domains: you can't pSERious?* Structure, 2001. **9**(3): p. R33-8.

31. Yaffe, M.B. and S.J. Smerdon, *The use of in vitro peptide-library screens in the analysis of phosphoserine/threonine-binding domain structure and function.* Annu Rev Biophys Biomol Struct, 2004. **33**: p. 225-44.

32. Durocher, D. and S.P. Jackson, *The FHA domain.* FEBS Lett, 2002. **513**(1): p. 58-66.

33. Mahajan, A., et al., *Structure and function of the phosphothreonine-specific FHA domain.* Sci Signal, 2008. **1**(51): p. re12.

34. Reynolds, D., et al., *Recruitment of Thr 319-phosphorylated Ndd1p to the FHA domain of Fkh2p requires Clb kinase activity: a mechanism for CLB cluster gene activation.* Genes Dev, 2003. **17**(14): p. 1789-802.

35. Featherstone, C. and S.P. Jackson, *DNA repair: the Nijmegen breakage syndrome protein.* Curr Biol, 1998. **8**(17): p. R622-5.

36. Sun, Z., et al., *Rad53 FHA domain associated with phosphorylated Rad9 in the DNA damage checkpoint.* Science, 1998. **281**(5374): p. 272-4.

37. Huen, M.S., et al., *RNF8 transduces the DNA-damage signal via histone ubiquitylation and checkpoint protein assembly.* Cell, 2007. **131**(5): p. 901-14.

38. Durocher, D., et al., *The molecular basis of FHA domain:phosphopeptide binding specificity and implications for phospho-dependent signaling mechanisms.* Mol Cell, 2000. **6**(5): p. 1169-82.

39. Shieh, S.Y., et al., *The human homologs of checkpoint kinases Chk1 and Cds1 (Chk2) phosphorylate p53 at multiple DNA damage-inducible sites.* Genes Dev, 2000. **14**(3): p. 289-300.

40. Hirao, A., et al., *DNA damage-induced activation of p53 by the checkpoint kinase Chk2.* Science, 2000. **287**(5459): p. 1824-7.

41. Varon, R., et al., *Nibrin, a novel DNA double-strand break repair protein, is mutated in Nijmegen breakage syndrome.* Cell, 1998. **93**(3): p. 467-76.

42. Carney, J.P., et al., *The hMre11/hRad50 protein complex and Nijmegen breakage syndrome: linkage of double-strand break repair to the cellular DNA damage response.* Cell, 1998. **93**(3): p. 477-86.

43. Bloom, G.S., *The UNC-104/KIF1 family of kinesins.* Curr Opin Cell Biol, 2001. **13**(1): p. 36-40.

44. Li, J., et al., *The FHA domain mediates phosphoprotein interactions.* J Cell Sci, 2000. **113 Pt 23**: p. 4143-9.

45. Li, H., et al., *Structure of human Ki67 FHA domain and its binding to a phosphoprotein fragment from hNIFK reveal unique recognition sites and new views to the structural basis of FHA domain functions.* J Mol Biol, 2004. **335**(1): p. 371-81.

46. Lee, H., et al., *Diphosphothreonine-specific interaction between an SQ/TQ cluster and an FHA domain in the Rad53-Dun1 kinase cascade.* Mol Cell, 2008. **30**(6): p. 767-78.

47. Bernstein, N.K., et al., *The molecular architecture of the mammalian DNA repair enzyme, polynucleotide kinase.* Mol Cell, 2005. **17**(5): p. 657-70.

48. Weng, J.H., et al., *Uncovering the Mechanism of Forkhead-Associated Domain-Mediated TIFA Oligomerization That Plays a Central Role in Immune Responses.* Biochemistry, 2015. **54**(40): p. 6219-29.

49. Koch, C.A., et al., *Xrcc4 physically links DNA end processing by polynucleotide kinase to DNA ligation by DNA ligase IV.* EMBO J, 2004. **23**(19): p. 3874-85.

50. Takagi, M., et al., *A novel nucleolar protein, NIFK, interacts with the forkhead associated domain of Ki-67 antigen in mitosis.* J Biol Chem, 2001. **276**(27): p. 25386-91.

51. Sueishi, M., M. Takagi, and Y. Yoneda, *The forkhead-associated domain of Ki-67 antigen interacts with the novel kinesin-like protein Hklp2.* J Biol Chem, 2000. **275**(37): p. 28888-92.

52. Zhou, B.B. and S.J. Elledge, *The DNA damage response: putting checkpoints in perspective.* Nature, 2000. **408**(6811): p. 433-9.

53. Abreu, C.M., et al., *Site-specific phosphorylation of the DNA damage response mediator rad9 by cyclin-dependent kinases regulates activation of checkpoint kinase 1.* PLoS Genet, 2013. **9**(4): p. e1003310.

54. Chen, S.H., M.B. Smolka, and H. Zhou, *Mechanism of Dun1 activation by Rad53 phosphorylation in Saccharomyces cerevisiae.* J Biol Chem, 2007. **282**(2): p. 986-95.

55. Emili, A., *MEC1-dependent phosphorylation of Rad9p in response to DNA damage.* Mol Cell, 1998. **2**(2): p. 183-9.

56. Vialard, J.E., et al., *The budding yeast Rad9 checkpoint protein is subjected to Mec1/Tel1-dependent hyperphosphorylation and interacts with Rad53 after DNA damage.* EMBO J, 1998. **17**(19): p. 5679-88.

57. Stone, J.M., et al., *Interaction of a protein phosphatase with an Arabidopsis serine-threonine receptor kinase.* Science, 1994. **266**(5186): p. 793-5.

58. Liao, H., et al., *Structure of the FHA1 domain of yeast Rad53 and identification of binding sites for both FHA1 and its target protein Rad9.* J Mol Biol, 2000. **304**(5): p. 941-51.

59. Olsen, J.V., et al., *Global, in vivo, and site-specific phosphorylation dynamics in signaling networks.* Cell, 2006. **127**(3): p. 635-48.

60. Dephoure, N., et al., *A quantitative atlas of mitotic phosphorylation.* Proc Natl Acad Sci U S A, 2008. **105**(31): p. 10762-7.

61. Mayya, V., et al., *Quantitative phosphoproteomic analysis of T cell receptor signaling reveals system-wide modulation of protein-protein interactions.* Sci Signal, 2009. **2**(84): p. ra46.

62. Johnson, S.A. and T. Hunter, *Kinomics: methods for deciphering the kinome.* Nat Methods, 2005. **2**(1): p. 17-25.

63. Manning, B.D. and L.C. Cantley, *Hitting the target: emerging technologies in the search for kinase substrates.* Sci STKE, 2002. **2002**(162): p. pe49.

64. Smolka, M.B., et al., *Proteome-wide identification of in vivo targets of DNA damage checkpoint kinases.* Proc Natl Acad Sci U S A, 2007. **104**(25): p. 10364-9.

65. Loyet, K.M., J.T. Stults, and D. Arnott, *Mass spectrometric contributions to the practice of phosphorylation site mapping through 2003: a literature review.* Mol Cell Proteomics, 2005. **4**(3): p. 235-45.

66. Dephoure, N., et al., *Mapping and analysis of phosphorylation sites: a quick guide for cell biologists.* Mol Biol Cell, 2013. **24**(5): p. 535-42.

67. Urban, P.L., *Quantitative mass spectrometry: an overview.* Philos Trans A Math Phys Eng Sci, 2016. **374**(2079).

68. Gafken, P.R. and P.D. Lampe, *Methodologies for characterizing phosphoproteins by mass spectrometry.* Cell Commun Adhes, 2006. **13**(5-6): p. 249-62.

69. Beausoleil, S.A., et al., *A probability-based approach for high-throughput protein phosphorylation analysis and site localization.* Nat Biotechnol, 2006. **24**(10): p. 1285-92.

70. Savitski, M.M., et al., *Confident phosphorylation site localization using the Mascot Delta Score.* Mol Cell Proteomics, 2011. **10**(2): p. M110 003830.

71. Baker, P.R., J.C. Trinidad, and R.J. Chalkley, *Modification site localization scoring integrated into a search engine.* Mol Cell Proteomics, 2011. **10**(7): p. M111 008078.

72. Montoya, A., et al., *Characterization of a TiO(2) enrichment method for label-free quantitative phosphoproteomics.* Methods, 2011. **54**(4): p. 370-8.

73. Lehr, S., et al., *Identification of major tyrosine phosphorylation sites in the human insulin receptor substrate Gab-1 by insulin receptor kinase in vitro.* Biochemistry, 2000. **39**(35): p. 10898-907.

74. Kange, R., et al., *Comparison of different IMAC techniques used for enrichment of phosphorylated peptides.* J Biomol Tech, 2005. **16**(2): p. 91-103.

75. Nika, H., et al., *Optimization of the beta-elimination/michael addition chemistry on reversed-phase supports for mass spectrometry analysis of O-linked protein modifications.* J Biomol Tech, 2013. **24**(3): p. 132-53.

76. Sawasdikosol, S., *Detecting tyrosine-phosphorylated proteins by Western blot analysis.* Curr Protoc Immunol, 2010. **Chapter 11**: p. Unit 11 3 1-11.

77. Vincent, E.E., et al., *Akt phosphorylation on Thr308 but not on Ser473 correlates with Akt protein kinase activity in human non-small cell lung cancer.* Br J Cancer, 2011. **104**(11): p. 1755-61.

78. Carey, K.D., et al., *The requirement of specific membrane domains for Raf-1 phosphorylation and activation.* J Biol Chem, 2003. **278**(5): p. 3185-96.

79. Migues, P.V., et al., *Phosphorylation of CaMKII at Thr253 occurs in vivo and enhances binding to isolated postsynaptic densities.* J Neurochem, 2006. **98**(1): p. 289-99.

80. Shen, J.X., et al., *Muscarinic receptors stimulate AC2 by novel phosphorylation sites, whereas Gbetagamma subunits exert opposing effects depending on the G-protein source.* Biochem J, 2012. **447**(3): p. 393-405.

81. Molgaard, S., et al., *Detection of phosphorylated Akt and MAPK in cell culture assays.* MethodsX, 2016. **3**: p. 386-98.

82. Bradbury, A.R., et al., *Beyond natural antibodies: the power of in vitro display technologies.* Nat Biotechnol, 2011. **29**(3): p. 245-54.

83. Lipman, N.S., et al., *Monoclonal versus polyclonal antibodies: distinguishing characteristics, applications, and information resources.* ILAR J, 2005. **46**(3): p. 258-68.

84. Lozano, F., et al., *Low cytoplasmic mRNA levels of immunoglobulin kappa light chain genes containing nonsense codons correlate with inefficient splicing.* EMBO J, 1994. **13**(19): p. 4617-22.

85. Baumann, B., M.J. Potash, and G. Kohler, *Consequences of frameshift mutations at the immunoglobulin heavy chain locus of the mouse.* EMBO J, 1985. **4**(2): p. 351-9.

86. Sroubek, J., et al., *The use of Bcl-2 over-expression to stabilize hybridomas specific to the HERG potassium channel.* J Immunol Methods, 2012. **375**(1-2): p. 215-22.

87. Grimsey, N.L., et al., *Specific detection of CB1 receptors; cannabinoid CB1 receptor antibodies are not all created equal!* J Neurosci Methods, 2008. **171**(1): p. 78-86.

88. Bohmer, T., N. Pfeiffer, and A. Gericke, *Three commercial antibodies against alpha1-adrenergic receptor subtypes lack specificity in paraffin-embedded sections of murine tissues.* Naunyn Schmiedebergs Arch Pharmacol, 2014. **387**(7): p. 703-6.

89. Pradidarcheep, W., et al., *Lack of specificity of commercially available antisera against muscarinergic and adrenergic receptors.* Naunyn Schmiedebergs Arch Pharmacol, 2009. **379**(4): p. 397-402.

90. Jensen, B.C., P.M. Swigart, and P.C. Simpson, *Ten commercial antibodies for alpha-1-adrenergic receptor subtypes are nonspecific.* Naunyn Schmiedebergs Arch Pharmacol, 2009. **379**(4): p. 409-12.

91. Couchman, J.R., *Commercial antibodies: the good, bad, and really ugly.* J Histochem Cytochem, 2009. **57**(1): p. 7-8.

92. Kinoshita, E., et al., *Phosphate-binding tag, a new tool to visualize phosphorylated proteins.* Mol Cell Proteomics, 2006. **5**(4): p. 749-57.

93. Kinoshita, E., et al., *Recognition of phosphate monoester dianion by an alkoxide-bridged dinuclear zinc(II) complex.* Dalton Trans, 2004(8): p. 1189-93.

94. Tanaka, T., et al., *Quantitative analysis of lysophosphatidic acid by time-of-flight mass spectrometry using a phosphate-capture molecule.* J Lipid Res, 2004. **45**(11): p. 2145-50.

95. Takeda, H., et al., *Matrix-assisted laser desorption/ionization time-of-flight mass spectrometry of phosphorylated compounds using a novel phosphate capture molecule.* Rapid Commun Mass Spectrom, 2003. **17**(18): p. 2075-81.

96. Inamori, K., et al., *Detection and quantification of on-chip phosphorylated peptides by surface plasmon resonance imaging techniques using a phosphate capture molecule.* Anal Chem, 2005. **77**(13): p. 3979-85.

97. Kinoshita, E. and E. Kinoshita-Kikuta, *Improved Phos-tag SDS-PAGE under neutral pH conditions for advanced protein phosphorylation profiling.* Proteomics, 2011. **11**(2): p. 319-23.

98. Kinoshita, E., et al., *Specific glutamic acid residues in targeted proteins induce exaggerated retardations in Phos-tag SDS-PAGE migration.* Electrophoresis, 2017. **38**(8): p. 1139-1146.

99. Kinoshita, E., E. Kinoshita-Kikuta, and T. Koike, *Phos-tag SDS-PAGE systems for phosphorylation profiling of proteins with a wide range of molecular masses under neutral pH conditions.* Proteomics, 2012. **12**(2): p. 192-202.

100. Kinoshita, E., E. Kinoshita-Kikuta, and T. Koike, *Zn(II)-Phos-Tag SDS-PAGE for Separation and Detection of a DNA Damage-Related Signaling Large Phosphoprotein.* Methods Mol Biol, 2017. **1599**: p. 113-126.

101. Kinoshita, E., E. Kinoshita-Kikuta, and T. Koike, *Separation and detection of large phosphoproteins using Phos-tag SDS-PAGE.* Nat Protoc, 2009. **4**(10): p. 1513-21.

102. Kinoshita, E., et al., *A Phos-tag SDS-PAGE method that effectively uses phosphoproteomic data for profiling the phosphorylation dynamics of MEK1.* Proteomics, 2016. **16**(13): p. 1825-36.

103. Takiyama, K., et al., *A Phos-tag-based fluorescence resonance energy transfer system for the analysis of the dephosphorylation of phosphopeptides.* Anal Biochem, 2009. **388**(2): p. 235-41.

104. Kinoshita, E., et al., *Novel immobilized zinc(II) affinity chromatography for phosphopeptides and phosphorylated proteins.* J Sep Sci, 2005. **28**(2): p. 155-62.

105. Kinoshita-Kikuta, E., et al., *Enrichment of phosphorylated proteins from cell lysate using a novel phosphate-affinity chromatography at physiological pH.* Proteomics, 2006. **6**(19): p. 5088-95.

106. Iliuk, A.B. and W.A. Tao, *Universal non-antibody detection of protein phosphorylation using pIMAGO.* Curr Protoc Chem Biol, 2015. **7**(1): p. 17-25.

107. Iliuk, A., et al., *Phosphorylation assay based on multifunctionalized soluble nanopolymer.* Anal Chem, 2011. **83**(7): p. 2767-74.

108. Pan, L., et al., *Multiplexed quantitation of protein expression and phosphorylation based on functionalized soluble nanopolymers.* J Am Chem Soc, 2012. **134**(44): p. 18201-4.

109. Pan, L., et al., *Sensitive measurement of total protein phosphorylation level in complex protein samples.* Analyst, 2015. **140**(10): p. 3390-6.

110. Bender, K.W., et al., *Autophosphorylation-based Calcium (Ca2+) Sensitivity Priming and Ca2+/Calmodulin Inhibition of Arabidopsis thaliana Ca2+-dependent Protein Kinase 28 (CPK28).* J Biol Chem, 2017. **292**(10): p. 3988-4002.

111. Ni, W., et al., *PPKs mediate direct signal transfer from phytochrome photoreceptors to transcription factor PIF3.* Nat Commun, 2017. **8**: p. 15236.

112. Hanes, J. and A. Pluckthun, *In vitro selection and evolution of functional proteins by using ribosome display.* Proc Natl Acad Sci U S A, 1997. **94**(10): p. 4937-42.

113. Kierny, M.R., T.D. Cunningham, and B.K. Kay, *Detection of biomarkers using recombinant antibodies coupled to nanostructured platforms.* Nano Rev, 2012. **3**.

114. Helma, J., et al., *Nanobodies and recombinant binders in cell biology.* J Cell Biol, 2015. **209**(5): p. 633-44.

115. Groff, K., J. Brown, and A.J. Clippinger, *Modern affinity reagents: Recombinant antibodies and aptamers.* Biotechnol Adv, 2015. **33**(8): p. 1787-98.

116. Kierny, M.R., et al., *Generating Recombinant Antibodies against Putative Biomarkers of Retinal Injury.* PLoS One, 2015. **10**(4): p. e0124492.

117. Huang, R., et al., *Directed Evolution of a Highly Specific FN3 Monobody to the SH3 Domain of Human Lyn Tyrosine Kinase.* PLoS One, 2016. **11**(1): p. e0145872.

118. Shih, H.H., et al., *An ultra-specific avian antibody to phosphorylated tau protein reveals a unique mechanism for phosphoepitope recognition.* J Biol Chem, 2012. **287**(53): p. 44425-34.

119. Vielemeyer, O., et al., *Direct selection of monoclonal phosphospecific antibodies without prior phosphoamino acid mapping.* J Biol Chem, 2009. **284**(31): p. 20791-5.

120. Koerber, J.T., et al., *Nature-inspired design of motif-specific antibody scaffolds.* Nat Biotechnol, 2013. **31**(10): p. 916-21.

121. Sivasubramanian, A., et al., *Toward high-resolution homology modeling of antibody Fv regions and application to antibody-antigen docking.* Proteins, 2009. **74**(2): p. 497-514.

122. Weitzner, B.D., et al., *Blind prediction performance of RosettaAntibody 3.0: grafting, relaxation, kinematic loop modeling, and full CDR optimization.* Proteins, 2014. **82**(8): p. 1611-23.

123. Bazan, J., I. Calkosinski, and A. Gamian, *Phage display--a powerful technique for immunotherapy: 1. Introduction and potential of therapeutic applications.* Hum Vaccin Immunother, 2012. **8**(12): p. 1817-28.

124. Cherf, G.M. and J.R. Cochran, *Applications of Yeast Surface Display for Protein Engineering.* Methods Mol Biol, 2015. **1319**: p. 155-75.

125. Pluckthun, A., *Ribosome display: a perspective.* Methods Mol Biol, 2012. **805**: p. 3-28.

126. Wang, H. and R. Liu, *Advantages of mRNA display selections over other selection techniques for investigation of protein-protein interactions.* Expert Rev Proteomics, 2011. **8**(3): p. 335-46.

127. Stahl, S. and M. Uhlen, *Bacterial surface display: trends and progress.* Trends Biotechnol, 1997. **15**(5): p. 185-92.

128. He, Y., et al., *Epitope mapping by random peptide phage display reveals essential residues for vaccinia extracellular enveloped virion spread.* Virol J, 2012. **9**: p. 217.

129. Horisawa, K., et al., *In vitro selection of Jun-associated proteins using mRNA display.* Nucleic Acids Res, 2004. **32**(21): p. e169.

130. Rothe, A., R.J. Hosse, and B.E. Power, *In vitro display technologies reveal novel biopharmaceutics.* FASEB J, 2006. **20**(10): p. 1599-610.

131. Smith, G.P., *Surface presentation of protein epitopes using bacteriophage expression systems.* Curr Opin Biotechnol, 1991. **2**(5): p. 668-73.

132. McCafferty, J., et al., *Phage antibodies: filamentous phage displaying antibody variable domains.* Nature, 1990. **348**(6301): p. 552-4.

133. Smith, G.P., *Filamentous fusion phage: novel expression vectors that display cloned antigens on the virion surface.* Science, 1985. **228**(4705): p. 1315-7.

134. Winter, G., et al., *Making antibodies by phage display technology.* Annu Rev Immunol, 1994. **12**: p. 433-55.

135. Kay, B.K., *Mapping protein-protein interactions with combinatorial peptides.* Comp Funct Genomics, 2001. **2**(5): p. 304-6.

136. Cho, W., J.D. Fowler, and E.M. Furst, *Targeted binding of the M13 bacteriophage to thiamethoxam organic crystals.* Langmuir, 2012. **28**(14): p. 6013-20.

137. Bessette, P.H., J.J. Rice, and P.S. Daugherty, *Rapid isolation of high-affinity protein binding peptides using bacterial display.* Protein Eng Des Sel, 2004. **17**(10): p. 731-9.

138. Lofblom, J., *Bacterial display in combinatorial protein engineering.* Biotechnol J, 2011. **6**(9): p. 1115-29.

139. Kenrick, S.A. and P.S. Daugherty, *Bacterial display enables efficient and quantitative peptide affinity maturation.* Protein Eng Des Sel, 2010. **23**(1): p. 9-17.

140. Seelig, B., *mRNA display for the selection and evolution of enzymes from in vitro-translated protein libraries.* Nat Protoc, 2011. **6**(4): p. 540-52.

141. Wilson, D.S., A.D. Keefe, and J.W. Szostak, *The use of mRNA display to select high-affinity protein-binding peptides.* Proc Natl Acad Sci U S A, 2001. **98**(7): p. 3750-5.

142. Levin, A.M. and G.A. Weiss, *Optimizing the affinity and specificity of proteins with molecular display.* Mol Biosyst, 2006. **2**(1): p. 49-57.

143. O'Connell, D., et al., *Phage versus phagemid libraries for generation of human monoclonal antibodies.* J Mol Biol, 2002. **321**(1): p. 49-56.

144. Zahnd, C., P. Amstutz, and A. Pluckthun, *Ribosome display: selecting and evolving proteins in vitro that specifically bind to a target.* Nat Methods, 2007. **4**(3): p. 269-79.

145. Schaffitzel, C., et al., *Ribosome display: an in vitro method for selection and evolution of antibodies from libraries.* J Immunol Methods, 1999. **231**(1-2): p. 119-35.

146. Yang, L.M., et al., *Construction and analysis of high-complexity ribosome display random peptide libraries.* PLoS One, 2008. **3**(5): p. e2092.

147. Benatuil, L., et al., *An improved yeast transformation method for the generation of very large human antibody libraries.* Protein Eng Des Sel, 2010. **23**(4): p. 155-9.

148. Hess, G.T., et al., *M13 bacteriophage display framework that allows sortase-mediated modification of surface-accessible phage proteins.* Bioconjug Chem, 2012. **23**(7): p. 1478-87.

149. Fagerlund, A., A.H. Myrset, and M.A. Kulseth, *Construction and characterization of a 9-mer phage display pVIII-library with regulated peptide density.* Appl Microbiol Biotechnol, 2008. **80**(5): p. 925-36.

150. Vazquez-Lombardi, R., et al., *Challenges and opportunities for non-antibody scaffold drugs.* Drug Discov Today, 2015. **20**(10): p. 1271-83.

151. Qi, H., et al., *Phagemid vectors for phage display: properties, characteristics and construction.* J Mol Biol, 2012. **417**(3): p. 129-43.

152. Marks, J.D., et al., *Molecular evolution of proteins on filamentous phage. Mimicking the strategy of the immune system.* J Biol Chem, 1992. **267**(23): p. 16007-10.

153. Olson, C.A., et al., *mRNA display selection of a high-affinity, modification-specific phospho-IkappaBalpha-binding fibronectin.* ACS Chem Biol, 2008. **3**(8): p. 480-5.

154. Kummer, L., et al., *Structural and functional analysis of phosphorylation-specific binders of the kinase ERK from designed ankyrin repeat protein libraries.* Proc Natl Acad Sci U S A, 2012. **109**(34): p. E2248-57.

155. Kummer, L., et al., *Knowledge-based design of a biosensor to quantify localized ERK activation in living cells.* Chem Biol, 2013. **20**(6): p. 847-56.

156. Huang, Y.M. and C.E. Chang, *Mechanism of PhosphoThreonine/Serine Recognition and Specificity for Modular Domains from All-atom Molecular Dynamics.* BMC Biophys, 2011. **4**: p. 12.

157. Pershad, K., K. Wypisniak, and B.K. Kay, *Directed evolution of the forkhead-associated domain to generate anti-phosphospecific reagents by phage display.* J Mol Biol, 2012. **424**(1-2): p. 88-103.

158. Pershad, K. and B.K. Kay, *Generating thermal stable variants of protein domains through phage display.* Methods, 2013. **60**(1): p. 38-45.

159. Venegas, L.A., et al., *A comparison of phosphospecific affinity reagents reveals the utility of recombinant Forkhead-associated domains in recognizing phosphothreonine-containing peptides.* N Biotechnol, 2016. **33**(5 Pt A): p. 537-43.

160. McGinnis, J. and B.K. Kay, *Generation of recombinant affinity reagents against a two-phosphosite epitope of ATF2.* New Biotechnology Under review.

Chapter 2

A comparison of phosphospecific affinity reagents reveals the utility of recombinant Forkhead-associated domains in recognizing phosphothreonine-containing peptides

This research has been published in

Venegas, L.A., Pershad, K., Bankole O, Shah N, Kay BK. *A comparison of phosphospecific affinity reagents reveals the utility of recombinant Forkhead-associated domains in recognizing phosphothreonine-containing peptides.* N Biotechnol, 2016. **33**(5 Pt A): p. 537-43.

2 Chapter 2

2.1 Abstract

Phosphorylation is an important post-translational event that has a wide array of functional consequences. With advances in the ability of various technologies in revealing and mapping new phosphosites in proteins, it is equally important to develop affinity reagents that can monitor such posttranslational modifications in eukaryotic cells. While monoclonal and polyclonal antibodies have been shown to be useful in assessing the phosphoproteome, we have expanded our efforts to exploit the Forkhead-associated 1 (FHA1) domain as scaffold for generating recombinant affinity reagents that recognize phosphothreonine-containing peptides. A phage display library of FHA1 variants was screened by affinity selection with 15 phosphothreonine-containing peptides corresponding to various human transcription factors and kinases, including human Myc, calmodulin-dependent protein kinase II (CaMKII), and extracellular-signal regulated kinases 1 and 2 (ERK1/2). The library yielded binding variants against 10 targets (66% success rate); success was largely determined by what residue occurred at the +3 position (C-terminal) to the pThr moiety (i.e., pT+3). The FHA domains binding Myc, CaMKII, and ERK1/2 were characterized and compared against commercially available antibodies. All FHA domains were shown to be phosphorylation-dependent and phosphothreonine-specific in their binding, unlike several commercial monoclonal and polyclonal antibodies. Both the pThr and the residue at the pT+3 position were major factors in defining the specificity of the FHA domains.

2.2 Introduction

Protein phosphorylation is an important post-translational modification that principally occurs on serine (89%), threonine (10%), and tyrosine (<1%) residues [1-4]. With over 100,000 phosphosites reported to date [5], there is a tremendous need for highly sensitive and specific probes to monitor the phosphorylation of particular residues in proteins during cell growth, differentiation, and disease [6]. One such class of reagents are antibodies, which can be generated by immunizing animals with phosphopeptides; such antibodies have allowed the identification of physiologically important phosphosites, changes in phosphorylation states, and subcellular translocation of particular proteins upon phosphorylation [7-10].

While monoclonal and polyclonal antibodies have been historically invaluable to the field of eukaryotic cell signaling, drawbacks include production cost, renewability [11], and limited control over specificity, which can result in cross-reactive reagents [12-16]. One strategy to overcome these limitations is to use recombinant affinity reagents, as they eliminate the need for animals, there is more control in epitope recognition, they are sequenced and renewable reagents and they are amenable to protein engineering [17, 18]. To this extent, several engineered phosphate-binding domains, such as the Src Homology 2 (SH2) domain [19], a recombinant phosphospecific antibody fragment [20], the 10th fibronectin type III domain (10FnIII) [21], and the Forkhead-associated 1 (FHA) domain [22], have all been used successfully for generating recombinant affinity reagents to phosphopeptides.

A major advantage of the FHA domain, compared to other engineered scaffolds, is its natural ability to recognize a phosphothreonine (pThr, pT) residue in a post-translationally

modified protein [23]. Within the FHA domain, there is a pocket that interacts with the γ-methyl group and phosphate of pThr, which allows the domain to discriminate between phosphoserine (pSer) and pThr [24]. Utilizing the domain's natural ability to discriminate between pSer and pThr, the specificity of one particular FHA domain, the FHA1 domain of yeast Rad53 protein, was reengineered through phage display [22]. In this report, we demonstrate that the engineered FHA domains are exquisitely selective in binding pThr, and not pSer- or phosphotyrosine (pTyr)-containing peptides, unlike several polyclonal and monoclonal antibodies tested. Furthermore, we also show that our library is capable of producing a variant that recognizes a doubly-phosphorylated peptide. In this regard, the FHA domain offers great promise in generating highly specific pThr-binding reagents, a feat not readily achievable through traditional immunological means.

2.3 Materials and methods

Reagents

Peptides were synthesized at University of Illinois at Chicago's Research Resource Center, with >90% purity. All peptides were biotinylated at their N-terminus and amidated at their C-terminus and included lysine and tyrosine residues to increase peptide solubility and for measuring absorbance, respectively. The cognate targets for the Myc, ERK1/2, and CaMKII FHA domain affinity reagents are FELLPpTPPLSPS (Myc-pT58), HTGFLpTEpYVATRW (ERK1-pT202/pY204 + ERK2-pT185/pY187), and LKGAILpTTMLATRN (CaMKII-pT305), respectively. The following peptides were used in a pThr substitution study: FELLPpTPPLSPS (pT58), FELLPpSPPLSPS (pT58pS), FELLPpYPPLSPS (pT58pY), FELLPTPPLSPS (T58), HTGFLpTEpYVATRW (pT202), HTGFLpSEpYVATRW (pT202pS), HTGFLpYEpYVATRW (pT202pY), HTGFLTEYVATRW (T202), LKGAILpTTMLATRN (pT305), LKGAILpSTMLATRN (pT305pS), LKGAILpYTMLATRN (pT305pY), LKGAILTTMLATRN (T305). Three commercial anti-phosphopeptide antibodies were compared to the recombinant FHA domains generated in this report. Two were polyclonal antibodies (pAb), pAbαMyc (Abnova, catalog# PAB0541) and pAbαCaMKII (Thermo Scientific, catalog# PA5-35521), and one was a monoclonal antibody (mAb) mAbαERK1- pT202/pY204 + ERK2-pT185/pY187 (mAbαERK1/2) (Abcam, catalog# ab136926). As all three are rabbit antibodies, a goat anti-rabbit immunoglobulin G (IgG), conjugated to Horseradish peroxidase (HRP; Abcam, catalog# ab97051), served as the common secondary reagent.

Another secondary reagent was the anti-Flag epitope mAb, M2, which was conjugated to HRP (Sigma–Aldrich, catalog# A8592).

DNA constructs

The coding sequences for individual FHA domains were amplified from virions by the polymerase chain reaction (PCR). The double-stranded DNA product was digested with Nco I and Not I restriction endonucleases and subcloned into the pET29b expression vector. These constructs included a 3XFlag1-tag sequence (DYKDHDGDYKDHDIDYKDDDDK), followed by a His6-tag, at the C-terminus of the fusion proteins. All constructs were verified by DNA sequencing.

Protein purification

Overexpression of the constructs and their purification was carried out using standard methods [25]. Briefly, BL21DE3 cells containing the expression vector were grown at 30°C for 24 hours using the Overnight Express^{TM} Autoinduction System 1 (Novagen). Bacterial cells were lysed using a Sonic Dismembrator (Branson Model 500). The lysate was mixed with Clontech His-60 Ni Superflow resin (Clontech Laboratories), and the His6-tagged proteins eluted with 50 mM sodium phosphate, 300 mM sodium chloride, 250 mM imidazole (pH 8.0). The purity and yield, and quality of the eluted protein is determined by SDS-PAGE electrophoresis and a fluorescence thermal shift assay, respectively.

Enzyme-linked immunosorbent assays (ELISA)

ELISAs were performed using an established protocol [25], except that non-specific binding in microtiter plate wells was blocked with 1% casein in phosphate buffered saline (PBS; 137 mM NaCl, 3 mM KCl, 8 mM Na2HPO4, 1.5 mM KH2PO4). The absorbance was read at 405 nm wavelength in 10-min intervals, for a total of 40 min. All experiments were performed in triplicate and repeated at least three times to confirm reproducibility of the data.

2.4 Results and discussion

Production of FHA domains by recombinant phage display

Phage display is a powerful technique that allows for the rapid and efficient production of affinity reagents, such as antibodies [26], without the need to immunize animals [27]. To generate recombinant affinity reagents that are phosphothreonine-specific, a phage display library was constructed by randomizing residues in the β4-β5 and β10-β11 loop regions of a thermostable variant (FHA1G2) of the FHA1 domain of the yeast Rad53 protein [22, 28] (Fig. 1a). The library was incubated separately with a variety of phosphothreonine-containing peptides, which were chosen based on the physiological importance of the pThr residue in a eukaryotic signaling pathway, and included protein kinases and transcription factors. After three rounds of affinity selection, individual clones were tested by an enzyme-linked immunosorbent assay (ELISA), and unique clones were identified by DNA sequencing (Fig. 1d). With biotinylated, phosphorylated forms of the peptides as targets, we were able to produce recombinant affinity reagents in less than two weeks for 10 out of 15 peptides attempted, reflecting a 66% success rate (Table 1). Biochemical and structural studies [29] have revealed that a major determinant of specificity for FHA domains is the +3 position (C-terminal) to the pThr moiety. To date, FHA domains can be categorized into three groups based on their recognition of the pT+3 position – pTxxD, pTxx(I/L), and pTxx(A/S) – with the yeast Rad53 protein FHA1 domain falling into the first category. We also confirmed this position to be important for binding to our FHA domains. As seen in Table 1, we isolated FHA domain variants to peptides

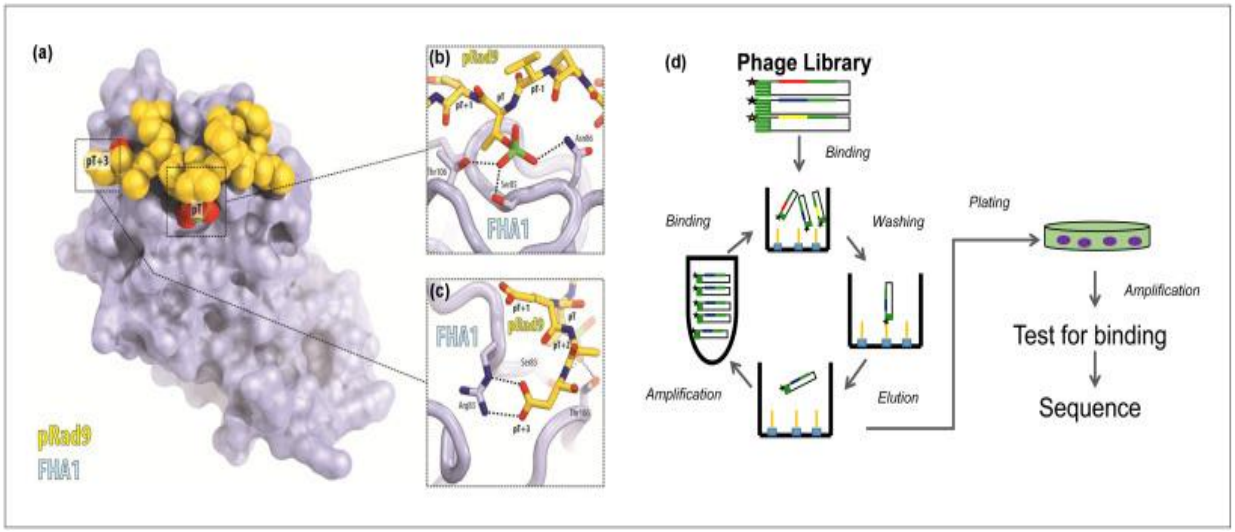

Figure 1 Generation of FHA affinity reagents via phage display. **A.** The FHA1 domain (PDB: 1G6G) interacting with its native peptide (SLEVpTEAD) from pRad9. The FHA1 domain and peptide are represented in surface view and as spheres, respectively, with the PyMOL Molecular Graphics System, Version 1.7.4 Schrödinger, LLC. **B.** A magnification of Ser85, Asn86, and Thr106 on FHA1 domain interacting with the phosphate on the pThr residue. **C.** A magnification of Arg83 on FHA1 domain interacting with Asp on pRad9 in the pT+3 position. **D.** Schematic of the process for isolating binders to phosphopeptides from a phage library displaying FHA1G2 variants. The biotinylated pThr-containing peptide is immobilized by Streptavidin. The library is incubated with the target and undergoes a series of washes. The phage is eluted and amplified to undergo two more rounds of selection. After the third round, *Escherichia coli* is infected with eluted phage and plated for amplification. Binding of individual clones is tested by phage ELISA. Clones are sequenced to check for any unique sequences.

Protein	Phosphosite	Peptide sequence	FHA reagent
Ca^{2+}/calmodulin-dependent protein kinase II	CaMKII-pT305	LKGAIL**pT**TM*L*ATRN	FHAαCaMKII
Family with Sequence Similarity 38, Member A	FAM38A-pT1811	NTRPQSD**pT**PE*I*RKYK	FHAαFAM38A
Mitogen-activated protein kinase kinase kinase kinase 4	MAP4K4-pT915	KRELYNG**pT**AD*I*TLRF	FHAαMAP4K4
Mitogen-activated protein kinase 3	MAPK3-pT197	ADPEHDH**pT**GF*L*TE	FHAαMAPK3*
Mitogen-activated protein kinase 1	MAPK1-pT185	HDHTGFL**pT**EY*V*AT	FHAαMAPK1*
Src homology 2 domain containing transforming protein 1	Shc-1-pT35	GSFVNKP**pT**RG*W*LH	FHAαShc-1
Transcription factor jun-B	JunB-pT25	EARSRDA**pT**PP*V*SP	FHAαJunB*
Transcription factor jun-D	JunD-pT245	ALKDEPQ**pT**VP*D*VP	FHAαJunD*
Transcription factor Myc	Myc-pT58	FELLP**pT**PP*L*SPS	FHAαMyc
RAF proto-oncogene serine/threonine protein kinase	Raf1-pT491	IGDFGLA**pT**VK*S*RWSG	FHAαRaf1

**Previously reported in [22]*

Table 1. A list of FHA variants isolated against phosphothreonine peptides corresponding to various human cell signaling proteins. The "p" proceeding the "T" indicates the phosphate attached to the T residue (bold). Italicized residues are in the pT+3 position, where the pT is assigned as the "0" position, and residues N-terminal and C-terminal to the pT are denoted as "−" and "+," respectively. Peptide sequence information was collected from http://www.phosphonet.ca/.

with D, L, V, P, S, and W, in the pT+3 position. We have yet to test phosphothreonine-containing peptides with A, C, Q, E, H, M, F, N, T, and Y at the pT+3 position.

The five peptides that failed to yield binders included pThr-containing phosphopeptides corresponding to nucleolin (NCL), histone H1, polo-like kinase 1 (PLK1), mitogen-activated protein kinase kinase 2 (MAP2K2), and isoform 1 of epidermal growth factor receptor precursor (EGFR). The inability to isolate FHA1 domains that bound to these particular phosphopeptides was reproducible; their sequences either contained K, R, and G at the pT+3 position. To our knowledge, an FHA domain that binds to any of these three amino acids at this position has not been observed before in nature. In the future, it will be interesting to see if an FHA domain scaffold can be devised, through directed evolution or computational design that recognizes such residues in the pT+3 position.

FHA domain variants are phosphorylation-dependent in binding.

To evaluate the specificity of the isolated FHA variants, their open reading frames (ORFs) were subcloned into an expression vector containing 3XFlag1- and His6-tags. The recombinant proteins were purified using immobilized-metal affinity chromatography (IMAC). Each of the variants produced high yields (>150 mg/L) and was shown to be >95% pure and properly folded by a fluorescence thermal shift assay. Binding of two variants, FHAαMyc (Fig. 2a) and FHAαCaMKII (Fig. 2b), to their cognate phosphorylated targets were assessed by ELISA and compared against commercially available antibodies. The ELISA is an ideal assay to test for peptide binding as it is a sensitive

assay format, as compared to western blotting where the peptides are too small to resolve properly by SDS-PAGE. All reagents showed a >1000-fold difference in signal between

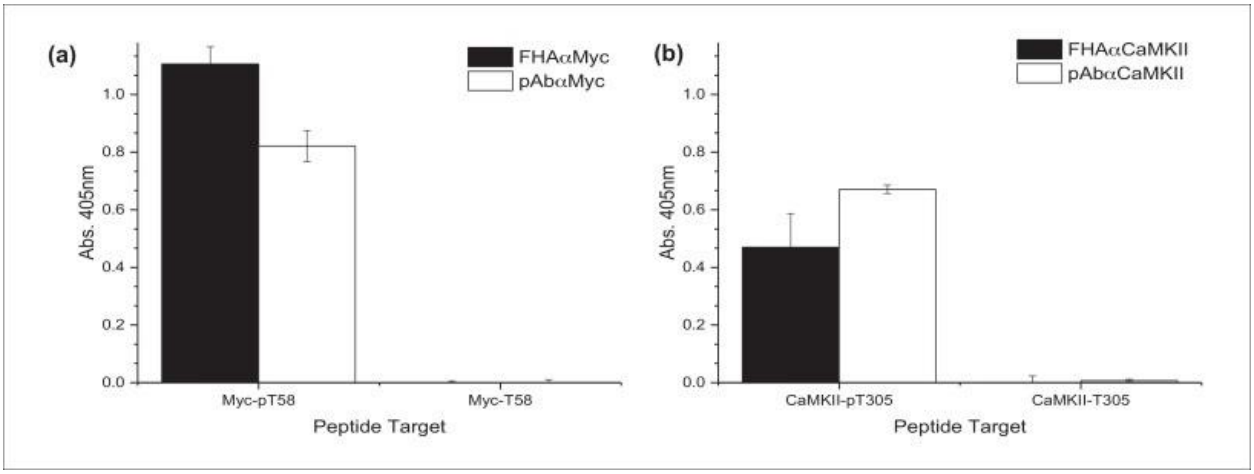

Figure 2 FHA variants are phosphorylation-dependent. A phosphorylated or unphosphorylated peptide was used as a target in an ELISA. Phosphospecific reagents were used as probe targets to test for phosphorylation dependence. The M2-HRP and goat α-rabbit-HRP antibodies were used to detect binding of the FHA variant or antibody, respectively. **A.** Binding of the FHAαMyc and pAbαMyc to the target peptide. **B.** Binding of the FHAαCaMKII and pAbαCaMKII to the target peptide.

the phosphorylated and non-phosphorylated peptide targets. These data indicate that binding of all reagents is phosphorylation-dependent.

A major challenge in generating pThr-specific affinity reagents is preventing cross-reactivity between peptides that contain pSer or pThr residues, which differ by the γ-methyl group. While the FHA1 naturally recognizes a pThr residue on pRad9 [30], it was uncertain whether the engineered variants would cross-react with pSer-containing versions of the phosphopeptides. To test for specificity, variants of the peptide sequences were synthesized with pSer or pTyr in place of pThr. The cognate target, pSer, pTyr, and unphosphorylated variant peptides were then used as targets in an ELISA (Fig. 3). Both FHAαMyc and FHAαCaMKII bound to their cognate peptide 100-fold better than phospho-peptides that carried pSer or pTyr in place of the pThr residue. These data demonstrate that the FHA domain variants are truly pThr-specific. Soluble forms of the FHA domains were then compared against commercially available monoclonal and polyclonal antibodies to the same targets. Like the FHA variants, all antibodies were shown to be phosphorylation-dependent in binding (Fig. 2). However, in evaluating the commercial antibodies for discrimination between peptides containing pSer, pThr, and pTyr, we observed that the pAbαMyc reagent binds equally well to the phosphopeptide variant containing pSer and pThr, but not pTyr (Fig. 3a). By contrast, for the polyclonal antibody against the pThr-containing phospho-peptide of CaMKII, we observed that the pAbαCaMKII reagent did not cross-react with the other phosphoresidues (Fig. 3b). Without the details of how these two polyclonal antibodies were prepared, it is difficult to speculate why one antibody is more selective than the other. Nevertheless, these data demonstrate that the FHA1 domains are more consistent in discriminating between pThr,

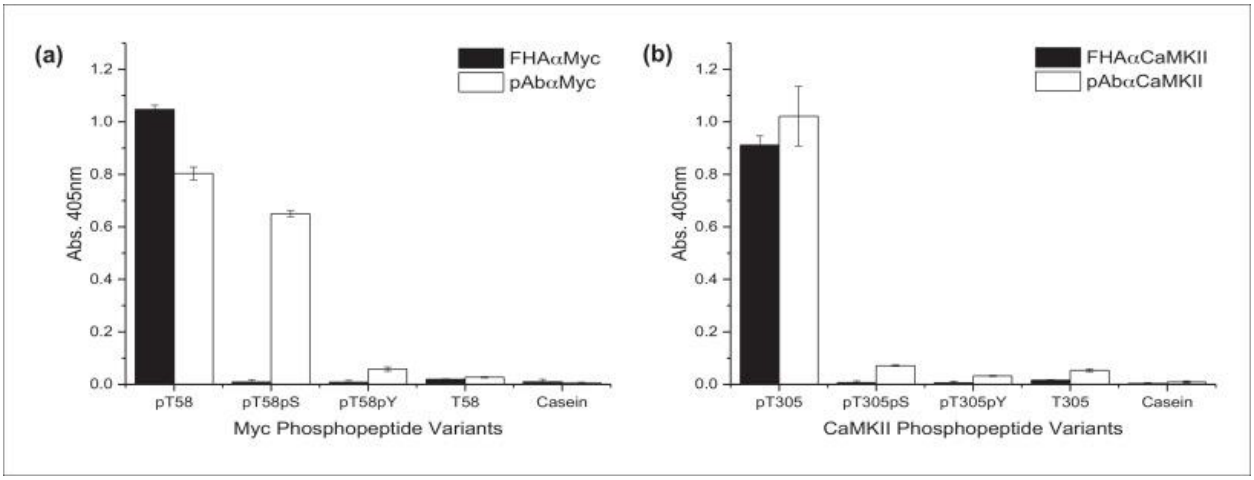

Figure 3 FHA variants are phosphothreonine-specific. The pThr for each of the cognate peptides was substituted with pSer or pTyr. These phosphopeptide variants, the cognate target, unphosphorylated target, and casein (negative control) served as targets in the ELISA. Phosphospecific reagents were used to probe targets to test for pThr-specificity. The M2-HRP and goatαrabbit-HRP were used to detect binding of the FHA1 variant or antibody, respectively. **A.** Binding of the FHAαMyc and pAbαMyc to the target peptides. **B.** Binding of the FHAαCaMKII and pAbαCaMKII to the target peptides.

pSer, and pTyr than commercial antibodies. In the FHA1 domain, the β4-β5 and β6-β7 loops create a structural pocket for the γ-methyl of the pThr to fill. More specifically, the histidine at position 88 (His88) of the β4-β5 loop interacts with Ser85 (β4-β5), Thr106 (β6-β7), Ile104 (β6-β7), and Gly108 (β6-β7) to create a pocket for the γ-methyl group as well as interacting with the phosphate (Fig. 1b) [24]. Given the structure of the FHA1 domain, and because we have been unable to isolate any variants against pSer- or pTyr-containing peptides, we are confident that FHA domain variants from the library share the same selectivity for pThr. Thus, one major advantage of the FHA1 domain as a scaffold for recombinant affinity reagent generation is its ability to discriminate between pThr and pSer residues.

Identifying positions important for FHA–peptide interaction

It has previously been reported that a major recognition determinant for naturally occurring FHA domains is the residue at the pT+3 position in the peptide ligand. Specifically, in the Rad53- FHA1, Arg83 interacts with the Asp in the pT+3 of the pRad9 peptide ligand (Fig. 1c). To confirm this for the recombinant FHA domain variants, alanine scanning was performed on the peptide ligand for the FHAαMyc domain; each residue from the pT+1 to the pT+4 was substituted to Ala. Two control peptides were used to confirm residue contribution: the first control peptide contains Ala at every position from pT+1 through pT+4 (AAApTAAAA), and the second control peptide contains Ala at positions pT+1, pT+2, and pT+4 with Leu at the pT+3 position (AAApTAALA). The signals for each phosphopeptide variant were normalized against the truncated cognate sequence (LLPpTPPLS). There was a 45%, 28%, and 20% reduction in signal using the

phosphopeptide variants containing the Ala substituted at positions pT+1, pT+2, and pT+4, respectively. A 96% reduction in signal was observed substituting the Leu (pT+3) for Ala (Fig. 4). Our findings confirm that the pT+3 position is critical for binding for this FHA domain variant. This is consistent with the previous finding of Pershad *et al.* [22], which demonstrated the importance of the pT+3 in the peptide ligand for the FHA domain that binds MAPK3. However, it is likely that other positions in the peptide likely contribute somewhat to binding, as the peptide AAApTAALA does not bind to the same level as the target sequence, LLPpTPPLS.

Identifying the important phosphoresidues for binding in dual-phosphorylated targets

As many proteins are doubly-phosphorylated during signal transduction in eukaryotes, we surveyed the phage-display library for members capable of binding a doubly-phosphorylated peptide target. We selected three proteins, activating transcription factor 2 (ATF2), extracellular signal-regulated kinase1/2 (ERK1/2), and myc, as important biological proteins that are dually phosphorylated, as targets for affinity selection. We were able to isolate FHA domain variants that bind to each of the three peptides. This prompted us to examine how doubly-phosphorylated peptides are recognized by FHA domain variants.

The cognate target for the FHAαERK1/2 variant contains a pThr residue as well as a pTyr residue at the pT+2 position in the peptide sequence, HTGFLpTEpYVATRW. While both the FHAαERK1/2 variant and monoclonal antibody, mAbαERK1/2, are phosphorylation-dependent in binding this peptide ligand (Fig. 5a), only the FHAαERK1/2

variant was shown to be pThr-specific, as mAbαERK1/2 bound to peptides with pSer or pTyr residues at position 185/202 (Fig. 5b). To assess which phosphoresidue is important for phosphospecific reagent binding, variants of the cognate target containing either pThr

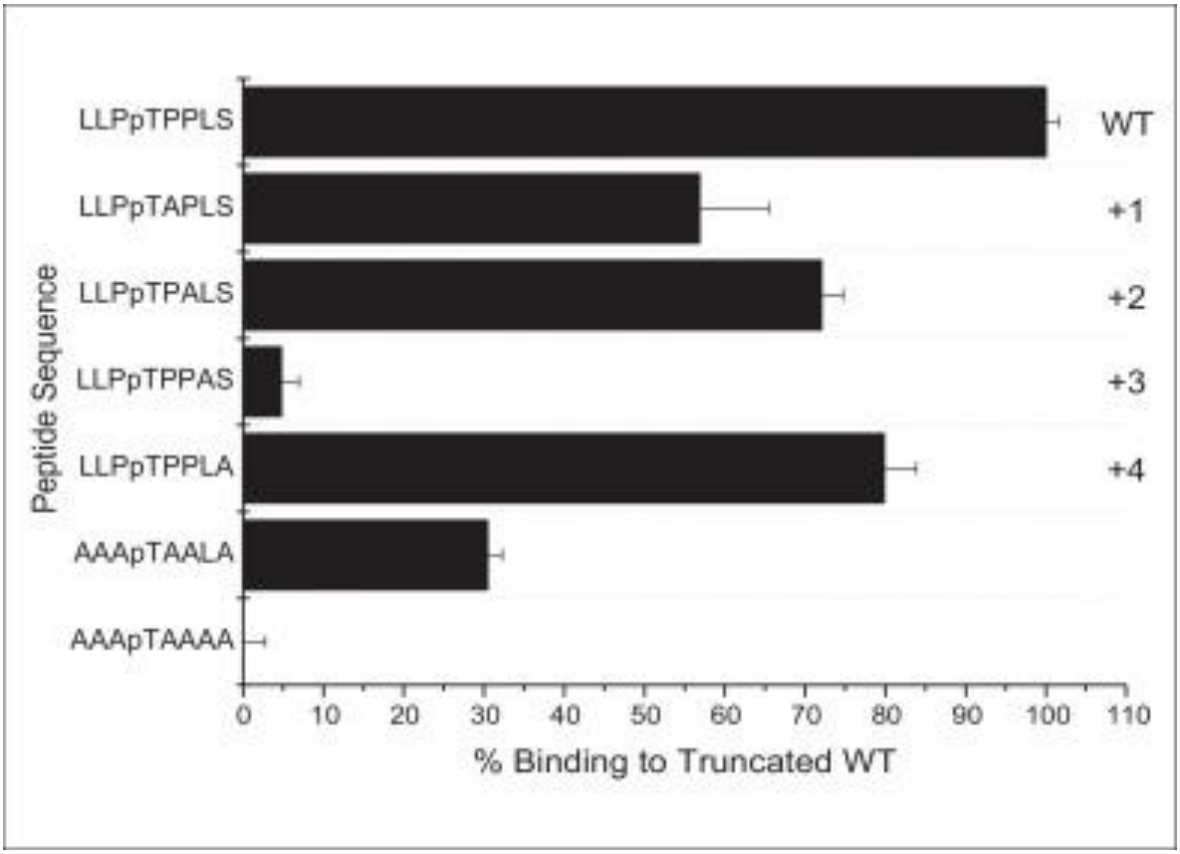

Figure 4 Identification of important residues for the FHA-peptide. An alanine scanning of the cognate peptide for FHAαMyc. Ala was substituted at positions pT+1, pT+2, pT+3, pT+4 in the cognate peptide ligand. Binding of the FHAαMyc to its cognate truncated target was set to 100% and the Myc phosphopeptide variants were compared against it.

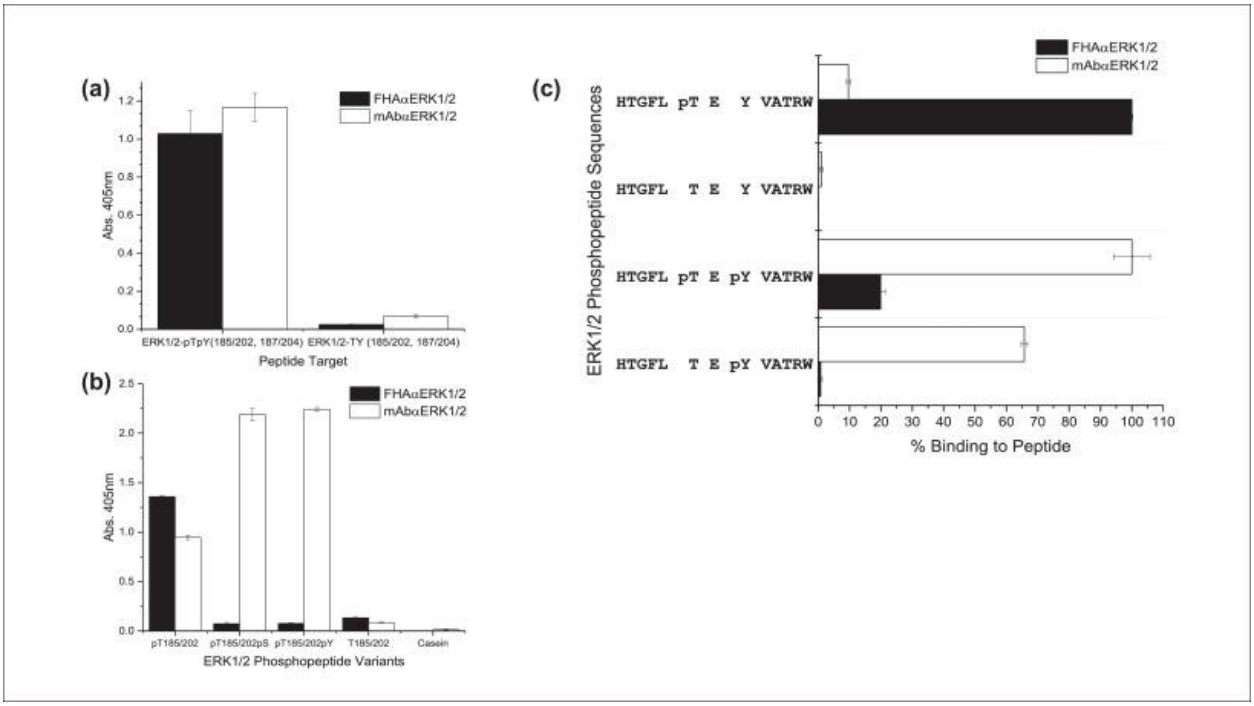

Figure 5 Comparison of phosphospecificαERK1/2 reagents. **A.** The FHAαERK1/2 and mAbαERK1/2 were used in an ELISA to assess phosphorylation dependence. **B.** The FHAαERK1/2 and mAbαERK1/2 were used in an ELISA to assess pThr-specificity **C.** Binding of the FHAαERK1/2 and mAbαERK1/2 to ERK1/2 phosphopeptide variants targets. Binding to the preferred target peptide was set to 100% and the phosphopeptide variants were compared against it.

or pTyr were created. The cognate target, the phosphorylated variants, and an unphosphorylated form of the cognate peptide served as targets in an ELISA (Fig. 5c). Interestingly, the FHAαERK1/2 variant bound the strongest to the monophosphorylated form of the peptide, HTGFLpTEYVATRW. By contrast, the mAbαERK1/2 bound to the doubly-phosphorylated peptide and nearly as well to the monophosphoryated pTyr peptide (HTGFLTEpYVATRW). Taken together, these data confirm the importance of the pThr and suggests that the pT+2 position contributes to binding to FHA domain for this variant, whereas the most important residue for the mAb-peptide interaction is the pTyr residue. One can take advantage of the differing specificities of the two classes of affinity reagents to monitor phosphorylation of ERK1/2 in cells. The localization of the ERK1/2 when phosphorylated on Thr (185/202) and Tyr (187/204) is a well described event in the cell that has a range of physiological consequences including activation of transcription factors [31]. Mass spectrometry has confirmed the three different phosphoforms of ERK1/2 [32]; however, there are currently no known biological consequences of these phosphorylated forms of ERK1/2.

The *in vitro* nature of phage display offers the ability to control epitope recognition, unlike immunization. In this way, it would be possible to continue to narrow the specificity of the FHAαERK1/2 through directed evolution experiments so that they only recognize the pThr-only variant target peptide and not the dual-phosphorylated target. Alternatively, it may be possible to evolve a FHA domain that discriminates between the mono- and doubly-phosphorylated targets. The availability of a set of recombinant affinity reagents with this narrow specificity may be useful in revealing a novel physiological aspect of this well-studied protein.

2.5 Conclusions

The FHA1 domain has been demonstrated to be an attractive alternative to commercially available antibodies. The domain has the innate ability to bind specifically to pThr, and not to pSer or pTyr, containing peptides. Accordingly, the FHA domain is very selective in binding certain phospho-peptides; our studies also confirms the pT+3 position contributes significantly to binding. It is conceivable that one could create a different FHA domain variant for every potential residue at this position. Thus, the FHA domain offers the potential to be used in a wide variety of biochemical and cellular applications that monitor phosphorylation of threonine residues.

2.6 References

1. Endicott, J.A., M.E. Noble, and L.N. Johnson, *The structural basis for control of eukaryotic protein kinases.* Annu Rev Biochem, 2012. **81**: p. 587-613.

2. Ubersax, J.A. and J.E. Ferrell, Jr., *Mechanisms of specificity in protein phosphorylation.* Nat Rev Mol Cell Biol, 2007. **8**(7): p. 530-41.

3. Lin, J., et al., *Understanding protein phosphorylation on a systems level.* Brief Funct Genomics, 2010. **9**(1): p. 32-42.

4. Mann, M., et al., *Analysis of protein phosphorylation using mass spectrometry: deciphering the phosphoproteome.* Trends Biotechnol, 2002. **20**(6): p. 261-8.

5. Nita-Lazar, A., H. Saito-Benz, and F.M. White, *Quantitative phosphoproteomics by mass spectrometry: past, present, and future.* Proteomics, 2008. **8**(21): p. 4433-43.

6. Dephoure, N., et al., *Mapping and analysis of phosphorylation sites: a quick guide for cell biologists.* Mol Biol Cell, 2013. **24**(5): p. 535-42.

7. Liu, P., et al., *Cell-cycle-regulated activation of Akt kinase by phosphorylation at its carboxyl terminus.* Nature, 2014. **508**(7497): p. 541-5.

8. Rardin, M.J., et al., *Monitoring phosphorylation of the pyruvate dehydrogenase complex.* Anal Biochem, 2009. **389**(2): p. 157-64.

9. Whittaker, R., et al., *Kinetics of the translocation and phosphorylation of alphaB-crystallin in mouse heart mitochondria during ex vivo ischemia.* Am J Physiol Heart Circ Physiol, 2009. **296**(5): p. H1633-42.

10. Yao, Z., et al., *Detection of partially phosphorylated forms of ERK by monoclonal antibodies reveals spatial regulation of ERK activity by phosphatases.* FEBS Lett, 2000. **468**(1): p. 37-42.

11. Bradbury, A.R., et al., *Beyond natural antibodies: the power of in vitro display technologies.* Nat Biotechnol, 2011. **29**(3): p. 245-54.

12. Grimsey, N.L., et al., *Specific detection of CB1 receptors; cannabinoid CB1 receptor antibodies are not all created equal!* J Neurosci Methods, 2008. **171**(1): p. 78-86.

13. Bohmer, T., N. Pfeiffer, and A. Gericke, *Three commercial antibodies against alpha1-adrenergic receptor subtypes lack specificity in paraffin-embedded sections of murine tissues.* Naunyn Schmiedebergs Arch Pharmacol, 2014. **387**(7): p. 703-6.

14. Pradidarcheep, W., et al., *Lack of specificity of commercially available antisera against muscarinergic and adrenergic receptors.* Naunyn Schmiedebergs Arch Pharmacol, 2009. **379**(4): p. 397-402.

15. Jensen, B.C., P.M. Swigart, and P.C. Simpson, *Ten commercial antibodies for alpha-1-adrenergic receptor subtypes are nonspecific.* Naunyn Schmiedebergs Arch Pharmacol, 2009. **379**(4): p. 409-12.

16. Couchman, J.R., *Commercial antibodies: the good, bad, and really ugly.* J Histochem Cytochem, 2009. **57**(1): p. 7-8.

17. Kierny, M.R., T.D. Cunningham, and B.K. Kay, *Detection of biomarkers using recombinant antibodies coupled to nanostructured platforms.* Nano Rev, 2012. **3**.

18. Sidhu, S.S., *Antibodies for all: The case for genome-wide affinity reagents.* FEBS Lett, 2012. **586**(17): p. 2778-9.

19. Kaneko, T., et al., *Superbinder SH2 domains act as antagonists of cell signaling.* Sci Signal, 2012. **5**(243): p. ra68.

20. Koerber, J.T., et al., *Nature-inspired design of motif-specific antibody scaffolds.* Nat Biotechnol, 2013. **31**(10): p. 916-21.

21. Olson, C.A., et al., *mRNA display selection of a high-affinity, modification-specific phospho-IkappaBalpha-binding fibronectin.* ACS Chem Biol, 2008. **3**(8): p. 480-5.

22. Pershad, K., K. Wypisniak, and B.K. Kay, *Directed evolution of the forkhead-associated domain to generate anti-phosphospecific reagents by phage display.* J Mol Biol, 2012. **424**(1-2): p. 88-103.

23. Durocher, D., et al., *The molecular basis of FHA domain:phosphopeptide binding specificity and implications for phospho-dependent signaling mechanisms.* Mol Cell, 2000. **6**(5): p. 1169-82.

24. Huang, Y.M. and C.E. Chang, *Mechanism of PhosphoThreonine/Serine Recognition and Specificity for Modular Domains from All-atom Molecular Dynamics.* BMC Biophys, 2011. **4**: p. 12.

25. Kierny, M.R., et al., *Generating Recombinant Antibodies against Putative Biomarkers of Retinal Injury.* PLoS One, 2015. **10**(4): p. e0124492.

26. Chames, P., et al., *Therapeutic antibodies: successes, limitations and hopes for the future.* Br J Pharmacol, 2009. **157**(2): p. 220-33.

27. Schmitz, U., et al., *Phage display: a molecular tool for the generation of antibodies--a review.* Placenta, 2000. **21 Suppl A**: p. S106-12.

28. Pershad, K. and B.K. Kay, *Generating thermal stable variants of protein domains through phage display.* Methods, 2013. **60**(1): p. 38-45.

29. Liao, H., I.J.L. Byeon, and M.D. Tsai, *Structure and function of a new phosphopeptide-binding domain containing the FHA2 of Rad53.* Journal of Molecular Biology, 1999. **294**(4): p. 1041-1049.

30. Liao, H., et al., *Structure of the FHA1 domain of yeast Rad53 and identification of binding sites for both FHA1 and its target protein Rad9.* J Mol Biol, 2000. **304**(5): p. 941-51.

31. Mebratu, Y. and Y. Tesfaigzi, *How ERK1/2 activation controls cell proliferation and cell death: Is subcellular localization the answer?* Cell Cycle, 2009. **8**(8): p. 1168-75.

32. Shi, T., et al., *Sensitive targeted quantification of ERK phosphorylation dynamics and stoichiometry in human cells without affinity enrichment.* Anal Chem, 2015. **87**(2): p. 1103-10.

Chapter 3

Generating a recombinant phosphothreonine-binding domain for a phosphopeptide of the human transcription factor, c-Myc

This research has been published in

Venegas, L.A., Kall, S.L, Bankole, O, Lavie, A, Kay B.K. *Generating a recombinant phosphothreonine-binding domain for a phosphopeptide of the human transcription factor, c-Myc.* N Biotechnol, 2018. pii: S1871-6784(18)30120-1.

3 Chapter 3

3.1 Abstract

Transcription factor c-Myc is an oncoprotein that is regulated at the post-translational level through phosphorylation of two conserved residues, Serine 62 (Ser62) and Threonine 58 (Thr58). A highly specific tool capable of recognizing Myc via pThr58 is needed to monitor activation and localization. Through phage display, we have isolated ten engineered Forkhead-associated (FHA) domains that selectively bind to a phosphothreonine (pThr)-containing peptide (53-FELLP**pT**PPLSPS-64) segment of human c-Myc. One domain variant was observed to bind to the Myc-pThr58 peptide with a K_D value of 800 nM and had > 1,000-fold discrimination between the phosphorylated and non-phosphorylated peptide. The crystal structure of the engineered FHA Myc-pThr-binding domain (Myc-pTBD) was solved in complex with its cognate ligand. The Myc-pTBD was observed to be structurally similar to the yeast Rad9 FHA1 domain, except that its β4-β5 and β10-β11 loops form a hydrophobic pocket to facilitate the interaction between the domain and the peptide ligand. The Myc-pTBD's specificity for its cognate ligand was demonstrated to be on par to three commercial polyclonal antibodies, suggesting that this recombinant reagent is a viable alternate to antibodies for monitoring Myc regulation.

3.2 Introduction

Transcription factor c-Myc (Myc) is an oncoprotein involved in many cellular functions, such as proliferation, growth, differentiation, and apoptosis [1]. Many tumors express constitutively active Myc, which is thought to be a driver of tumorigenesis [2-4], necessitating a tight regulation of Myc's activity for the normal cell to prevent tumor formation. Regulation is accomplished at multiple levels: transcriptional [5], via mRNA stability [6], at the translational level [7], by regulation of protein stability [8], and at the post-translational level [9, 10].

The interdependent phosphorylation of the conserved Serine 62 (Ser62) and Threonine 58 (Thr58) residues regulates Myc protein stability, such that the protein is not prone to degradation [11]. The extracellular signal-regulated kinase (ERK) or cyclin-dependent kinase (CDK) phosphorylates Myc at Ser62, causing it to undergo a conformational change. The Myc-pSer62 conformation activates transcriptional activity and prevents it from becoming ubiquitinated by ligases and therefore degraded by the proteasome. When Glycogen synthase kinase-3β (GSK3β) phosphorylates Myc at Thr58, there is an additional conformational change [12], which prompts the dephosphorylation of Ser62 by protein phosphatase 2A (PP2A) [13], ubiquitylation by SCF-Fbw7 E3 ligase, and ultimately degradation by the proteasome [9]. Mutations affecting Fbw7's WD40 domain, which contacts the pThr58 in Myc, have been reported in a number of human cancers [14-17]; Myc cannot be ubiquitinated when mutant Fbw7 fails to bind pThr58.

The biological consequence of the cell's inability to degrade Myc-pThr58 is unknown. While probing with antibodies is one option to study Myc-pThr58, many commercially available antibodies do not distinguish between Myc-pThr58pSer62 and Myc-pThr58 due

to cross-reactivity, which is often observed for anti-phosphopeptide antibodies [18-23]. Non-antibody recombinant scaffold proteins are attractive alternatives to antibody technology, as they offer a high level of control over their specificity [24], they are small (<200 amino acids), express well in *Escherichia coli*, are soluble at high concentrations, are thermally stable, lack cysteine residues (that can lead to expression and aggregation problems associated with disulfide bonds), are not prone to aggregation [25], and have demonstrated success in phosphosite detection [26-30].

The specificity of a naturally occurring phosphorecognition domain [31], the Forkhead-associated 1 (FHA1) domain, was altered for use as a scaffold in phage display affinity selection [29]. Through directed evolution, a phage library of variants was generated [32] and used in phage display selection to isolate variants against either monophosphorylated or dual phosphorylated peptide targets [29, 32, 33]. Reagents were successfully isolated against 14 out of 17 targets, reflecting an 82% success rate. All isolated reagents were demonstrated to be both pThr-specific and dependent, as opposed to their antibody counterparts [34].

In this study, we present the results of affinity selection of an engineered FHA domain that binds to a phosphopeptide corresponding to Myc-pThr58. The crystal structure of the FHAαMyc-pThr58 binding domain, termed Myc-pTBD for convenience in this report, was determined in complex with its phosphopeptide ligand, and, in conjunction with biochemical assays, revealed the molecular determinants of specificity and selectivity. Additionally, the specificity of the Myc-pTBD was determined to be comparable to three commercially available antibodies, thus demonstrating its potential utility as a probe to study the consequences of Myc-pThr58.

3.3 Materials and methods

Peptides

Peptides were synthesized with >90% purity at University of Illinois at Chicago's Research Resource Center. All peptides were biotinylated at their N-terminus and amidated at their C-terminus and included lysine and tyrosine residues to increase peptide solubility and for measuring absorbance, respectively. The cognate targets for the Myc-pTBD is 53-FELLPpTPPLSPS-64 (Myc-pT58) of human Myc. The following peptides were probed to test Myc-pTBD specificity: FELLPpTPPLSPS (pT58 L61), FELLPpTPPVSPS (pT58 L61V), FELLPpTPPISPS (pT58 L61I), and FELLPpTPPASPS (pT58 L61A).

Antibodies

Three commercial polyclonal antibodies (pAbs) of Abcam (ab28842), AMSBIO (500-11834), and GeneTex (GTX79007) were compared to the recombinant Myc-pTBD. A goat anti-rabbit immunoglobulin G (IgG), conjugated to Horseradish peroxidase (HRP; Abcam ab97051), served as the common secondary reagent. The secondary reagent for Myc-pTBD detection was the anti-Flag epitope monoclonal Ab (mAb), M2, which was conjugated to HRP (Sigma-Aldrich A8592).

Cloning recombinant Myc-pTBDs into protein expression vectors

The coding sequences for individual FHA domains were amplified from the pKP700-phagemid by polymerase chain reaction (PCR) using the OmpA Up (5'-CTGTCATAAAGTTGTCACGGC-3') and FHA1G2Rv (5'-

GTAAATGAATTTTCTGTATGGGGTTTTGC-3') primers. The double-stranded DNA product was digested with *Nco* I and *Not* I restriction endonucleases and subcloned into the pET29b expression vector. These constructs included a 3xFlag-tag sequence (DYKDHDGDYKDHDIDYKDDDDK), followed by a His_6-tag, at the C-terminus of the fusion proteins.

DNA fragments encoding the truncated FHA domain were commercially prepared as gBlocks® Gene Fragments (Integrated DNA Technologies, Inc.). All coding regions were codon-optimized for expression in *Escherichia coli*. DNA fragments were cleaved with *Nde* I and *Bam* HI-HF (New England BioLabs) and subsequently ligated into a modified version of the pET14b expression vector, where the N-terminal His_6-tag is followed by SUMO. The resulting DNA constructs (verified by sequencing) were transformed into *E. coli* strain BL21 C41(DE3) (Lucigen).

Phage display affinity selection

To isolate Myc-pTBDs, three rounds of affinity selection were performed with the FHA1G2 library and the Myc-pThr58 peptide, following a modified version of a published protocol [29]. All the selection steps were performed at room temperature using a KingFisher™ mL Purification System (ThermoFisher Scientific). The biotinylated peptide (3 ng/µL, 400 µL) was immobilized using Dynabeads™ M-270 Streptavidin (ThermoFisher Scientific catalog#65305) and blocked with 2% skim milk in phosphate buffered saline (PBS; 137 mM NaCl, 3 mM KCl, 8 mM Na_2HPO_4, 1.5 mM KH_2PO_4). A 10-fold excess of the phage library (2.8×10^{10} phage particles) was incubated with the blocked target for 1 hour (h), followed by 3 washes with PBS-0.1% Tween 20 (PBST) and three washes with PBS.

Phage particles bound to the target were eluted using trypsin (100 µg/ml in 400µl), and used to infect 800 µL of TG1 cells at mid-logarithmic phase for 40 minutes (min) at 37°C. The cells were plated after infection, scraped the next day, and the phage was amplified. Phage particles were precipitated using 24% PEG8000 and 3 M NaCl, and the pellet was resuspended in 0.6 mL PBS. The second and third rounds of affinity selection were conducted in the same manner with minor exceptions. The target concentration for rounds two and three were 1.5 ng/µL in 400 µL and the number of washes with PBST and PBS increased by three and six, respectively. After the third round of affinity selection, 96 individual clones were propagated as phage, followed by phage-ELISA [29] to identify functional clones that recognize the peptide ligand. Positive binding clones were sequenced.

Protein Purification

Overexpression of the pET29b-Myc-pTBD constructs and their purification was carried out using a previously described protocol [34]. Briefly, BL21(DE3) cells containing the expression vector, were grown in 2xYT media containing all components of the Overnight Express™ Autoinduction System 1 (Novagen). The cells were grown at 30°C for 24 h and then lysed using a Sonic Dismembrator (Branson Model 500). Clontech His-60 Ni Superflow resin (Clontech Laboratories) was mixed the lysate for one hour at room temperature, and the His_6-tagged proteins eluted with 50 mM NaH_2PO_4, 300 mM NaCl, 250 mM imidazole (pH 8.0).

For structural analysis, bacterial cells carrying pET14b-SUMO-MycpTBD plasmid were grown at 30ºC in Overnight Express™ Autoinduction System 1 (Novagen), which was supplemented with 50 µg/mL carbenicillin, and cultured overnight. Cells were harvested

by centrifugation at 5000 rpm, washed with 200 mM KCl, 50 mM Tris, pH 7.4, and lysed by sonication in 25 mM Tris, pH 7.4, 200 mM KCl, 10 mM $MgCl_2$, 10% glycerol, 1% Triton X-100, 1 mM phenylmethylsulfonyl fluoride (PMSF). The lysate was centrifuged at 20000 rpm for 30 min. Clarified supernatant was loaded onto 5 mL HisTrap^{TM} HP Ni^{2+} Sepharose column (GE Healthcare). The column was subsequently washed with 25 mM Tris, pH 7.4, and 500 mM NaCl, supplemented with 10 mM and 25 mM imidazole. Recombinant protein was eluted from the column in the same buffer supplemented with 500 mM imidazole. The His_6-SUMO tag was cleaved with SUMO protease while dialyzing against 25 mM Tris, pH 7.4, 500 mM NaCl, 10 mM imidazole, and the tag was removed by loading the sample back onto a nickel column. Collected fractions containing purified protein were concentrated and injected onto a S-200 size exclusion column (GE Healthcare), equilibrated with 25 mM Tris-HCl, pH 7.4, 500 mM NaCl, 3 mM DTT, and 1 mM EDTA. To assess purity, collected samples were analyzed by SDS-PAGE and detected with Coomassie Brilliant Blue staining. All purified proteins were concentrated and stored at -80ºC.

Surface plasmon resonance

The affinity of the Myc-pTBD was measured using a Biacore200 following a similar protocol described in [35]. The Myc-pT58, Myc-pT58pS62, and Myc-T58 biotinylated peptide were diluted to 0.1 μM with PBS followed by immobilization at each channel with 20 μL/min flow rate for 2 min on a sensor chip coated with streptavidin (SA). A blank channel without any immobilized peptide served as a control. The analyte was added in a series of increasing concentration (0.01-5 μM) to all four channels, at 25 μL/min flow rate, for 180 seconds of dissociation.

ELISA

ELISAs were performed using an established protocol [34, 36]. The final concentration of each peptide was 5 ng/μL. Myc-pTBDs were diluted in PBST and added to a final concentration of 0.5 μM. The absorbance was read at 405 nm wavelength in 10 min intervals, for a total of 40 min. All experiments were performed in triplicate and repeated at least three times to confirm reproducibility of the data.

Crystallization of Myc-pTBD with Myc-pT58

All crystals were grown at 20ºC using sitting drop vapor diffusion method. Crystals of the protein-peptide complex were grown in 1.4 M sodium malonate pH 6.0. Drops of 1 μL protein at 6.0 mg/mL were prepared with a 5:1 molar ratio of peptide to protein. This complex mixture was set at a 1:1 ratio with reservoir solution. Crystals took 8 months to appear as rectangular prisms. Prior to data collection, the Myc-pTBD plus peptide crystals were cryoprotected in mother liquor containing 30% glycerol.

Data Collection and Structure Determination of Myc-pTBD with Myc-pT58

Diffraction data for [Myc-pTBD + peptide] was obtained at the Life Sciences Collaborative Access Team ID beamlines 21-ID-F at the Advanced Photon Source, Argonne National Laboratory (wavelength, 0.979 Å; temperature, 100ºK) (refer to Table I for data collection and refinement statistics). Data processing was executed using XDS [37]. The peptide-bound structure of Myc-pTBD was solved using MOLREP [38] molecular replacement software using PDB ID:1G6G as a model. Further refinement of the model was done using REFMAC5 software [39]. B factors were calculated for the

main chain residues using bAverage software from CCP4i [40]. All structural figures were generated with PyMOL (PyMol™ Molecular Graphics System, version 1.7.2.3; Schrodinger, LLC).

Structure	Myc-pTBD
PDB ID	6C4U
Data Collection	
Space Group	P 2 2 2_1
Cell dimensions	
a, b, c (Å)	70.18 72.37 280.35
α, β, γ (º)	90
Resolution (Å)	54.43-2.54 (2.70-2.54)
R_{merge} (%)	6.4 (117.1)
R_{meas} (%)	6.9 (128.5)
CC1/2	99.9 (86.7)
I/σI	16.08 (1.17)
Completeness (%)	98.4% (90.9%)
Reflections (Unique/total)	47879/333127
Refinement	
Resolution (Å)	2.60
R_w/R_f (%)	23.4/27.6
No. Atoms	
Protein	6417
Water	51
Average FHA main chain B values for monomers A, B, C, D. E.& F ($Å^2$)	96, 87, 88, 95, 88, 102
Average peptide main chain B values for the peptides associated with monomers A, B, C, D, E, & F. ($Å^2$)	124, 114, 108, 115, 98, 117
R.M.S.D	
Bond Length (Å)	0.013
Bond Angles (º)	1.796
Ramachandran Plot (%)	
Most Favored*	95.9
Allowed	3.7
Disallowed	0.4

Table I. Refinement statistics for Myc-pTBD + Myc-pT58

3.4 Results

A Myc phosphothreonine-binding domain (Myc-pTBD) was isolated against a phosphothreonine-containing peptide of c-Myc

To generate a recombinant affinity reagent that recognizes Myc-pThr58, a synthetic peptide corresponding to residues 53-64 of human c-Myc, with pThr at position 58 (Fig. 1), was synthesized and used for affinity selection experiments. The thermostable FHA1 domain was randomized at 10 positions with NNK codons to create a library (10^9) of FHA variants [29]. After three rounds of selection, 96 clones were examined by phage ELISA. Of these, 46 clones were confirmed to bind to the Myc-pT58 peptide, of which ten had a > 1,000-fold difference in binding between the phosphorylated and non-phosphorylated forms of the peptide (Fig. 2A). Additionally, the ten clones were observed not to bind to peptides bearing phosphomimetic substitutions (i.e., Asp, Glu) for the phosphothreonine residue (data not shown).

DNA sequencing of these ten Myc-pTBDs revealed that they are all unique. A comparison (Fig. 2B) of the β4-β5 and β10-β11 loops, which were randomized in the library [29], reveal that five clones contain leucine (Leu), proline (Pro), and valine (Val) at positions 82-84, respectively, in the β4-β5 loop. Six clones contain an arginine (Arg) at position 133 in the β10-β11 loop. Finally, seven clones contain a threonine (Thr) at position 134 in the β10-β11 loop. Taken together, these data suggest that 82-Leu-Pro-Val-84 and 133-Arg-Thr-134 in the Myc-pTBD play a role in recognizing the phosphopeptide, or in stabilizing the structure of the domain so that is adopts the binding-competent conformation.

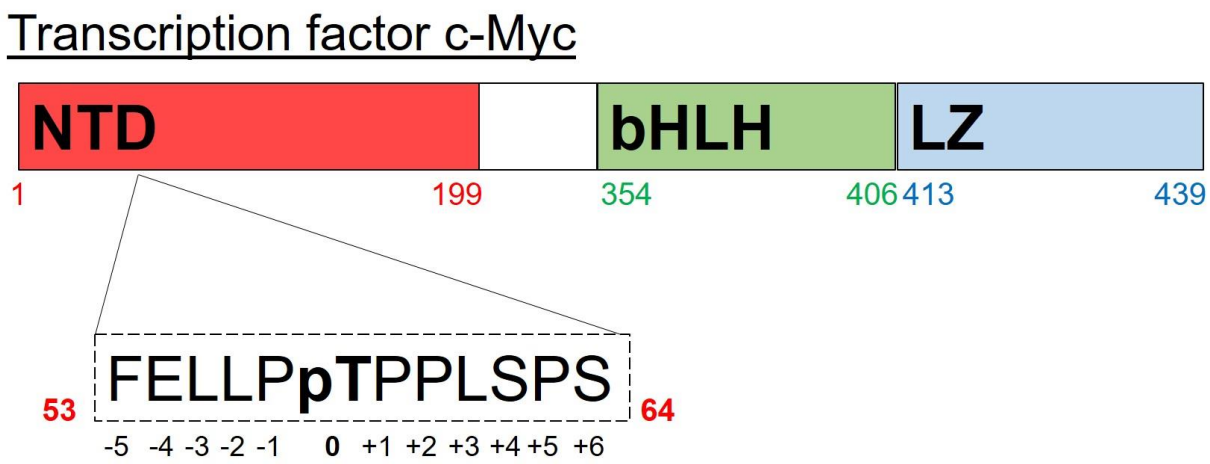

Figure 1. The structural domains of transcription factor c-Myc. c-Myc contains several domains, including the N-terminal domain (NTD, red), a basic helix-loop-helix domain (bHLH, green), and a leucine zipper domain (LZ, blue). The insert of residues 53-64 of the NTD represent where the phosphorylation events regulating c-Myc occur, and correspond to the peptide used in this work. The resides N-terminal to the pThr are denoted with a (-), the pThr is the 0 position, and residues C-terminal to the pThr are denoted with a (+).

A.

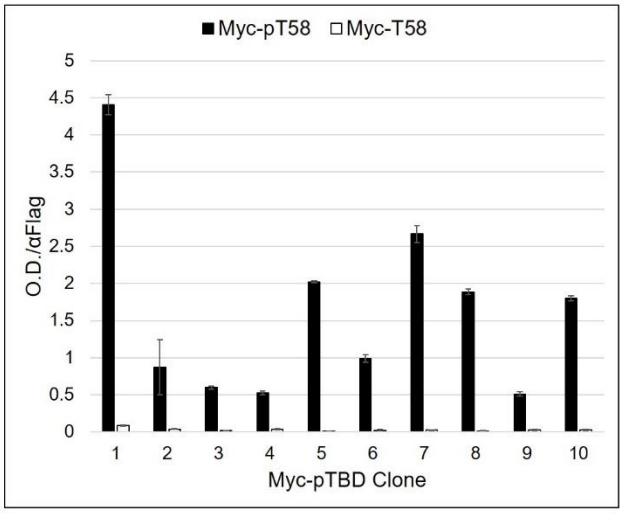

B.

Myc-pTBD Clone	β4-β5 (82-84)	β10-β11 (133-139)
FHA1 (WT)	SRL	GVGVESD
1	LPV	RTDPTGT
2	SFM	VTSPRWG
3	LPV	RTDPNGN
4	LPV	RTARRGH
5	LPV	RTGLQGR
6	RHY	KARGPNS
7	LPV	RTAAPGR
8	LVV	RTRPVGP
9	RHA	PGPYAPR
10	IYW	PARNRHQ

Figure 2. FHA variants were isolated against Myc-pT58. Three rounds of affinity selection were performed to isolate binders from the phage library of FHA domain variants. **(A)** Evaluation of ten phage clones derived from FHA by measuring their binding to the biotinylated peptides, Myc-pT58 (53-FELLPpTPPLSPS-64) and Myc-T58 (53-FELLPTPPLSPS-64), by ELISA. **(B)** Amino acid sequences of the two variable loops isolated in each clone. Many contained a Leu-Pro-Val sequence in loop β4-β5. Loop β10-β11 was more variable, but often contained basic residues or additional Prolines, neither of which were present in the parent construct. Residues in the clones that differ from the parental residues are represented in red.

The Myc-pTBD builds a network of interactions with the pThr moiety

To learn more about the recognition of the engineered Myc-pTBD with its peptide ligand, the structure of clone 1 of the Myc-pTBD (Fig. 2B) in complex with the Myc-derived phosphorylated peptide NH_2-KLLP(pT)PPLS-COOH was solved by X-ray crystallography. The asymmetric unit contained six copies of Myc-pTBD, each interacting with the phosphopeptide. Alignment of all six copies showed low R.M.S.D. values, ranging from 0.09 to 0.17 Å over 98 to 101 common Cα atoms, indicating strong structural similarity between all monomers. The B monomer + H peptide was used for analysis, as it had the lowest average B-factors for the main chain (87 $Å^2$ compared to 88 $Å^2$ to 102 $Å^2$ for the other 5 monomers; Fig. 3A). The Myc-pTBD retained the general architecture of the FHA1 domain (Fig. 3B); specifically, monomer A + peptide E of 1G6G to monomer B + peptide H of Myc-pTBD gave an R.M.S.D. value of 0.41 Å over 105 common Cα atoms. The most notable change in the backbone architecture was the loss of an α-helix in the β10-β11 loop. The pThr residue of Myc-pT58 rests in the same pocket as the pThr of phosphorylated Rad9 in the wild-type FHA1 structure (Fig. 3C). The electron density is clearly seen for eight of the nine residues in the peptide (Fig. 3D).

Inspection of the complex reveals that Arg70, Ser85, Asn86 (both the backbone and side chain), and Thr106 in the Myc-pTBD form hydrogen bonds with the phosphoryl group (Fig. 4). These residues were expected to interact with the pThr moiety based on other structures, and thus were not randomized during the library construction in order to retain phosphospecific binding.

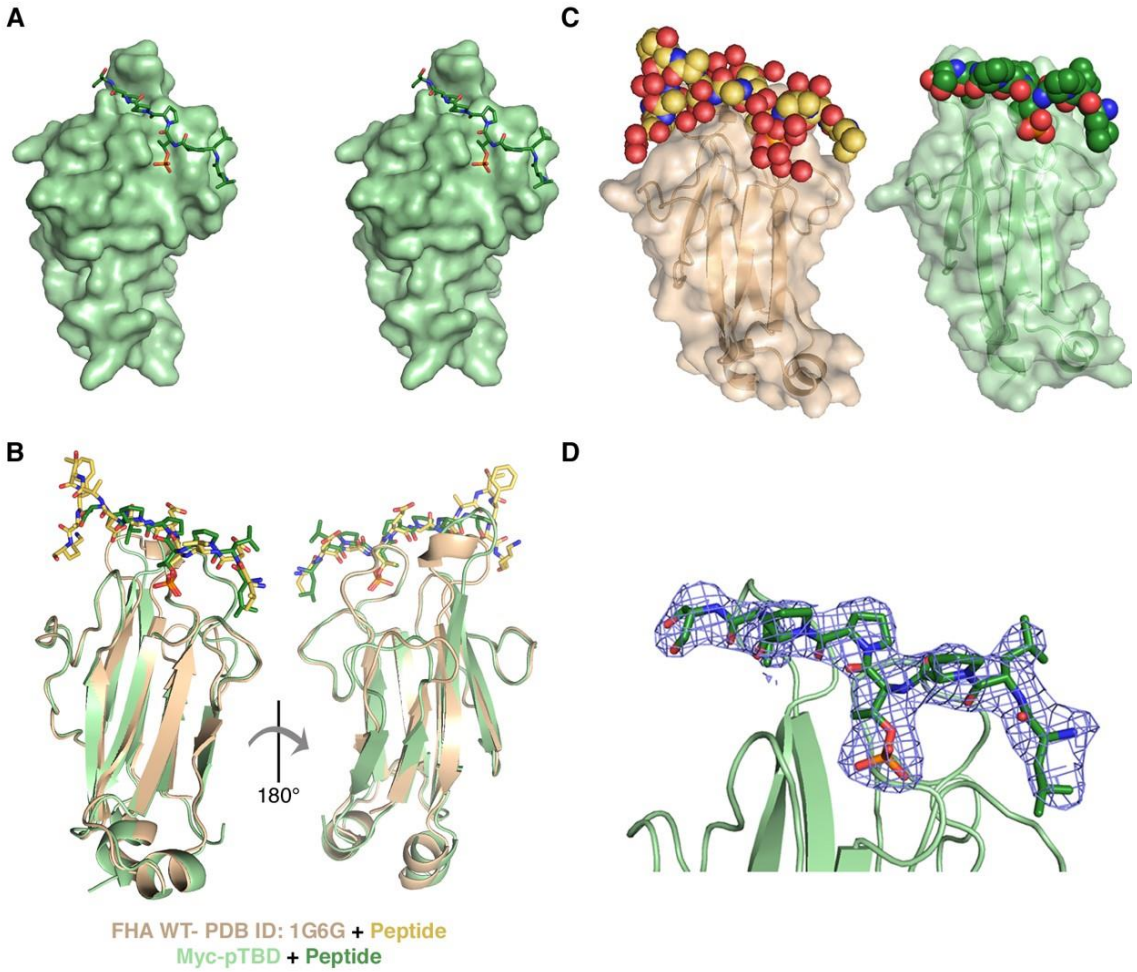
A
C
B
D
180°
FHA WT- PDB ID: 1G6G + Peptide
Myc-pTBD + Peptide

Figure 3. The engineered Myc-pTBD strongly resembles the structure of the yeast FHA1 domain and how it interacts with a phosphopeptide. (A) Stereo image of the 2.5 Å complex of engineered FHA with a Myc-derived phosphothreonine peptide, designated Myc-pTBD. **(B)** Cartoon overlay of the published FHA1 domain wild-type structure (PDB ID: 1G6G; wheat) with its peptide ligand (yellow) and the Myc-pTBD (pale green) + Myc-pT58 peptide (forest). The overlays show the general structure of the domain is conserved in both structures, and the Myc peptide binds in the same binding groove and orientation. R.M.S.D. for the overlay is 0.41 Å. **(C)** A space-filling model of cognate peptide ligands bound to the FHA1 (top) and Myc-pTBD for Myc-pT58 (bottom) shows how the peptide ligands occupy space along one face of the FHA protein, driving specificity. **(D)** A close-up of the Myc-pTBD's peptide-binding region with the $2F_o$-F_c electron density map for the peptide. Note there is clear electron density for the bound peptide through the pT+3 position. The map is contoured to 1.0 σ within 1.4 Å.

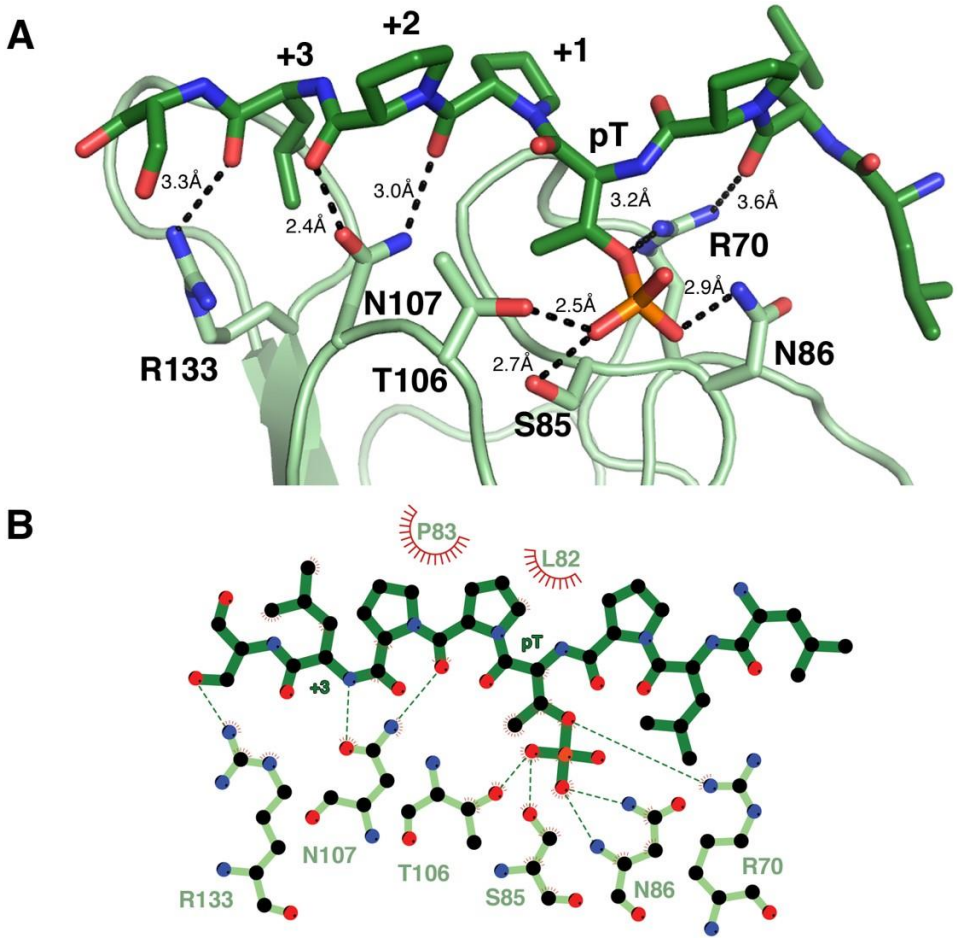

Figure 4. The Myc-pTBD creates a large electrostatic pocket for the binding of pThr. (A) A close-up view of the Myc-pT58 peptide bound to the Myc-pTBD. The key residues of the domain responsible for orienting the pThr of the peptide are Arg70, Ser85, Asn86, and Thr106. Asn107 is also crucial in orienting the peptide, as it is orienting the Myc-derived peptide backbone at the Pro(+2) and the Leu(+3) positions. Arg70 and Arg133 form additional salt bridges with the peptide backbone. **(B)** The Ligplot analysis of peptide binding additionally reveals that Leu82 and Pro83 are responsible for hydrophobic interactions with the pT+1 and pT+2 prolines of the peptide.

Both ionic and hydrophobic interactions were important for the formation of the protein-peptide complex. Hydrophobic forces drove the specificity of the interaction based on the residues surrounding the pThr of the peptide. Meanwhile, the interaction between the phosphorylated moiety of peptide and Myc-pTBD was largely driven by ionic interactions between the pThr and the domain.

Previous work [34] demonstrated that there was no cross-reactivity with a Myc-pT58 peptide variant containing pSer in place of pThr. We speculate that the different rotamer bias between pThr and pSer led to a preference for pThr. Interestingly, just as pSer could not replace pThr, the phosphomimetic carboxylic acid residues Asp and Glu likewise could not replace pThr in the peptide. Here again, the requirement for pThr could be due to rotamer bias. We note that proline residues, which would act to limit the conformational flexibility of the peptide, flank the pThr moiety. Hence, it is possible that replacement of pThr by pSer, Asp, or Glu also affect the peptide conformation such as to prefer a state that is not optimal for interacting with the Myc-pTBD. In other words, the special property of being a beta-branched amino acid endows threonine, but not the other amino acids, the ability to adopt the binding-competent conformation.

The Myc-pTBD interacts with the Leu at the pT+3 position through a hydrophobic network

As mentioned before, the peptide residue three positions C-terminal to the pThr moiety, pT+3, is critical for the protein-peptide interaction for both naturally occurring and engineered FHA domains [29, 34, 41, 42] and was demonstrated to be the major determinant of specificity for the naturally-occurring FHAs [42]. We also observe a key

role for the leucine at the +3 position, Leu(+3), in facilitating the binding of the Myc-pThr peptide to the Myc-pTBD. Specifically, the side chain of Leu(+3) fills a hydrophobic cavity that is lined by two proline residue (Pro83 and Pro136), and the carbon atoms of the Arg133 side chain. The outward-facing extended conformation of Arg133 is stabilized by an interaction within the Myc-pTBD (to carbonyl atom of Asn107) and by an interaction with the peptide (OG atom of Ser at the +4 position).

The insertion of the Leu(+3) side chain into this well-fitting cavity (Fig. 5A) suggests an important role of this residue for binding. To examine this point, a set of eight different pThr-containing peptides, each with a different pT+3 residue, was probed to establish the specificity of the Myc-pTBD. Results showed that the Myc-pTBD bound to some degree with pThr-containing peptides that also contained an Ile or Val at the pT+3 position. We wondered if the observed cross-reactivity was due to the similarity between the Leu and Val/Ile. To test this idea, variants of the Myc-pT58 peptide were generated by substituting Leu at the pT+3 with Val (Myc-pT58 L61V), Ile (Myc-pT58 L61I), or Ala (Myc-pT58 L61A). Binding of the Myc-pTBD to each of the peptide variants was compared in an ELISA (Fig. 5B). Compared to the cognate peptide, there was an 85% and 95% reduction in signal with Myc-pT58 L61V and Myc-pT58 L61A, respectively, but only a 10% reduction in signal with Myc-pT58 L61I. To better understand the discrimination between Ile, Val, and Ala at +3, each residue was modeled in the structure (Fig. 5C), which indicated that the discrimination between the three amino acids is likely due to side chain length: Ile has a longer side chain and is thus able to fill the hydrophobic pocket created by the β4-β5 and β10-β11 loops, whereas the side chains for Val and Ala are too short to fill the

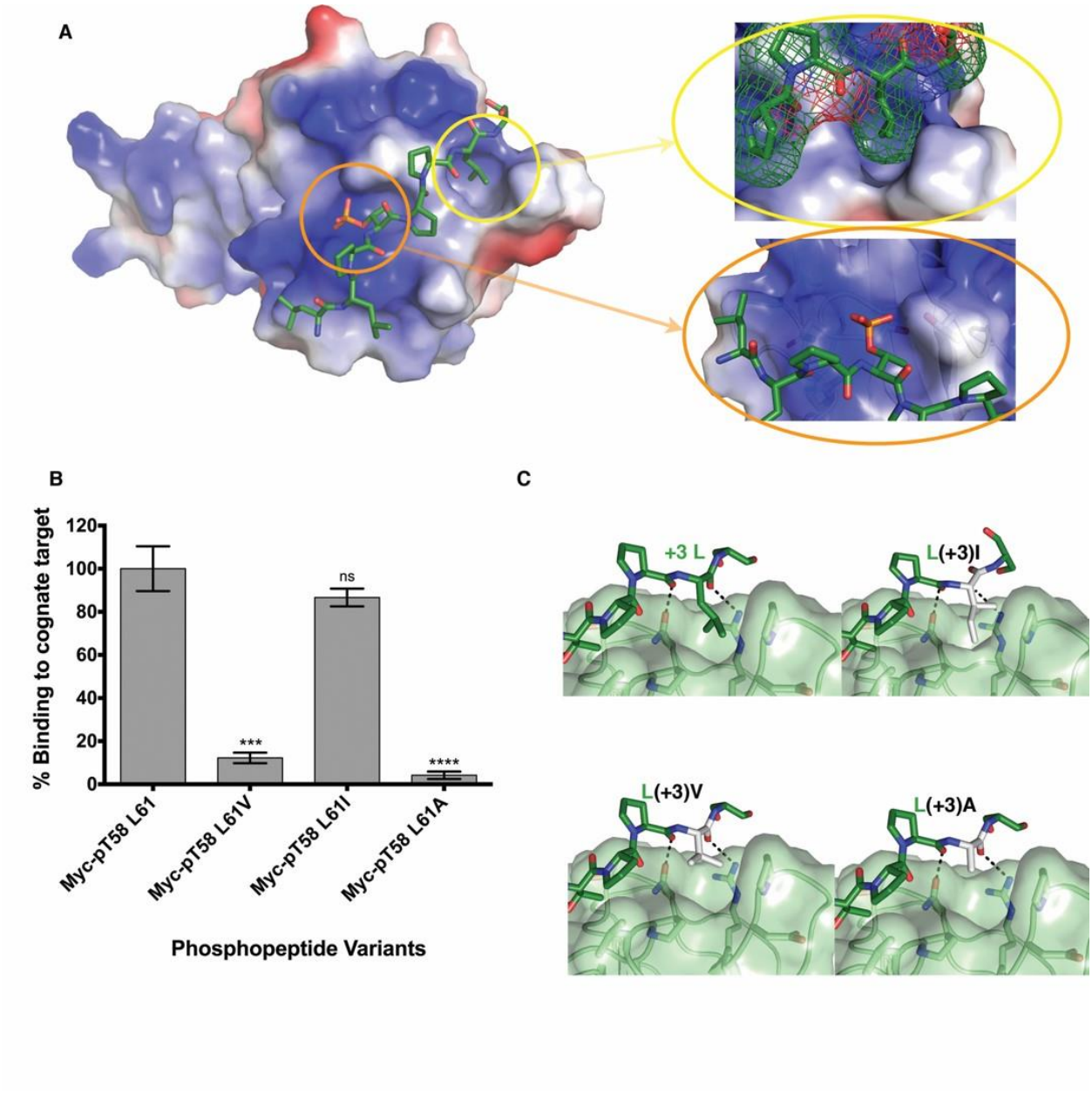
A
B
% Binding to cognate target
120
100
80
60
40
20
0
ns
***
****
Myc-pT58 L61
Myc-pT58 L61V
Myc-pT58 L61I
Myc-pT58 L61A
Phosphopeptide Variants
C
+3 L
L(+3)I
L(+3)V
L(+3)A

Figure 5. The pT+3 position is the major determinant of specificity. Binding of the pThr peptide is driven by the pThr moitey and Leu+3. A) The surface map of Myc-pTBD with its peptide ligand shows the electrostatic charge along the surface of the domain. The yellow insert shows a close-up of the hydrophobic binding pocket occupied by Leu+3. A mesh overlay has been added to demonstrate how Leu fits in this hydrophobic pocket formed by the Myc-pTBD. The orange insert shows a close-up of the pThr moiety of the peptide. Note the surface of Myc-pTBD as formed by in particular Arg70 and Asn86 along the left-hand side contributes a basic surface for the negatively-charged phosphate group to interact with. **B)** Myc-pT58 peptide variants were probed in an ELISA. The experiment showed that while the engineered FHA domain could bind to the peptide when Ile was swapped for Leu, it could not do so for Ala or Val substitutions. The Myc-pTBD served as the probe and detected using a mAbαFlag-HRP secondary antibody. The Myc-pT58A served as the negative control. All signals were normalized to signal from the cognate target. N=3 and error bars refer to standard deviation. P-values ***=0.0001 ****<0.0001 n.s.=not significant. **C)** Models of the FHA with the +3 residue-mutated Myc-pTBD help illustrate why this pT+3 residue is important for specificity. In the case of the actual structure (+3 L, top left) and the predicted Ile substitution (L+3I, top right), both side chains extend into a deep pocket formed by the FHA domain. In the case of both Val (L+3V, bottom left) and Ala (L+3A, bottom right), the side chains as modelled do not occupy enough space to fill that hydrophobic pocket, which could explain the loss of binding.

hydrophobic pocket. Taken together, these data indicate that the pT+3 position is major contributor to Myc-pTBD binding and specificity. These results also suggest that in order to generate an FHA domain that could tightly bind pThr-containing peptides with residues other than Leu or Ile at the pT+3 position, a redesign of the β4-β5 and β10-β11 loops would be necessary.

Probing the specific role of FHA residues from the β4-β5 and β10-β11 loops

To reveal the specific importance to the binding of the phosphorylated peptide by the phage-display selected β4-β5 and β10-β11 loop residues, we conducted an alanine scan of the two loops (Table II). Myc-pTBD variants were generated by sequentially mutating each position to Ala. Each of the mutants was examined for binding to various phosphopeptides by ELISA, and absorbance values normalized to those observed for the wild-type Myc-pTBD domain.

In the β4-β5 loop, the L82A mutation resulted in an 80% loss in binding. This result reveals the importance of the hydrophobic interaction between the side chains of Myc-pTBD Leu82 and the peptide's Leu(-2), and to some extent, with Pro(+1). In contrast, the P83A mutation only had a minor (i.e., 13%) decrease in binding; this observation suggests that an alanine can mostly retain the hydrophobic nature of the cavity binding Leu(+3). Surprisingly, since the side chain is facing into the domain and is not directly interacting with the peptide, the V84A mutation led to a 96% loss in binding. The reduction in peptide binding by the V84A mutation is probably due to an indirect effect, which can be attributed to a global change in conformation of the β4-β5 loop.

For the β10-β11 loop's contribution, we discovered that the precise nature of the residues was less critical as six out of the seven residues impacted peptide binding to by

Myc-pTBD			
Sequence			
Clone	β4-β5	β10-β11	% Binding
W.T.	**LPV**	**RTDPTGT**	**100**
L82A	APV	RTDPTGT	20
P83A	LAV	RTDPTGT	87
V84A	LPA	RTDPTGT	4
R133A	LPV	ATDPTGT	39
T134A	LPV	RADPTGT	67
D135A	LPV	RTAPTGT	97
P136A	LPV	RTDATGT	100
T137A	LPV	RTDPAGT	88
G138A	LPV	RTDPTAT	60
T139A	LPV	RTDPTGA	100

Table II. Alanine scanning of the Myc-pTBD

less than 40%. Arg133 is the most critical residue on this loop, as the mutation resulted in a 61% reduction in binding. As mentioned previously, the carbon atoms of the Arg133 side chain contribute to the hydrophobic cavity that binds Leu(+3). Therefore, the R133A mutation takes away one face of the cavity, which may rationalize the large detrimental impact on the affinity to the peptide.

The Myc-pTBD is as specific to the c-Myc's different phosphorylation states as commercially available antibodies

To investigate whether the Myc-pTBD has the same cross-reactivity limitations as polyclonal antibodies, we compared their binding to a set of peptides corresponding to the different phosphorylation states of c-Myc (Fig. 6A). Each of the pAbs were raised against a peptide containing the Myc-pT58 phosphosite. The Myc-pTBD and pAbs were only able to bind to the cognate peptide and the dually phosphorylated Myc-pT58pS62 peptide and showed little to no discrimination for either. To confirm that the Myc-pTBD does not a have a significant preference for the Myc-pT58 and Myc-pT58pS62 targets, the affinity to the dual phosphorylated peptides was measured by surface plasmon resonance (SPR) using the same conditions as the Myc-pT58 (Table III) and showed no significant difference. Taken together, these data indicate that the isolated Myc-pTBD is comparable in specificity to the three commercially available antibodies.

A.

Myc Phosphopeptide Sequences

Myc-pS62:		LLP	T	PPL	**pS** PSRRSGY
Myc-pT58pS62:	FELLP	**pT**	PPL	**pS**	PSY
Myc-pT58:	FELLP	**pT**	PPL	S	PSY
Myc-TS:	FELLP	T	PPL	S	PSY

B

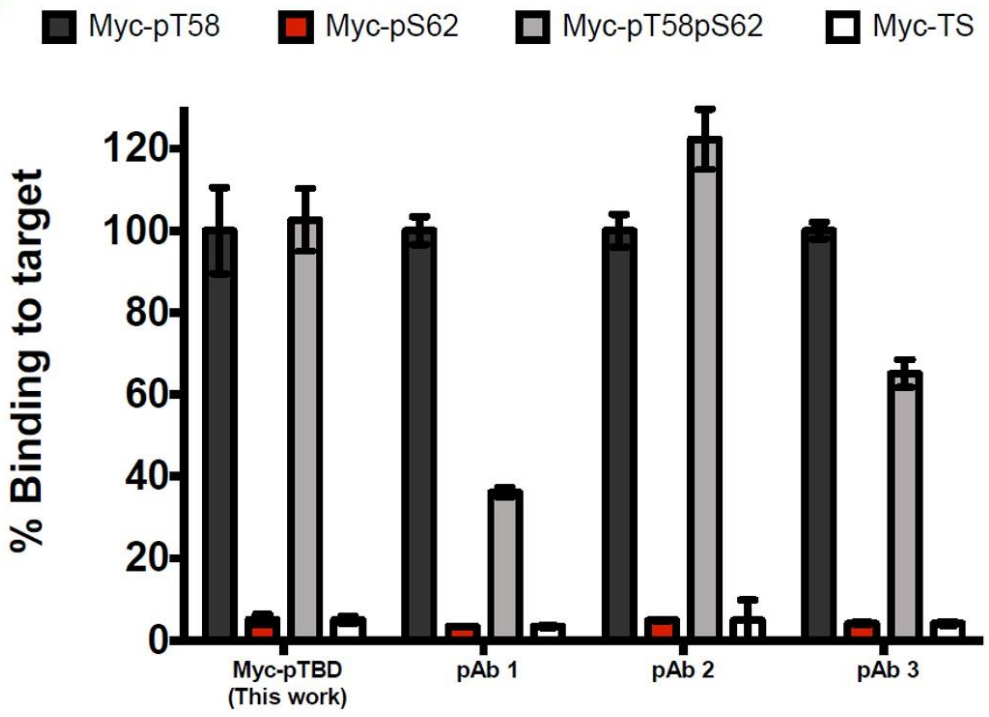

Figure 6. The Myc-pTBD is as specific as commercially available antibodies. (A) A panel of Myc peptides corresponding to the different phosphorylation states of Myc. **(B)** A panel of Myc peptides were probed in an ELISA with the Myc-pTBD and three pAbs. The Myc-pTBD was detected using a mAb αFlag-HRP secondary antibody, whereas the pAbs were detected with a goat anti-rabbit IgG-HRP secondary antibody. Absorbance values were normalized to the Myc-pT58 signal. N=3 and error bars refer to standard deviation.

3.5 Discussion

Through affinity selection of a phage library displaying FHA domain variants, ten pThr-specific and pThr-dependent variants were isolated. The clone with the highest apparent affinity was further characterized and demonstrated to be comparable in specificity to three commercially available antibodies. Using both biochemical and structural approaches, the engineered Myc-pTBD was analyzed and characterized to reveal the molecular determinants of its specificity.

The FHA domain is an advantageous scaffold to isolate phosphospecific affinity reagents against pThr-containing peptide targets, as it is naturally capable of interacting with the pThr moiety. It was previously observed that critical residues for successfully isolating FHA variants were the pThr itself as well as the residue in the pT+3 position (C-terminal to pThr) [34]. Structural analysis of the FHA1 revealed the importance of the pThr [43]. Here, our Myc-pTBD's structure, when overlaid with the previously published WT FHA1 domain, emphasizes again how the engineered Myc-pTBD's phosphorylation-dependence and pThr-specificity are crucial for binding. The side chains of residues Arg70, Ser85, Asn86, and Thr106 act in concert to accommodate the phosphorylated Thr residue of the peptide. This large binding pocket precludes interaction with a non-phosphorylated Thr and adds specificity via ionic interactions with the phospho-group on pThr.

We further probed Myc-pTBD's structure in order to understand the importance of the pT+3 position. A comparison of the primary structures of the ten Myc-pTBD clones showed that half of them shared the motif, Leu82-Pro83-Val84 along with Arg133, suggesting that these four residues together are important for binding in both a direct and

indirect manner. Structural analysis revealed that Pro83 in the Myc-pTBD β4-β5 loop contributes to a hydrophobic pocket for the Leu at the pT+3 position of the peptide ligand to occupy, as do Pro136 and the side chain carbon atoms of Arg133 from the β10-β11 loop. The side chain of Leu+3 fills the hydrophobic pocket created by the variable loop regions and by doing so contributes to the pTBD's affinity and specificity. When Leu at the pT+3 position was substituted with Ile, Val, and Ala, only the Myc-pT58 Ile (+3) peptide variant was able to interact with the pTBD, most likely due to Ile's side chain being sufficiently long enough to fill the pocket. Additionally, future work could focus on designing new combinatorial libraries to create a pocket specific for other amino acids. Because of the importance of the pT+3 position, and the work here that establishes the role of the β4-β5 and β10-β11 loops in creating space for this residue, it stands to reason that future libraries could focus on developing scaffolding domains specific to pThr peptides with specific residues at the pT+3 position.

The specificities of three engineered FHA domains binding to Myc, Ca^{2+}/calmodulin-dependent protein kinase II (CaMKII), and extracellularly regulated kinase 1/2 (ERK1/2) were previously compared with commercially available monoclonal or polyclonal antibodies and were determined to be comparable or better in some cases [34]. The specificity of the Myc-pTBD was also compared to three commercially available pAbs. The comparison revealed that the pTBD has a similar level of specificity to the pAbs. We observed that the pTBD is unable to discriminate between the Myc-pT58 and Myc-pT58p62 peptides. The inability of the pTBD to discriminate between the two peptides is likely due to the lack of the contribution to the interaction from the pT+4 position, i.e. the position which corresponds to Ser62. An approach for improving the Myc-pTBD specificity

could be to link the domain with a different scaffold, such as the fibronectin type III (FN3) monobody, to create an affinity clamp [44]. The linked FN3 domain might interact with residues N-terminal and/or C-terminal to the phosphothreonine, which could improve the specificity and affinity of the pTBD reagent.

The FHA domain has proven to be an effective scaffold for isolating a recombinant affinity reagent against Myc-pT58. The work presented in this report has demonstrated the specificity of the reagent using phosphopeptides. With this level of understanding and structural analysis, the scaffold has the potential for generating a set of Myc reagents, such as a dual-specific and pSer-specific FHA domains, to probe for activation and localization in living cells.

3.6 References

1. Meyer, N. and L.Z. Penn, *Reflecting on 25 years with MYC.* Nat Rev Cancer, 2008. **8**(12): p. 976-90.

2. Nesbit, C.E., J.M. Tersak, and E.V. Prochownik, *MYC oncogenes and human neoplastic disease.* Oncogene, 1999. **18**(19): p. 3004-16.

3. D'Cruz, C.M., et al., *c-MYC induces mammary tumorigenesis by means of a preferred pathway involving spontaneous Kras2 mutations.* Nat Med, 2001. **7**(2): p. 235-9.

4. Pelengaris, S., M. Khan, and G. Evan, *c-MYC: more than just a matter of life and death.* Nat Rev Cancer, 2002. **2**(10): p. 764-76.

5. Lang, J.C., et al., *Transcriptional regulation of the human c-myc gene.* Br J Cancer Suppl, 1988. **9**: p. 62-6.

6. Weidensdorfer, D., et al., *Control of c-myc mRNA stability by IGF2BP1-associated cytoplasmic RNPs.* RNA, 2009. **15**(1): p. 104-15.

7. Wall, M., et al., *Translational control of c-MYC by rapamycin promotes terminal myeloid differentiation.* Blood, 2008. **112**(6): p. 2305-17.

8. Li, S., et al., *Regulation of c-Myc protein stability by proteasome activator REGgamma.* Cell Death Differ, 2015. **22**(6): p. 1000-11.

9. Wang, X.Y., et al., *Phosphorylation Regulates c-Myc's Oncogenic Activity in the Mammary Gland.* Cancer Research, 2011. **71**(3): p. 925-936.

10. Escamilla-Powers, J.R. and R.C. Sears, *A conserved pathway that controls c-Myc protein stability through opposing phosphorylation events occurs in yeast.* J Biol Chem, 2007. **282**(8): p. 5432-42.

11. Sears, R.C., *The life cycle of C-myc - From synthesis to degradation.* Cell Cycle, 2004. **3**(9): p. 1133-1137.

12. Sears, R., et al., *Multiple Ras-dependent phosphorylation pathways regulate Myc protein stability.* Genes & Development, 2000. **14**(19): p. 2501-2514.

13. Yeh, E., et al., *A signalling pathway controlling c-Myc degradation that impacts oncogenic transformation of human cells.* Nature Cell Biology, 2004. **6**(4): p. 308-318.

14. O'Neil, J., et al., *FBW7 mutations in leukemic cells mediate NOTCH pathway activation and resistance to gamma-secretase inhibitors.* Journal of Experimental Medicine, 2007. **204**(8): p. 1813-1824.

15. Welcker, M. and B.E. Clurman, *FBW7 ubiquitin ligase: a tumour suppressor at the crossroads of cell division, growth and differentiation.* Nat Rev Cancer, 2008. **8**(2): p. 83-93.

16. Calhoun, E.S., et al., *BRAF and FBXW7 (CDC4, FBW7, AGO, SEL10) mutations in distinct subsets of pancreatic cancer: potential therapeutic targets.* Am J Pathol, 2003. **163**(4): p. 1255-60.

17. Aifantis, I., E. Raetz, and S. Buonamici, *Molecular pathogenesis of T-cell leukaemia and lymphoma.* Nat Rev Immunol, 2008. **8**(5): p. 380-90.

18. Grimsey, N.L., et al., *Specific detection of CB1 receptors; cannabinoid CB1 receptor antibodies are not all created equal!* J Neurosci Methods, 2008. **171**(1): p. 78-86.

19. Bohmer, T., N. Pfeiffer, and A. Gericke, *Three commercial antibodies against alpha1-adrenergic receptor subtypes lack specificity in paraffin-embedded sections of murine tissues.* Naunyn Schmiedebergs Arch Pharmacol, 2014. **387**(7): p. 703-6.

20. Pradidarcheep, W., et al., *Lack of specificity of commercially available antisera against muscarinergic and adrenergic receptors.* Naunyn Schmiedebergs Arch Pharmacol, 2009. **379**(4): p. 397-402.

21. Jensen, B.C., P.M. Swigart, and P.C. Simpson, *Ten commercial antibodies for alpha-1-adrenergic receptor subtypes are nonspecific.* Naunyn Schmiedebergs Arch Pharmacol, 2009. **379**(4): p. 409-12.

22. Couchman, J.R., *Commercial antibodies: the good, bad, and really ugly.* J Histochem Cytochem, 2009. **57**(1): p. 7-8.

23. Sahara, N., et al., *Phosphorylated p38MAPK specific antibodies cross-react with sarkosyl-insoluble hyperphosphorylated tau proteins.* J Neurochem, 2004. **90**(4): p. 829-38.

24. Groff, K., J. Brown, and A.J. Clippinger, *Modern affinity reagents: Recombinant antibodies and aptamers.* Biotechnol Adv, 2015. **33**(8): p. 1787-98.

25. Zhao, N., M.A. Schmitt, and J.D. Fisk, *Phage display selection of tight specific binding variants from a hyperthermostable Sso7d scaffold protein library.* FEBS J, 2016. **283**(7): p. 1351-67.

26. Olson, C.A., et al., *mRNA display selection of a high-affinity, modification-specific phospho-IkappaBalpha-binding fibronectin.* ACS Chem Biol, 2008. **3**(8): p. 480-5.

27. Kummer, L., et al., *Knowledge-based design of a biosensor to quantify localized ERK activation in living cells.* Chem Biol, 2013. **20**(6): p. 847-56.

28. Kummer, L., et al., *Structural and functional analysis of phosphorylation-specific binders of the kinase ERK from designed ankyrin repeat protein libraries.* Proc Natl Acad Sci U S A, 2012. **109**(34): p. E2248-57.

29. Pershad, K., K. Wypisniak, and B.K. Kay, *Directed evolution of the forkhead-associated domain to generate anti-phosphospecific reagents by phage display.* J Mol Biol, 2012. **424**(1-2): p. 88-103.

30. Venegas, L.A., et al., *Reagents for detecting phosphosites within proteins.* J Bioinform, Genomics, Proteomics, 2017. **2**(3).

31. Durocher, D., et al., *The molecular basis of FHA domain:phosphopeptide binding specificity and implications for phospho-dependent signaling mechanisms.* Mol Cell, 2000. **6**(5): p. 1169-82.

32. Pershad, K. and B.K. Kay, *Generating thermal stable variants of protein domains through phage display.* Methods, 2013. **60**(1): p. 38-45.

33. McGinnis, J. and B.K. Kay, *Generation of recombinant affinity reagents against a two-phosphosite epitope of ATF2.* New Biotechnology Under review.

34. Venegas, L.A., et al., *A comparison of phosphospecific affinity reagents reveals the utility of recombinant Forkhead-associated domains in recognizing phosphothreonine-containing peptides.* N Biotechnol, 2016. **33**(5 Pt A): p. 537-43.

35. Lee, H., et al., *Diphosphothreonine-specific interaction between an SQ/TQ cluster and an FHA domain in the Rad53-Dun1 kinase cascade.* Mol Cell, 2008. **30**(6): p. 767-78.

36. Kierny, M.R., et al., *Generating Recombinant Antibodies against Putative Biomarkers of Retinal Injury.* PLoS One, 2015. **10**(4): p. e0124492.

37. Kabsch, W., *Xds.* Acta Crystallogr D Biol Crystallogr, 2010. **66**(Pt 2): p. 125-32.

38. Vagin, A. and A. Teplyakov, *MOLREP: an automated program for molecular replacement.* J. Appl. Cryst., 1997. **30**: p. 1022-1025.

39. Winn, M.D., G.N. Murshudov, and M.Z. Papiz, *Macromolecular TLS refinement in REFMAC at moderate resolutions.* Methods Enzymol, 2003. **374**: p. 300-21.

40. Winn, M.D., et al., *Overview of the CCP4 suite and current developments.* Acta Crystallogr D Biol Crystallogr, 2011. **67**(Pt 4): p. 235-42.

41. Durocher, D. and S.P. Jackson, *The FHA domain.* FEBS Lett, 2002. **513**(1): p. 58-66.

42. Weng, J.H., et al., *Uncovering the Mechanism of Forkhead-Associated Domain-Mediated TIFA Oligomerization That Plays a Central Role in Immune Responses.* Biochemistry, 2015. **54**(40): p. 6219-29.

43. Huang, Y.M. and C.E. Chang, *Mechanism of PhosphoThreonine/Serine Recognition and Specificity for Modular Domains from All-atom Molecular Dynamics.* BMC Biophys, 2011. **4**: p. 12.

44. Huang, J., et al., *Structural basis for exquisite specificity of affinity clamps, synthetic binding proteins generated through directed domain-interface evolution.* J Mol Biol, 2009. **392**(5): p. 1221-31.

Chapter 4

Improving the apparent affinity of the Myc-pTBD through dimerization

4 Chapter 4

4.1 Abstract

The FHA1 domain has proven to be an ideal scaffold for isolating phosphothreonine-binding domains (pTBDs) against various kinases and transcription factors using phage display affinity selection. However, pTBDs have a modest affinity (K_d ~1 μM) for their phosphopeptide ligands, making it difficult to use them in biochemical assays due to the short half-life (i.e., seconds) of the pTBD-peptide complexes. Three pTBDs, which were affinity selected to bind pThr-containing peptides corresponding to human transcription factor c-Myc (FELLP**pT**PP*L*SPS), Ca^{2+}/calmodulin kinase II (CaMKII, LKGAIL**pT**TM*L*ATRN), and extracellular regulated kinase 1/2 (Erk1/2, HTGFL**pT**E**pY**VATRW), were demonstrated to be both phosphorylation dependent and pThr-specific in ELISA. To enhance apparent affinity of these pTBDs, they were converted to homodimers by either fusing the domains to a leucine zipper (LZ) dimerizing sequence (to generate pTBD LZs) or linking them in tandem (to generate pTBD-Tandem repeats, TR). To estimate the affinity of the various constructs, the concentration of each that gives the half maximal response (EC_{50}) was measured in an ELISA. Monomers were observed to have an average EC_{50} value of 10^{-8} M, whereas pTBD-LZs and pTBD-TRs had EC_{50} values of 10^{-9} M and 10^{-10} M, respectively. Interestingly, there was no apparent loss of specificity for either dimeric form of the three pTBDs tested. The utility of Myc-pTBD LZ was further evaluated by probing western blots of lysates of HEK 293 cells engineered to overexpress Myc-pT58. Curiously, while the Myc-pTBD LZ failed to detect Myc-pT58, it bound to two unrelated, phosphorylated protein species.

4.2 Introduction

Affinity is the quantitative measure of the strength of the interaction between a protein and its ligand. To describe the interaction, one can begin by measuring the time it takes for unbound protein (P) to associate with unbound ligand (L) to form a protein-ligand complex (PL):

$$P + L \rightleftarrows PL$$

The dissociation constant (K_d) is a way to describe the affinity of a protein to its ligand:

$$K_d = [P]*[L] / [PL]$$

where [P], [L], and [PL] are the molar (M) concentrations of the unbound protein, ligand, and the protein-ligand complex, respectively. The K_d describes the [L] at which the [PL] equals the concentration of [P] [1]. A high [PL] means that there is a high concentration of the protein-ligand complex, and thus, low concentrations of [P] and [L]. The lower the K_d value, the longer it takes for the protein-ligand complex to dissociate, which means there is a strong interaction between the protein and its ligand (i.e., a high affinity). For example, proteins with a nanomolar (nM) dissociation constants have dissociation rates around $0.001s^{-1}$ and half-lives >10 min. Proteins with a micromolar (μM) dissociation constants have dissociation rates around $1s^{-1}$ and half-lives of 0.7 seconds [2].

In the specific case of an antibody or affinity reagent binding to its target, one would describe the association constant:

$$P + L \rightleftarrows PL$$

$$K_a = [P*L] / [P]*[L]=1/K_d$$

This ratio describes both the on-rate (k_{on}) and off-rate (k_{off}) constants:

$$K_a = k_{on} / k_{off}$$

While two reagents may have the same affinities, they may have different on- and off-rates.

Using the FHA1 domain to generate anti-phosphospecific reagents through affinity selection is a useful approach for isolating pThr-specific variants with an average affinity of ~1 μM. Dr. Kritika Pershad previously used the Myc phosphothreonine-binding domain (Myc-pTBD) and extracellular-regulated kinase 1/2-pTBD (ERK-pTBD) as probes in western blots to identify activation of Myc-pT58 and ERK1/2-pT202/pY204, respectively, in whole cell lysates. When neither pTBDs reacted with a protein on the blots, she attributed their failure to their modest affinity (i.e., 1 μM). Through Dr. Michael Kierny's work with recombinant antibodies, the Kay lab estimated that a K_d value of <300 nM is required for a reagent to yield a band on a western blot. Since the affinities of the pTBDs were unsuitable for western blots, developing a strategy for increasing the affinity of the domains was necessary.

Common strategies for improving a reagent's affinity include affinity clamping [3], affinity maturation [4-6], and multimerization [7, 8]. Affinity maturation was the first method that I employed to improve the affinity of pTBDs. Using the Myc-pTBD, I began with stochastic approaches that included Error prone PCR (epPCR) across the domain's coding region and saturation mutagenesis [9-12] within the variable loop regions (i.e., the β4-β5 and the β10-β11 loops), but I was not able to isolate a variant with an improved affinity. I attributed the inability of the affinity maturation approach to the few contact sites

between the FHA domain and the peptide. I then turned to increasing the affinity of the pTBDs through multimerization.

In nature, multivalency often increase the apparent strength of interactions between two multimeric proteins or ligands [13]. Immunoglobulin M (IgM) is an example of a naturally occurring multivalent protein (pentamer) that is capable of interacting with up to 10 sites on an antigen complex (i.e., glycoproteins on a bacterial cell surface) [14]. The affinity of a protein describes the single interaction strength between the protein and its ligand. If a protein can interact with multiple ligands, these interactions act synergistically to improve the protein's apparent affinity. This effect, known as avidity, occurs if the ligands are within a close proximity of each other so that each monomeric unit can interact simultaneously [15]. Increasing a protein's valency in turn increases the overall affinity due to a slower off-rate [7]. Avidity is what allows IgMs to bind to mulitivalent antigens (i.e., virus, bacterial cell) very tightly despite the low affinity of monomeric igM molecules. Improving the affinity of recombinant affinity reagents through avidity has been achieved by fusing the affinity reagent to an oligomerization domain [7, 16-18]. Specifically, fusing a protein to a leucine zipper domain has proven to be an effective approach for creating homodimeric and tetrameric constructs with high apparent affinity (K_d <10 nM) [17].

To improve the affinity of pTBDs through multimerization, I fused three previously isolated pTBDs, via a Gly-Ser linker, to the N-terminus of a leucine zipper (LZ) domain from the yeast GCN4 protein. I also linked two pTBDs via a Gly-Ser linker to create a tandem repeat homodimer. Both types of homodimers were expressed and purified in *Escherichia coli* and characterized. The Myc-pTBD LZ was then used as a probe for detection of the phosphorylated form of c-Myc on a western blot.

4.3 Materials

Reagents

Peptides were synthesized at University of Illinois at Chicago's Research Resource Center, with >90% purity. All peptides were biotinylated at their N-terminus and amidated at their C-terminus and included lysine and tyrosine residues to increase peptide solubility and measure their concentration (through absorbance), respectively. The peptide ligands for the Myc-, ERK1/2-, and CaMKII-pTBDs are FELLPpTPPLSPS, HTGFLpTEpYVATRW, and LKGAILpTTMLATRN, respectively. As all pTBDs carry the 3xFlag-tag epitope (DYKDHDGDYKDHDIDYKDDDDK), the secondary antibody was an anti-Flag epitope monoclonal antibody, M2, which was conjugated to horseradish peroxidase (HRP) (Sigma–Aldrich).

Antibodies

The polyclonal antibodies (pAb), pAb anti-Myc-pT58 (Abnova) and pAb anti-β-actin (Abcam) were used to detect Myc-pT58 and β-actin, respectively. The human transcription factor c-Myc containing the hemagglutinin (HA)-epitope (YPYDVPDYA) was detected using a biotinylated monoclonal antibody (mAb). A goat anti-rabbit immunoglobulin G (IgG), conjugated to HRP (Abcam), served as the common secondary reagent for detection of anti-Myc-pT58 and anti-β-actin on western blots. Streptavidin conjugated HRP (ThermoFisher Scientific) served as the secondary reagent for detection of mAbαHA.

DNA constructs

The coding sequences for the individual FHA domains were amplified from virions by the polymerase chain reaction (PCR). The double-stranded DNA products were digested with *Nco* I-HF and *Not* I-HF (New England BioLabs) restriction endonucleases and subcloned into the pET29b expression vector (Novagen). DNA fragments encoding the Linker sequence $(Gly_4S)_X$ + Leucine Zipper (RMKQLEDKVEELLSKNYHLENEVARLKKLVGER) and Linker + pTBD were commercially prepared as gBlocks® Gene Fragments (Integrated DNA Technologies, Inc.). The linker length (x) was repeated either four or ten times where indicated. All coding regions were codon-optimized for expression in *Escherichia coli*. DNA fragments were cleaved with *Not* I-HF and *XhoI*-HF (New England BioLabs) and subsequently ligated into a modified version of the pET29b expression vector. These constructs included a 3xFlag-tag sequence (DYKDHDGDYKDHDIDYKDDDDK), followed by a His_6-tag, at the C-terminus of the fusion proteins. All constructs were verified by DNA sequencing.

Protein purification

Overexpression of the constructs and their purification was carried out using standard methods [19]. Briefly, BL21DE3 cells containing the expression vector was grown at 30°C for 24 hours using the Overnight Express™ Autoinduction System 1 (Novagen). Bacterial cells were lysed using a Sonic Dismembrator (Branson Model 500). The lysate was mixed with Clontech His-60 Ni Superflow resin (Clontech Laboratories), and the His_6-tagged proteins eluted with 50 mM sodium phosphate, 300 mM sodium chloride, 250 mM imidazole (pH 8.0).

The monomeric state and purity of dimeric pTBDs were assessed by size-exclusion chromatography in a Superdex 200 GL column with a ÄKTA FPLC system (GE Healthcare). The Gel Filtration Calibration Kit LMW (GE Healthcare) served as molecular weight standards.

Enzyme-linked immunosorbent assays (ELISA)

ELISAs were performed using an established protocol [19], except that non-specific binding in microtiter plate wells was blocked with 1% casein in phosphate buffered saline (PBS; 137 mM NaCl, 3 mM KCl, 8 mM Na_2HPO_4, 1.5 mM KH_2PO_4). Optical absorbance was read at 405 nm wavelength in 10-min intervals, for a total of 40 min. All experiments were performed in triplicate and repeated three or more times.

Immunoprecipitation and western blotting

Immunoprecipitation (IP) experiments were performed by Mr. Colin Daniel at the Oregon Health Science University, according to a described protocol [20]. Briefly, the anti-HA mAb (Applied Biological Materials) were bound to Protein G-Sepharose Fast Flow beads (GE Healthcare) overnight 4°C. Separately, transfected HEK 293 cells (ATCC) were lysed using a sonicator (Branson Sonifier 450) and mixed with the antibody-coated beads overnight at 4°C. The beads were pelleted at 2,000 x g for 1 minute at 4°C, washed four times with IP buffer (20 mM Tris pH 7.5, 50 mM NaCl, 0.5% Triton X-100, 0.5% deoxycholic acid, 0.5% SDS, and 1 mM EDTA). The washed beads were resuspended in 40 µL of 1.5xSDS sample buffer and boiled at 95°C for 10 minutes.

Boiled samples were loaded in an AnykD™ Mini-PROTEAN TGX™ Precast Protein gel (Bio-Rad) for electrophoresis. The resolved proteins were transferred to a PVDF membrane for western blotting. After the transfer, the polyvinylidene fluoride (PVDF) membranes were rinsed with distilled water and blocked for 1 hour in 2% skim milk, followed by the addition of the anti-HA, anti-Myc-pT58 pAb, and Myc-pTBD LZ for 1-hour incubation. After three washes with PBS, the blot was incubated with the secondary antibodies conjugated to HRP (see above). The blot was washed three times with PBS. Bands were detected using the Pierce ECL substrate (Thermo Fisher Scientific) by HyBlot CL Autoradiography Film (Denville Scientific) using the SRX-101A (Konica Minolta).

4.4 Results

Generating dimeric phosphothreonine-binding domains

To improve the affinity of phosphothreonine-binding domains (pTBDs), I designed homodimers by fusing the pTBD to the leucine zipper domain from the yeast GCN4 transcription factor (Fig.1), For the Leucine Zipper (LZ) construct, a Glycine (Gly)-Serine (Ser) linker region connected the pTBD to the LZ (Fig. 3A); the linker region was designed by repeating Gly_4-Ser four times, $(Gly_4\text{-}Ser)_4$, for a total length of 20 amino acids. The coding regions for the Myc-pTBD, ERK-pTDB, and the Ca^{2+}/calmodulin kinase II-pTBD (CaMKII-pTBD) were subcloned into the pET29b-pTBD-Leucine Zipper expression vector to yield the Myc-pTBD LZ, ERK-pTDB LZ, and CaMKII-pTBD LZ protein constructs.

Similarly, a Glycine-Serine linker region connected two copies of the same pTBD in the Tandem Repeat (TR) construct (Fig. 2). Three TRs were designed to identify an optimal linker length. The Tandem Repeat 10 (TR10), Tandem Repeat 20 (TR20), and Tandem Repeat 40 (TR40) contain a 10, 20, or 40 amino acid linker length, respectively. The Myc-pTBD coding region was subcloned into the pET29b-pTBD-Tandem Repeat expression vector to yield Myc-pTBD TR10, Myc-pTBD TR20, and the Myc-pTBD TR40. All dimers were expressed in bacteria with the pET29b vector (Fig. 3) and purified as through immobilized metal affinity chromatography [21]. Table I lists their yields and calculated molecular weights (https://web.expasy.org/protparam/). All proteins migrated in an SDS-PAGE according to their anticipated monomeric, molecular weight (Fig. 4). To verify that the LZs formed dimers when overexpressed in bacteria, they were analyzed by size-exclusion chromatography (SEC) and determined to be dimeric (Fig. 5).

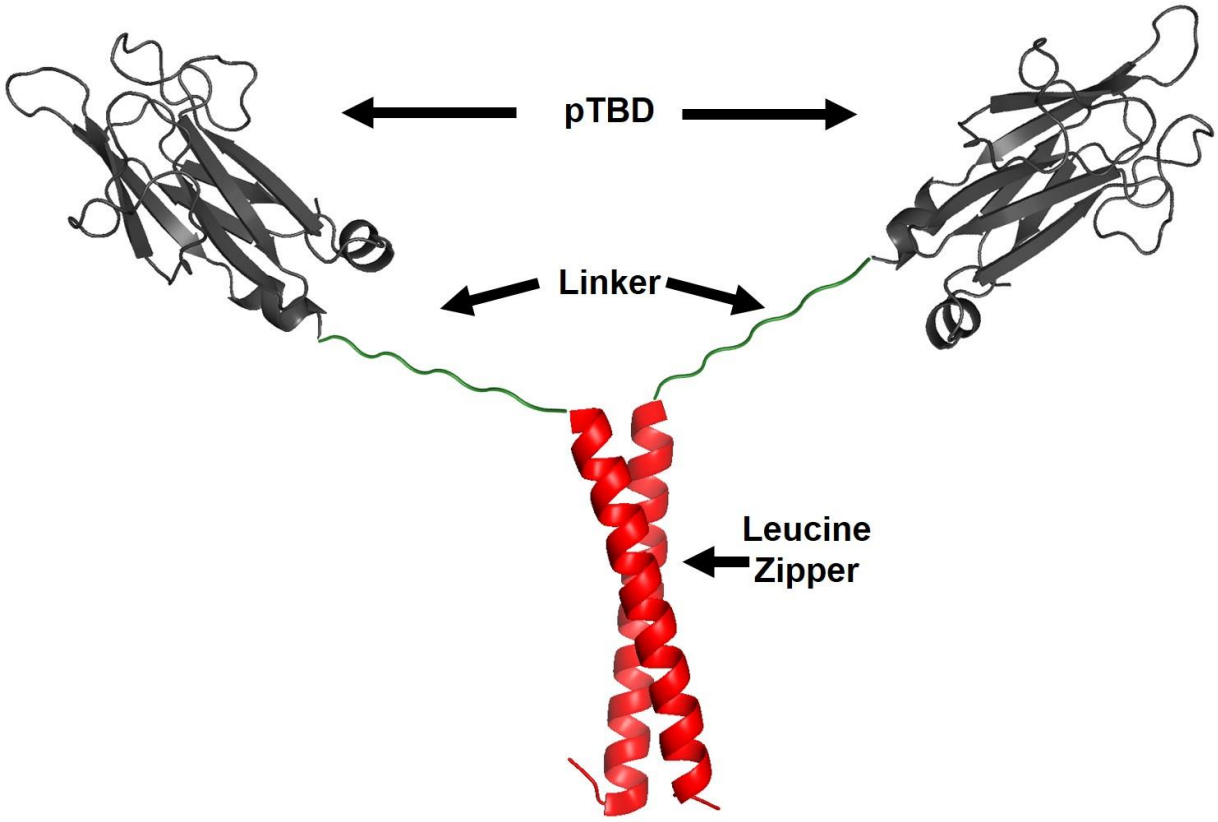

Figure 1. Diagram of the pTBD-Leucine Zipper affinity reagent. The three-dimensional structure of Myc-pTBD is represented in a cartoon format (Gray), the linker region is represented as a line (Green), and the GCN4's leucine zipper domain (PDB 4DMD) is represented in a cartoon format (Red). Not drawn to scale. All structural figures were generated with PyMOL (PyMOL™ Molecular Graphics System, version 1.7.2.3; Schrodinger, LLC).

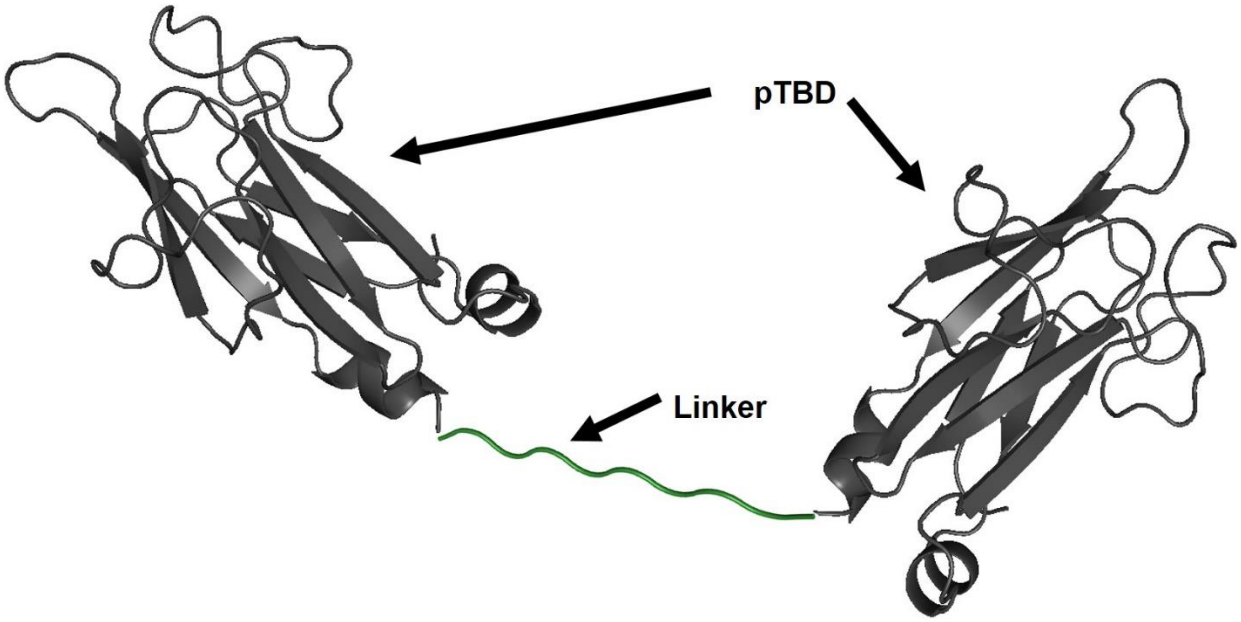

Figure 2. Diagram of the pTBD-Tandem Repeat affinity reagent. The pTBD is represented as a cartoon (Gray). The linker region is represented as a line (Green). All structural figures were generated with PyMOL (PyMOL™ Molecular Graphics System, version 1.7.2.3; Schrodinger, LLC).

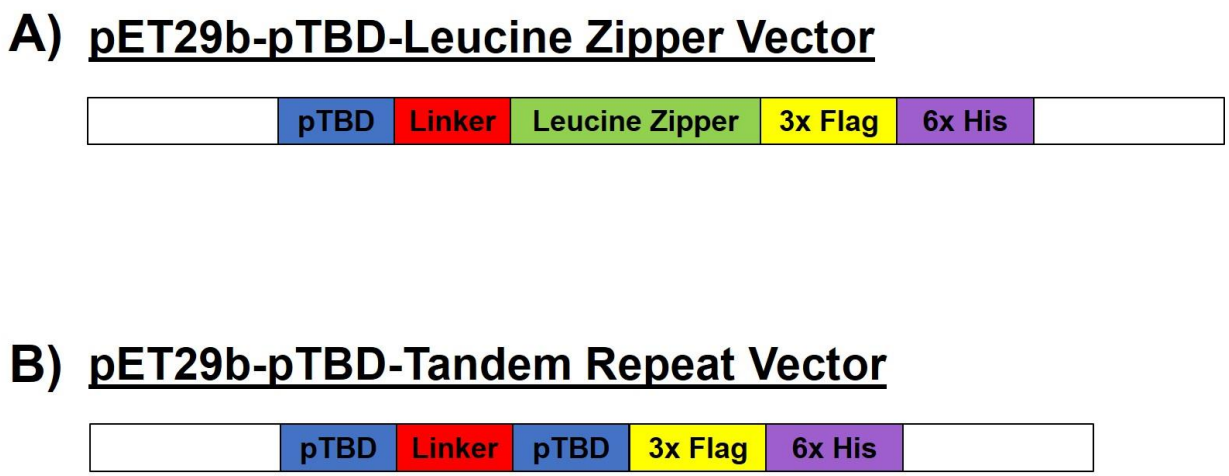

Figure 3. Diagram pTBD coding region in the pET29b vector. Dimeric pTBDs were constructed using the pET29b vector. **A.** The pTBD coding region (Blue). The pTBD and the Leucine Zipper domain (Green) are fused using a $(Gly\text{-}Gly\text{-}Gly\text{-}Gly\text{-}Ser)_4$ linker sequence (Red). A trimeric Flag tag (3x Flag, Yellow) and a six-Histidine (6x His, Purple) follow the LZ domain. **B.** The same pTBD coding regions (Blue) are linked using a (Gly-Gly-Gly-Gly-Ser) linker sequence (Red). A trimeric Flag tag (3x Flag, Yellow) and a six-Histidine (6x His, Purple) follow the second pTBD domain.

FHA Reagent	Calculated Molecular Weight (kDa)	Average Yield (mg/L)
Leucine Zipper	57.4	147.9
Tandem Repeat 10	43.5	80.7
Tandem Repeat 20	44.7	150.2
Tandem Repeat 40	45.9	58.2

Table I. Molecular weight and yield of dimeric pTBDs.

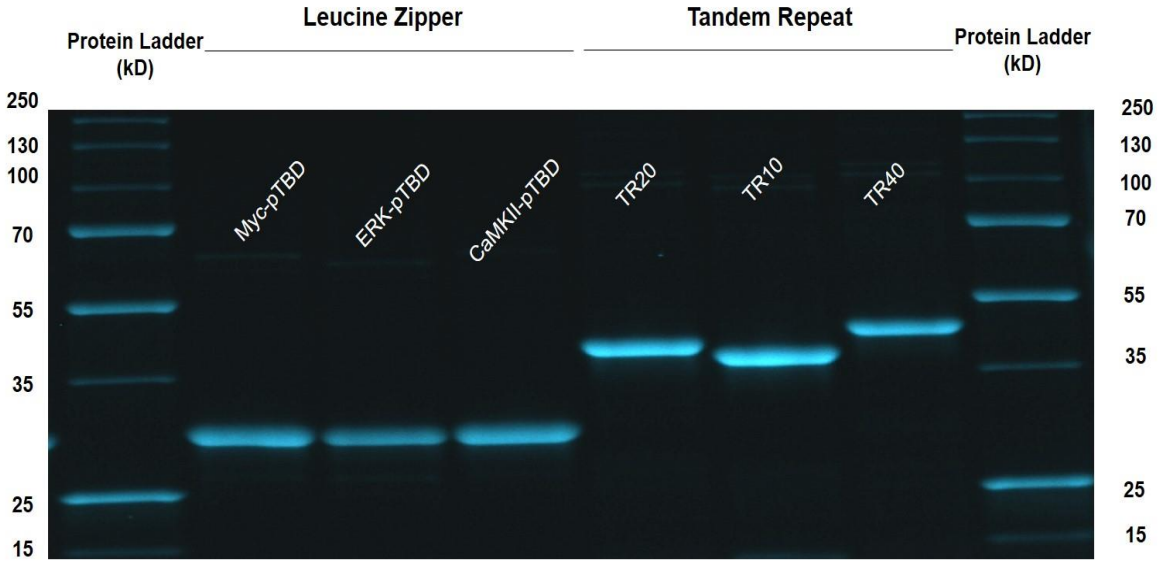

Figure 4. Image of sodium dodecyl sulfate polyacrylamide gel electrophoresis (SDS-PAGE) of purified dimeric pTBDs. The Myc-, ERK, and CaMKII-pTBD Leucine Zipper dimers (Left) migrated as monomers by SDS-PAGE and are ~ 27 kDa in size. The Myc-pTBD Tandem Repeat dimers (Right); their size varies according to the different linker lengths.

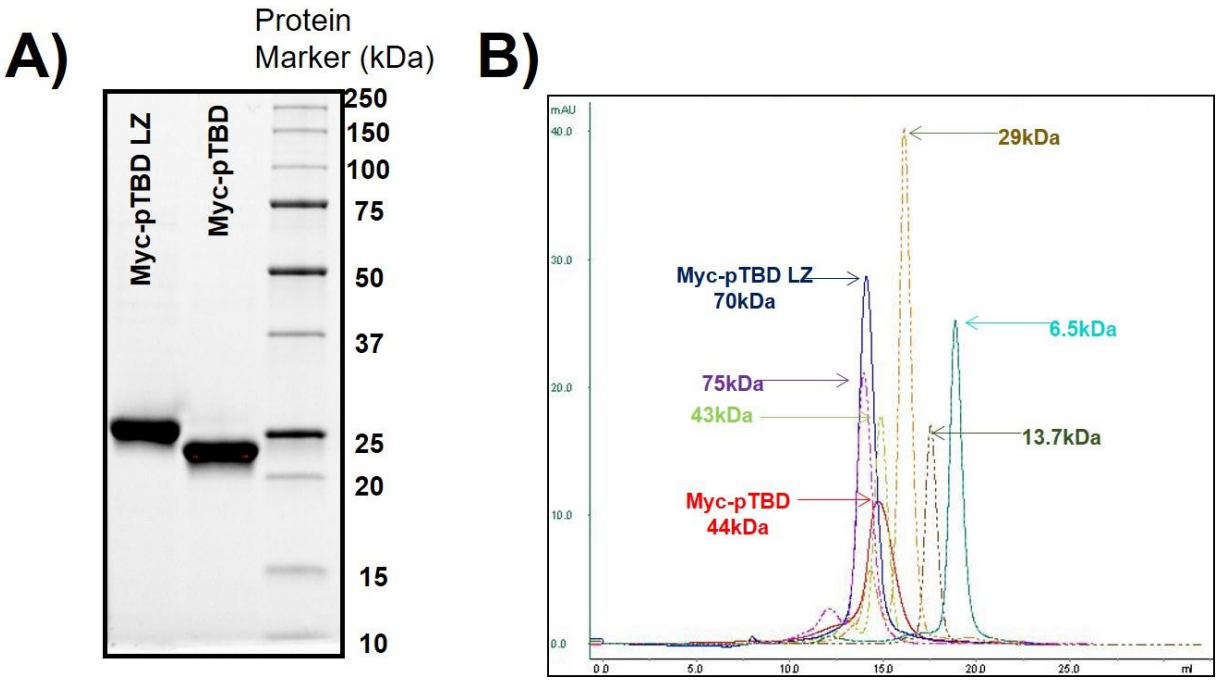

Figure 5. Confirmation of pTBD-Leucine Zipper dimerization. A. The Myc-pTBD LZ (Left) and Myc-pTBD (Right) chromatograph as monomers by SDS-PAGE gel. **B.** A representative image of size-exclusion chromatography LZ dimers. The Myc-pTBD LZ (Navy) and Myc-pTBD (Red) were chromatographed in parallel. Molecular weight standards of 6.5 kDa, 13.7 kDa, 29 kDa, 43 kDa, and 75 kDa were to elution times of the soluble Myc-pTBD LZ and Myc-pTBD proteins.

Dimeric pTBDs have improved apparent affinities

The apparent affinity of the dimers was evaluated by titrating the reagent to determine the concentration that gives the half maximal response (EC_{50}) in an ELISA. If there is an increase in the reagent's apparent affinity, the EC_{50} values for the dimers would be expected to be lower compared to the monomer due to avidity. If there is no difference in the EC_{50} values, then the interaction between the dimer and the ligand should be 1:1, just like the monomeric form of pTBD. The EC_{50} values for the monomeric and dimeric forms of the Myc-pTBD (Fig. 6), ERK-pTBD (Fig. 7), and the CaMKII-pTBD (Fig. 8) were determined. Similarly, the EC_{50} for each of the three TRs (Fig. 9) were also evaluated. There was between a 10-fold and 100-fold difference between the EC_{50} values of the monomers and dimers (Table II), suggesting that the apparent affinity has improved due to avidity.

Target density is a major factor when measuring the affinity of multimeric proteins [17]. If the target density is too low, then one would be unable to properly evaluate whether there was an improvement in affinity due to avidity. If the target density is too high, then one would not see an improved affinity. While I did observe an improvement in the apparent affinity of the dimers, it was less than the 1000-fold improvement reported in the literature [13, 16, 17]. To determine whether the target density in the ELISAs was affecting the results, I titrated the Myc-pT58 target peptide and used the three TRs as probes. The results demonstrated that the target densities are too high in ELISAs to establish an improvement in the affinity by avidity (Fig. 10) consistent with [22].

Linker size impacts the ability of a multimeric reagent to interact with multiple epitopes simultaneously. If the linker size is too short, then multimers would be unable to interact

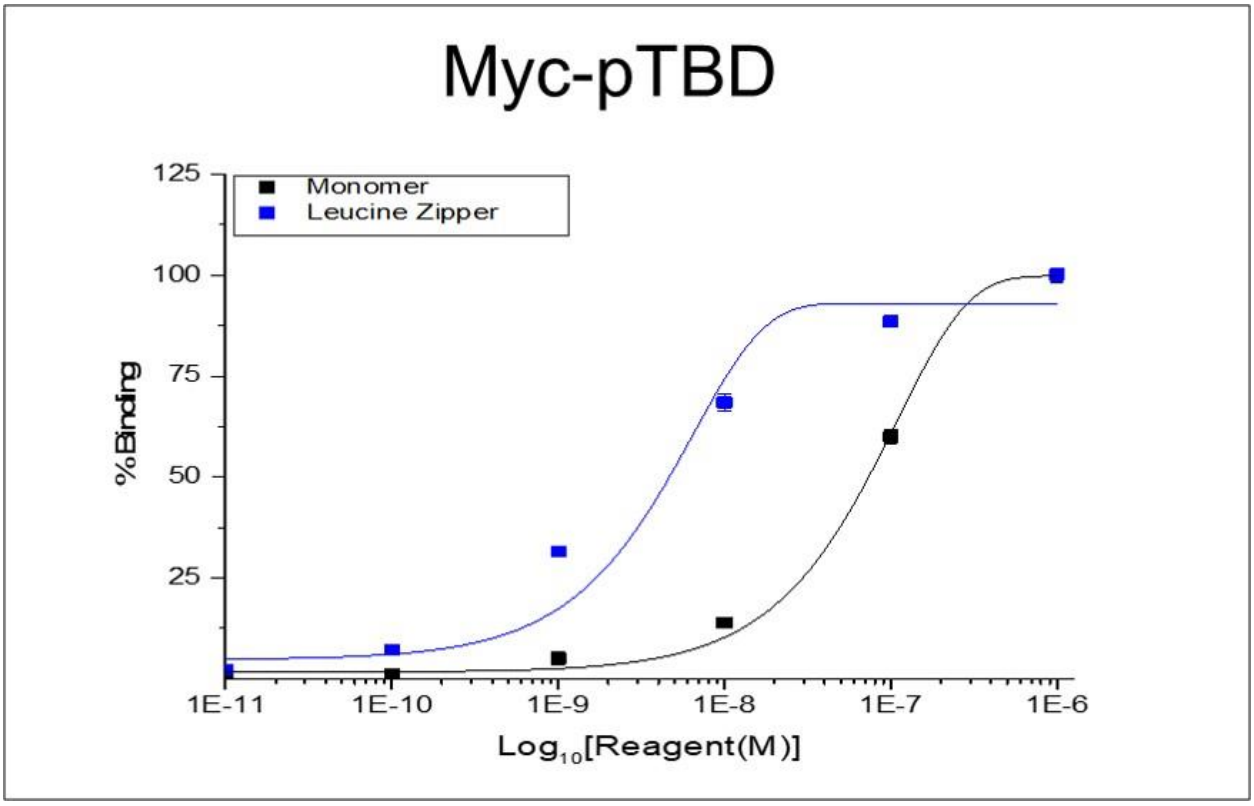

Figure 6. Titration of the Myc-pTBD monomer and Myc-pTBD dimer. The Myc-pT58 peptide was used as a target in an ELISA. The monomeric and dimeric Myc-pTBDs were titrated to determine their EC_{50} values. The M2-HRP antibody was used to detect binding of the pTBDs to the peptide target captured on the surface of microtiter plate wells. All experiments were performed in triplicate and repeated three times to confirm reproducibility. Error bars represent the standard deviation. Absorbance values were recorded at 405 nm wavelength.

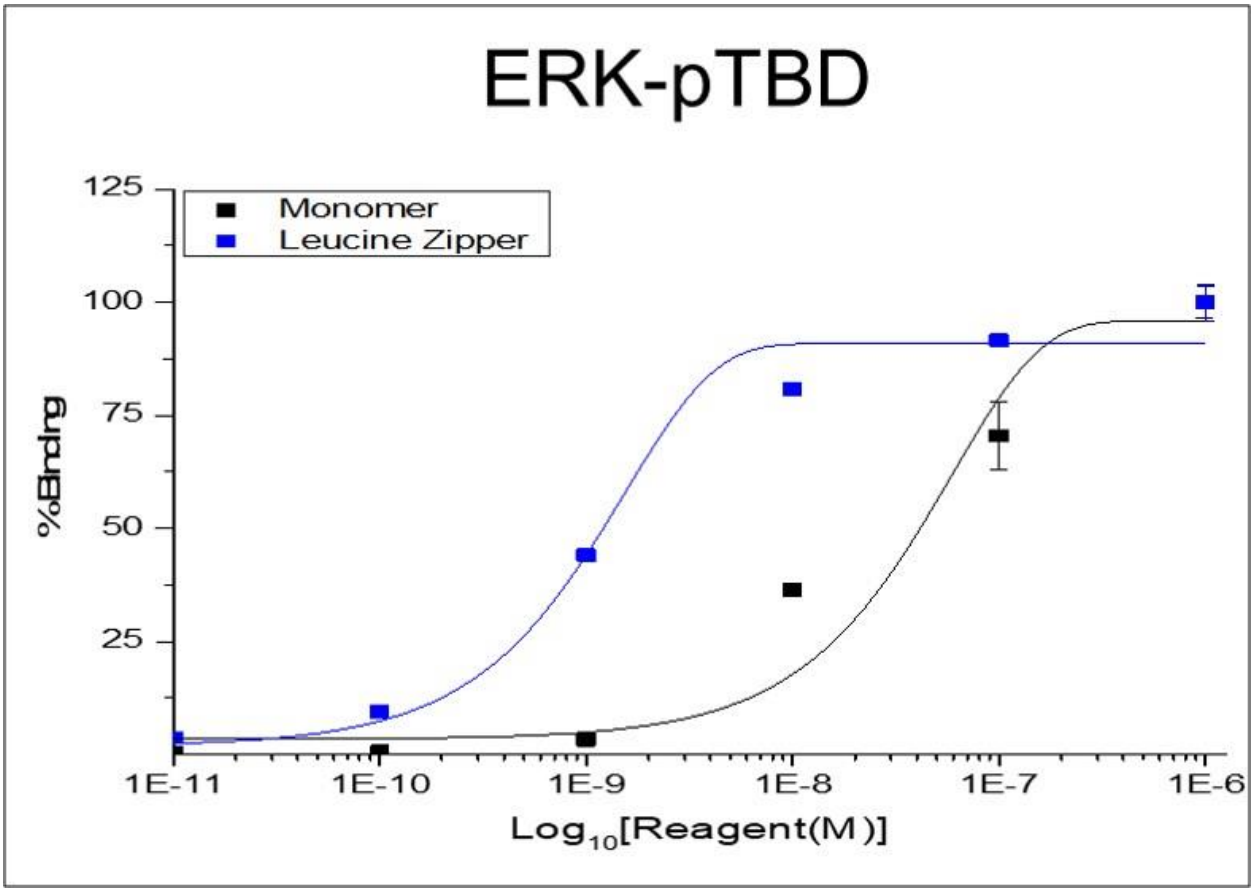

Figure 7. Titration of the ERK-pTBD monomer and ERK-pTBD dimer. The ERK-pT202/pY204 peptide was used as a target in an ELISA. The monomeric and dimeric Myc-pTBDs were titrated to determine their EC_{50} values. The M2-HRP antibody was used to detect binding of the pTBDs to the peptide target captured on the surface of microtiter plate wells. All experiments were performed in triplicate and repeated three times to confirm reproducibility. Error bars represent the standard deviation. Absorbance values were recorded at 405 nm wavelength.

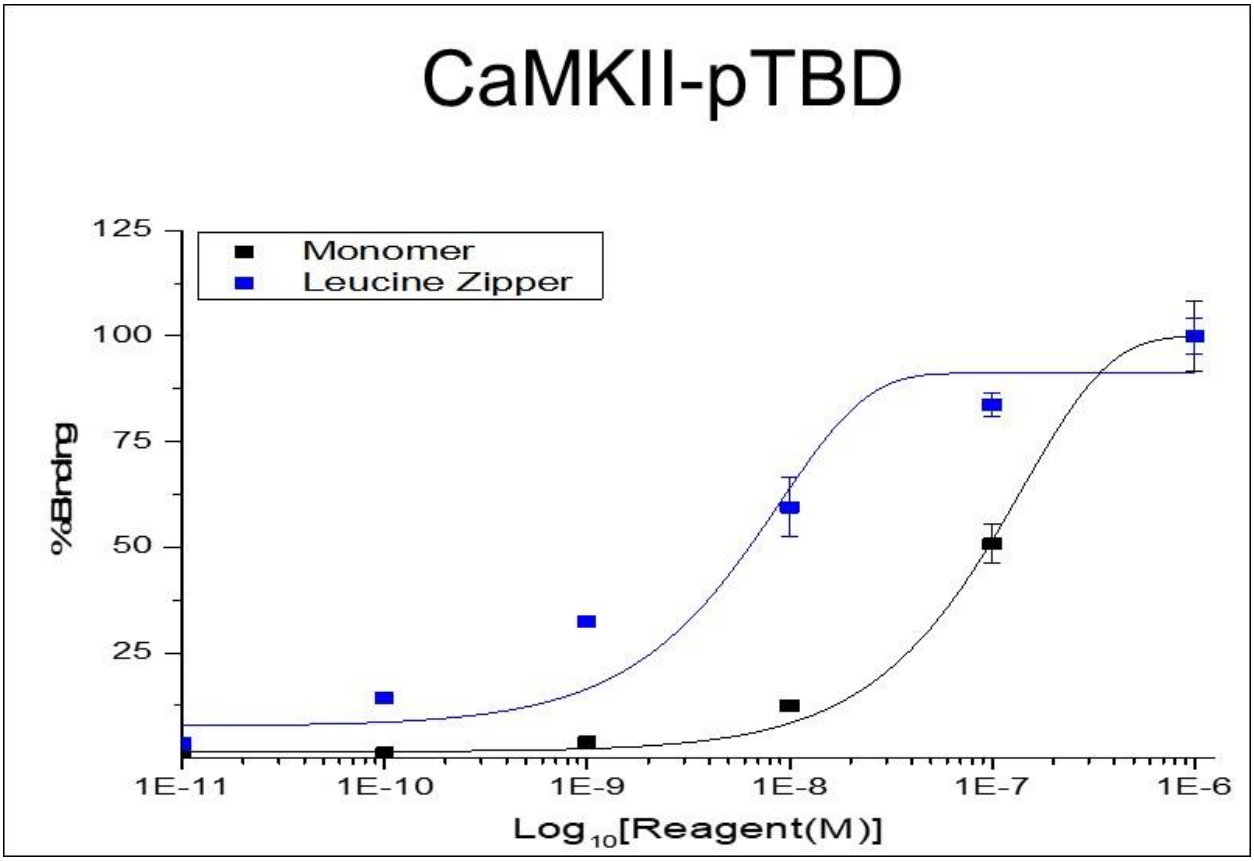

Figure 8. Titration of the CaMKII-pTBD monomer and CaMKII-pTBD dimer. The CaMKII-pT305 peptide was used as a target in an ELISA. The monomeric and dimeric Myc-pTBDs were titrated to determine their EC_{50} values. The M2-HRP antibody was used to detect binding of the pTBDs to the peptide target captured on the surface of microtiter plate wells. All experiments were performed in triplicate and repeated three times to confirm reproducibility. Error bars represent the standard deviation. Absorbance values were recorded at 405 nm wavelength.

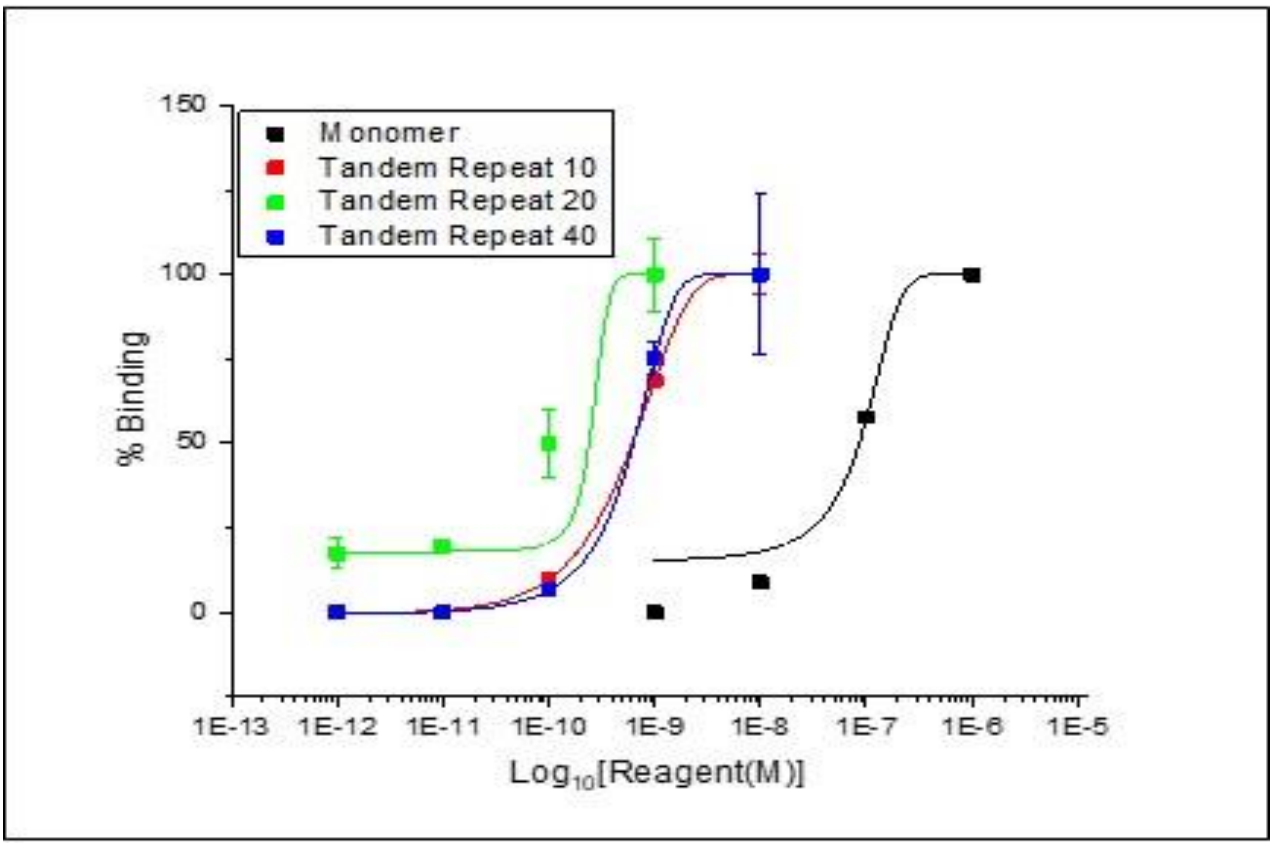

Figure 9. Titration of the Myc-pTBD monomer and Myc-pTBD Tandem Repeats. The Myc-pT58 captured on the surface of a microtiter plate well. The monomeric and dimeric Myc-pTBDs proteins were added well as a range of concentrations to determine their EC_{50} values in this assay format. The amount of pTBDs that were retained in microtiter plate wells with captured target peptide was revealed with the M2-HRP antibody, H_2O2, and a chromogenic substrate. All experiments were performed in triplicate and repeated three times to confirm reproducibility. Error bars represent the standard deviation. Absorbance values were recorded at 405 nm wavelength.

pTBD	Reagent	EC_{50} (M)
Myc	Monomer	$8.5x10^{-8}$
	Leucine Zipper	$4.7x10^{-9}$
	Tandem Repeat 10	$6.1x10^{-10}$
	Tandem Repeat 20	$2.4x10^{-10}$
	Tandem Repeat 40	$6.2x10^{-10}$
ERK	Monomer	$4.2x10^{-8}$
	Leucine Zipper	$1.2x10^{-9}$
CaMKII	Monomer	$9.6x10^{-8}$
	Leucine Zipper	$6.4x10^{-9}$

Table II. EC_{50} values for monomeric and dimeric pTBDs

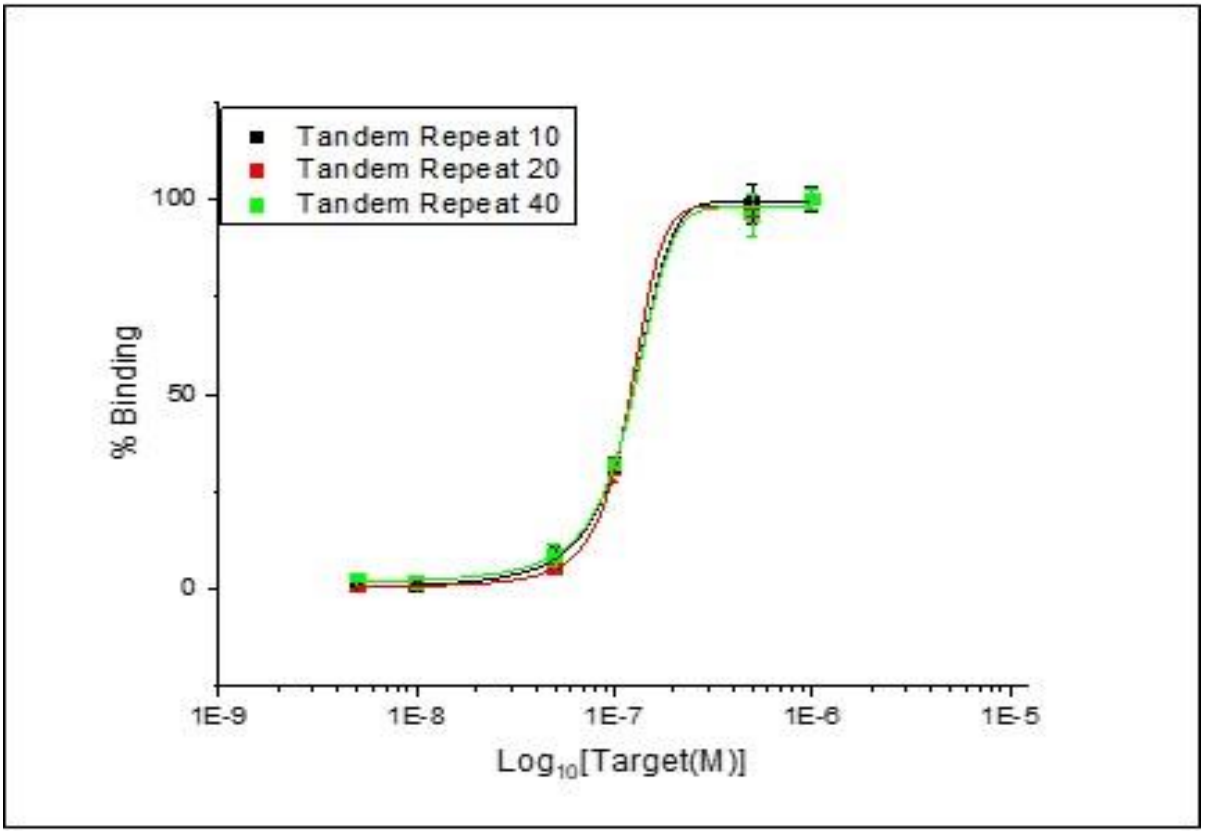

Figure 10. Titration of the Myc-pT58 peptide target. The Myc-pT58 peptide was used as a target in an ELISA. To test the effect of target density, a dilution series of the peptide was used. The TR forms of the pTBDs, with 10, 20, and 40 amino acid long linkers were used as probes in the assay. The M2-HRP antibody was used to detect binding of the pTBDs to the peptide target. All experiments were performed in triplicate and repeated three times to confirm reproducibility. Error bars represent the standard deviation.

with an adjacent peptide ligand. I decided to optimize the linker length by designing a new LZ construct that extends the linker length from 20 to 50 amino acids. This new design would allow the dimer to interact with ligands if the density of the target is low as the extended linker length would allow for a further reach. If successful, in theory I would extend the linker length of the TR reagents. The Myc-pTBD was chosen as a test case because of the detailed characterization for this pTBD that is described in Chapter 3. Although it is difficult to measure the affinity of multimeric reagents using immobilized targets because of avidity [13, 14, 22], surface plasmon resonance (SPR) has been used to measure the affinity of multivalent recombinant antibodies [13, 16, 23] to see if there is an effect. The affinities of the monomer and new Myc-pTBD LZ homodimer and were measured by SPR. The K_d values were 800 nM and 100 nM for the monomer and dimers, respectively (Table III). The data from the SPR experiment suggest that the increase in affinity of the Myc-pTBD homodimer is not due to avidity. This was a surprising result as I was expecting at least a 100-fold improvement in affinity. The modest improvement could have been a result of low target density.

The Myc-pTBD LZ can be used to probe for a phosphorylated target

As previously described in Chapter 3, Myc is phosphorylated on the conserved Serine 62 (Ser62) and Threonine 58 (Thr58) [24]. Phosphorylation on Ser62, by the extracellular signal-regulated kinase (ERK) or cyclin-dependent kinase (CDK), activates transcriptional activity and prevents it from becoming ubiquitinated by ligases and therefore degraded by the proteasome. When Glycogen synthase kinase-3β (GSK3β) phosphorylates Myc at Thr58, there is an additional conformational change [25], which prompts the

	Myc-pT58		
Reagent	**$k_a(M^{-1}s^{-1})$**	**k_d (s^{-1})**	**$K_D(M)$**
Myc-pTBD	$3.2*10^{4}$	$2.6*10^{-2}$	$7.9*10^{-7}$
Myc-pTBD LZ	$2.2*10^{5}$	$1.1*10^{-3}$	$1.0*10^{-7}$

Table III. Affinity measurements of the monomeric and dimeric Myc-pTBD.

dephosphorylation of Ser62 by protein phosphatase 2A (PP2A) [26], ubiquitylation by SCF-Fbw7 E3 ligase, and ultimately degradation by the proteasome [27]. Without the phosphorylation of Ser62, Myc is transcriptionally inactive and GSK3β cannot phosphorylate Thr58. Commercially available antibodies have been used to study Myc activation through western blotting. I took advantage of the Myc activation system to test the Myc-pTBD LZ's ability to probe for the phosphorylation of the full-length Myc protein at Thr58, using the commercially available reagents as controls. Mr. Colin Daniel, in Dr. Rosalie Sears' group at the Oregon Health Science University, prepared HEK 293 cells that ectopically express HA-tagged wild-type and mutant (S62A and T58A) forms of c-Myc. Given the interdependent phosphorylation of Myc, the S62A mutant would serve as the unphosphorylated control and the T58A would serve as a negative control.

The HEK 293 cells that ectopically expressed either the WT or mutant forms of Myc were lysed, electrophoresed, and transferred to a PDVF membrane for blotting. The Myc-pTBD LZ and a polyclonal antibody (pAb) against Myc-pT58 (pAbαMyc-pT58) were used in parallel to probe for Myc-pT58 in the cell lysates. The pAb is specific for Myc-pT58 as no bands were present in blotted lanes containing the S62A or T58A mutants (Fig. 11). The Myc-pTBD LZ failed to detect Myc-pT58 but did react with detected two protein species (>75k Da) in every lane (Fig. 12).

Detecting Myc-pT58 proved to be difficult even for the pAb. This may have been due to a low target density for Myc-pT58. To enrich the target density, Mr. Daniel immunoprecipitated wildtype Myc and each of the mutants from the HEK 293 cell lines with antibodies to the HA tag. The pAbαMyc-pT58 and Myc-pTBD LZ were again used as probes on the western blots. The pAbαMyc-pT58 detected Myc-pT58, whereas the Myc-

pTBD LZ did not (Fig. 13). The signal from the blot demonstrated that the target had been enriched but was still relatively weak suggesting that the target density is still too low. This may explain why, despite the improved affinity, the Myc-pTBD LZ is still unable to probe its target.

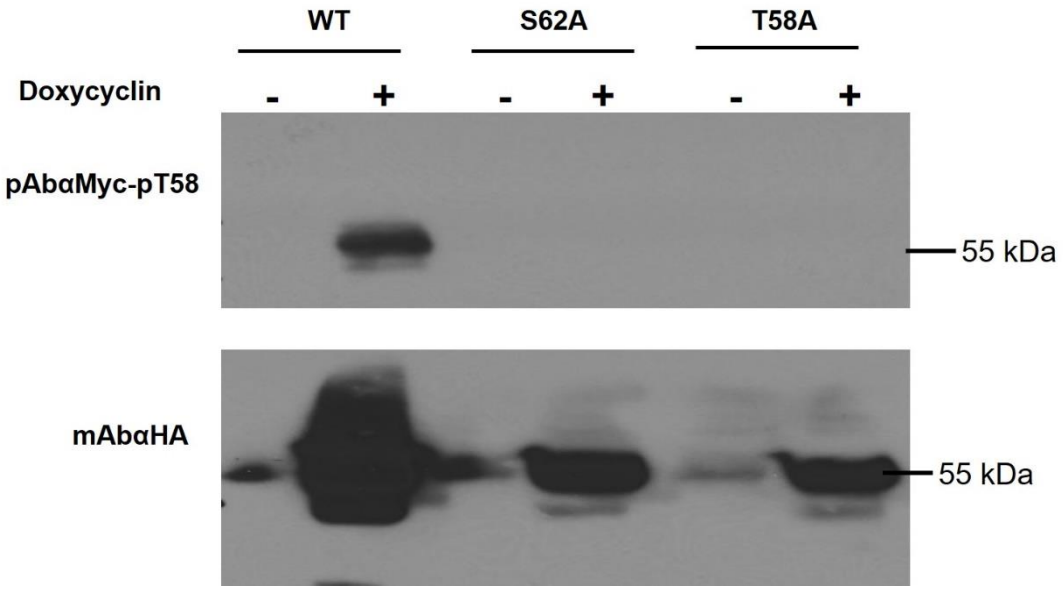

Figure 11. Detection of phosphorylated c-Myc using a commercially available antibody. HA-tagged c-Myc wildtype (WT), c-Myc S62A, and c-Myc T58A recombinant proteins were expressed in HEK 293 stably transfected cell lines. The cells were incubated with Doxycyclin (1µg/ml) 24 hours prior to lysis. The pAbαMyc-pT58 was used as a probe to detect phosphorylation of Thr58. The anti-HA mAb was used to detect the presence of the recombinant Myc protein. The experiment was repeated three times to confirm reproducibility.

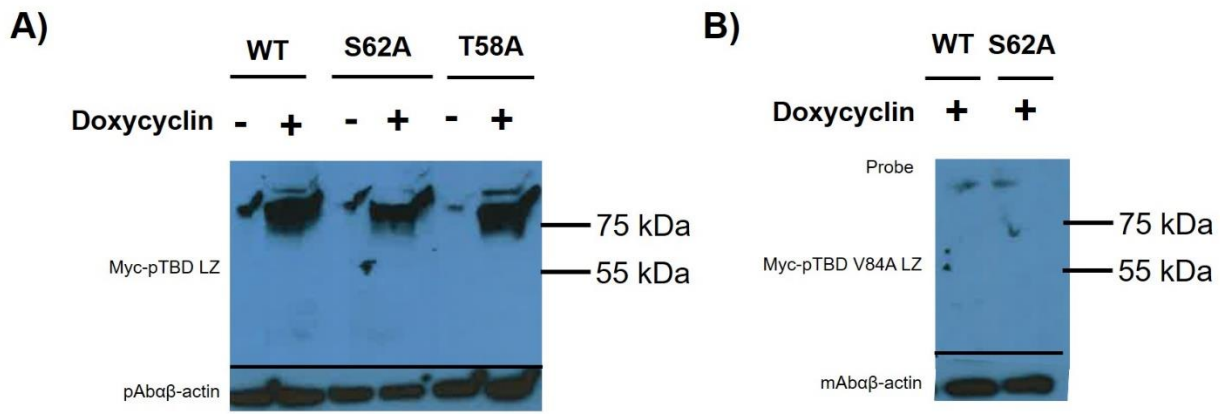

Figure 12. Detection of phosphorylated c-Myc using dimeric Myc-pTBD. HA-tagged c-Myc wildtype (WT), c-Myc S62A, and c-Myc T58A recombinant proteins were expressed in HEK 293 cells. The cells were incubated with Doxycycline 24 hours prior to lysis. Lithium chloride (LiCl) was supplement to all lysates to reduce non-specific binding of the pAbαMyc-pT58. As WT is destabilized due to pThr and prone to ubiquitination and degradation, the WT lysate was supplemented with twice the amount of protease inhibitors. **A.** The Myc-pTBD LZ was used as a probe to detect phosphorylation of Thr58. The pAbαβ-actin served as a loading control. The same set of samples were used in all lanes. **B.** The Myc-pTBD V84A LZ was used as a negative control for detecting pThr58. Actin (detected with a pAbα-Actin antibody, 45 kDa) served as a loading control. The experiment was repeated three times to confirm reproducibility. The blot images are stacked.

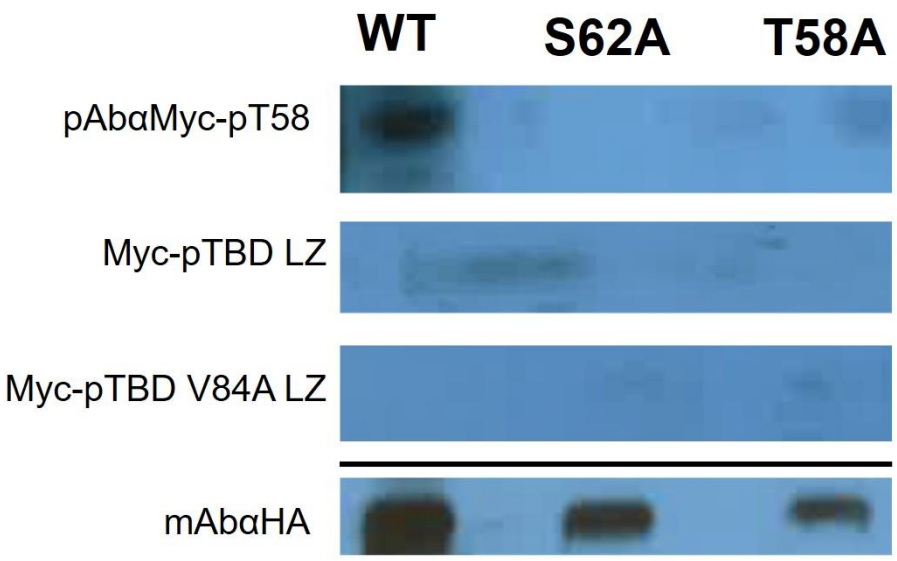

Figure 14. Immunoprecipitation of recombinant c-Myc in HEK 293 cells. Recombinant HA-tagged c-Myc WT, S62A, and T58A proteins were immunoprecipitated from HEK 293 cells using the anti-HA mAb. The pAbαMyc-pT58 (Top), Myc-pTBD LZ (Middle), and Myc-pTBD V84A LZ (bottom) were used as probes for detecting WT Myc. The anti-HA mAb served as a control to detect the presence of the HA-tagged proteins. The experiment was repeated three times to confirm reproducibility

4.5 Discussion

Three pTBDs were dimerized in two manners to improve the apparent affinity of the domain through avidity. While there was an improvement in the binding strength of the Myc-pTBD, it was not as dramatic as seen elsewhere [17]. This may have been due to a low-target density on the membrane, which negatively affects the ability of a multivalent reagent to interact with multiple epitopes. Conversely, the low improvement may be due to the inability of two pTBDs to bind two peptide ligands simultaneously due to steric hinderance. To overcome the target density issue, an alternative larger oligomerization domain may be used. One novel strategy would be to fuse the pTBD to the WD domain that adopts an eight-bladed beta-propeller architecture allowing the pTBD to be displayed eight times. Alternatively, the pTBD could be fused to the CaMKII protein as it folds into a dodecameric structure [28]. which would display the pTBD molecule 20 times per complex. Another potential oligomerization strategy would be to fuse the pTBDs to self-assembling protiens, such as those recently developed by Fallas and colleagues [29]. These homo-oligomers were designed to assemble into dimeric, trimeric, tetrameric, and pentameric stable complexes. Lastly, one could take advantage of using dendrimers for oligomerization of self-assembling ligands [30].

With an enhanced apparent affinity, I used a homodimeric Myc-pTBD to probe for phosphorylated Myc. The Myc-pTBD LZ was unable to detect phosphorylated Myc but it did interact with two proteins in the lysate. Both proteins are established to not be Myc as neither was the correct molecular weight nor did the pAbαMyc-pT58 react with either protein species. Despite the improvement in the Myc-pTBD's affinity, the probable reason

for the reagent's inability to react with Myc is likely due to a low target density on the membrane.

The identity of the two proteins that the Myc-pTBD LZ reacted with on the western blot are unknown. Based on the Myc-pTBD's characterization presented in Chapter 3, the two proteins detected by the domain must be phosphorylated on at least one threonine residue. The top band on the blot is estimated to be ~90 kDa in size, and this band was only present when Myc was either phosphorylated on both S62 and T58 or phosphorylated on S62. As previously described, Myc can only transcribe its downstream targets when it is phosphorylated on Ser62. Both the WT and T58A lines express Myc in this phosphorylated state. As the protein is only detectable by the Myc-pTBD-LZ50 in the lines with Myc-pSer62, it is probable that the larger of the two proteins is a Myc-target gene. Zeller and colleagues [31] have developed a database of genes responsive to Myc. Among the list of genes that are upregulated by Myc is Heat shock 90kDa protein I, alpha-like 3 (HSPCAL3), which is confirmed to be phosphorylated on Thr99 by mass spectrometry [32]. While HSPCAL3 contains an Asp at the pT+3 position, I have not tested to see whether the Myc-pTBD can bind when this particular residue is at the pT+3 position.

In the case of the second band of 75 kDa, this protein is present regardless of Myc's phosphorylation state and only appears in the doxycycline treated cells. Because there is a high level of Myc expression in the induced cells, the second band may be a chaperone protein that is needed to fold the overexpressed Myc protein. The 70 kDa heat shock protein (Hsp70) is involved in the folding and assembly of newly synthesized proteins [33, 34] and have been confirmed to be phosphorylated [35]. Using mass spectrometry, Tsai,

et al. [36] confirmed that Hsp70 is phosphorylated on Thr47 and three residues C-terminal to the pThr47 is a Leu residue. Given that the Myc-pTBD favors Leu at the pT+3 position, it is possible that the Myc-pTBD LZ is reacting with this protein in the blot. Predicting the identity of these two unknown proteins will be useful in optimizing the specificity of the Myc-pTBD and understanding the reagent's inability to recognize phosphorylated Myc.

Continuing to improve upon the pTBD's affinity to make it suitable for use as a probe in western blots remains a challenge. Despite improvements in the Myc-pTBD's affinity as a homodimer, the reagent failed to recognize phosphorylated Myc. Other strategies for improving the domain's utility should be considered. Such strategies include increasing the valency, reformatting for use as an affinity clamp [3], and generating a heterodimeric phosphospecific-reagent. These approaches would expand the utility of pTBDs.

4.6 References

1. Bjorkelund, H., L. Gedda, and K. Andersson, *Comparing the epidermal growth factor interaction with four different cell lines: intriguing effects imply strong dependency of cellular context.* PLoS One, 2011. **6**(1): p. e16536.

2. Pollard, T.D., *A guide to simple and informative binding assays.* Mol Biol Cell, 2010. **21**(23): p. 4061-7.

3. Koide, S. and J. Huang, *Generation of high-performance binding proteins for peptide motifs by affinity clamping.* Methods Enzymol, 2013. **523**: p. 285-302.

4. Richards, J., et al., *Engineered fibronectin type III domain with a RGDWXE sequence binds with enhanced affinity and specificity to human alphavbeta3 integrin.* J Mol Biol, 2003. **326**(5): p. 1475-88.

5. Crook, Z.R., et al., *Mammalian display screening of diverse cystine-dense peptides for difficult to drug targets.* Nat Commun, 2017. **8**(1): p. 2244.

6. Lofdahl, P.A. and P.A. Nygren, *Affinity maturation of a TNFalpha-binding affibody molecule by Darwinian survival selection.* Biotechnol Appl Biochem, 2010. **55**(3): p. 111-20.

7. Duan, J., et al., *Fibronectin type III domain based monobody with high avidity.* Biochemistry, 2007. **46**(44): p. 12656-64.

8. Willuda, J., et al., *Tumor targeting of mono-, di-, and tetravalent anti-p185(HER-2) miniantibodies multimerized by self-associating peptides.* J Biol Chem, 2001. **276**(17): p. 14385-92.

9. Nishimiya, Y., et al., *Thermodynamic consequences of grafting enhanced affinity toward the mutated antigen onto an antibody. The case of anti-lysozyme antibody, HyHEL-10.* J Biol Chem, 2000. **275**(17): p. 12813-20.

10. Yang, W.P., et al., *CDR walking mutagenesis for the affinity maturation of a potent human anti-HIV-1 antibody into the picomolar range.* J Mol Biol, 1995. **254**(3): p. 392-403.

11. Chowdhury, P.S. and I. Pastan, *Improving antibody affinity by mimicking somatic hypermutation in vitro.* Nat Biotechnol, 1999. **17**(6): p. 568-72.

12. Chowdhury, P.S., *Targeting random mutations to hotspots in antibody variable domains for affinity improvement.* Methods Mol Biol, 2002. **178**: p. 269-85.

13. Pluckthun, A. and P. Pack, *New protein engineering approaches to multivalent and bispecific antibody fragments.* Immunotechnology, 1997. **3**(2): p. 83-105.

14. Todorovska, A., et al., *Design and application of diabodies, triabodies and tetrabodies for cancer targeting.* J Immunol Methods, 2001. **248**(1-2): p. 47-66.

15. Vauquelin, G. and S.J. Charlton, *Exploring avidity: understanding the potential gains in functional affinity and target residence time of bivalent and heterobivalent ligands.* Br J Pharmacol, 2013. **168**(8): p. 1771-85.

16. Pack, P., et al., *Improved bivalent miniantibodies, with identical avidity as whole antibodies, produced by high cell density fermentation of Escherichia coli.* Biotechnology (N Y), 1993. **11**(11): p. 1271-7.

17. Pack, P., et al., *Tetravalent miniantibodies with high avidity assembling in Escherichia coli.* J Mol Biol, 1995. **246**(1): p. 28-34.

18. Radnai, L., et al., *Affinity, avidity, and kinetics of target sequence binding to LC8 dynein light chain isoforms.* J Biol Chem, 2010. **285**(49): p. 38649-57.

19. Kierny, M.R., et al., *Generating Recombinant Antibodies against Putative Biomarkers of Retinal Injury.* PLoS One, 2015. **10**(4): p. e0124492.

20. Daniel, C.J., X. Zhang, and R.C. Sears, *Detection of c-Myc protein-protein interactions and phosphorylation status by immunoprecipitation.* Methods Mol Biol, 2013. **1012**: p. 65-76.

21. Venegas, L.A., et al., *A comparison of phosphospecific affinity reagents reveals the utility of recombinant Forkhead-associated domains in recognizing phosphothreonine-containing peptides.* N Biotechnol, 2016. **33**(5 Pt A): p. 537-43.

22. Muller, K.M., K.M. Arndt, and A. Pluckthun, *Model and simulation of multivalent binding to fixed ligands.* Anal Biochem, 1998. **261**(2): p. 149-58.

23. Adams, G.P., et al., *Prolonged in vivo tumour retention of a human diabody targeting the extracellular domain of human HER2/neu.* Br J Cancer, 1998. **77**(9): p. 1405-12.

24. Sears, R.C., *The life cycle of C-myc - From synthesis to degradation.* Cell Cycle, 2004. **3**(9): p. 1133-1137.

25. Sears, R., et al., *Multiple Ras-dependent phosphorylation pathways regulate Myc protein stability.* Genes & Development, 2000. **14**(19): p. 2501-2514.

26. Yeh, E., et al., *A signalling pathway controlling c-Myc degradation that impacts oncogenic transformation of human cells.* Nature Cell Biology, 2004. **6**(4): p. 308-318.

27. Wang, X.Y., et al., *Phosphorylation Regulates c-Myc's Oncogenic Activity in the Mammary Gland.* Cancer Research, 2011. **71**(3): p. 925-936.

28. Chao, L.H., et al., *A mechanism for tunable autoinhibition in the structure of a human Ca2+/calmodulin- dependent kinase II holoenzyme.* Cell, 2011. **146**(5): p. 732-45.

29. Fallas, J.A., et al., *Computational design of self-assembling cyclic protein homo-oligomers.* Nat Chem, 2017. **9**(4): p. 353-360.

30. Franc, G., et al., *Dendritic structures within dendritic structures: dendrimer-induced formation and self-assembly of nanoparticle networks.* Nanoscale, 2009. **1**(2): p. 233-7.

31. Zeller, K.I., et al., *An integrated database of genes responsive to the Myc oncogenic transcription factor: identification of direct genomic targets.* Genome Biol, 2003. **4**(10): p. R69.

32. Martins-de-Souza, D., et al., *Phosphoproteomic differences in major depressive disorder postmortem brains indicate effects on synaptic function.* Eur Arch Psychiatry Clin Neurosci, 2012. **262**(8): p. 657-66.

33. Mayer, M.P. and B. Bukau, *Hsp70 chaperones: cellular functions and molecular mechanism.* Cell Mol Life Sci, 2005. **62**(6): p. 670-84.

34. Mayer, M.P., *Recruitment of Hsp70 chaperones: a crucial part of viral survival strategies.* Rev Physiol Biochem Pharmacol, 2005. **153**: p. 1-46.

35. Cho, H.S., et al., *Enhanced HSP70 lysine methylation promotes proliferation of cancer cells through activation of Aurora kinase B.* Nat Commun, 2012. **3**: p. 1072.

36. Tsai, C.F., et al., *Large-scale determination of absolute phosphorylation stoichiometries in human cells by motif-targeting quantitative proteomics.* Nat Commun, 2015. **6**: p. 6622.

Chapter 5

Conclusions

Dr. Stefanie Kall rendered all structural images.

5 Chapter 5

5.1 Introduction

While antibodies have proven to be useful tools for monitoring phosphorylation events, there are limitations in their production, renewability, and specificity [1-8]. Recombinant affinity reagents are attractive alternatives for studying protein phosphorylation as they do not have the same deficiencies as antibodies. In this thesis, I describe the generation of recombinant affinity reagents to pThr-containing peptides corresponding to a variety of human protein kinases and transcription factors. I characterize and identify the molecular determinants of specificity for the affinity reagents, termed phosphothreonine binding domains (pTBDs), through various biochemical and structural analyses. I also demonstrate that pTBDs are comparable in specificity to commercially available antibodies, which indicates that these reagents can be considered potential alternatives to antibodies. Finally, I improve the affinity of the reagents through homodimerization, which may enable them to be used as probes in western blots.

The work described in this thesis provides an in-depth characterization of a single, engineered pTBD. With this level of characterization, one can move forward in improving the affinity and specificity of the FHA scaffold. In the final chapter of my thesis, I use structural analysis to explain the changes that were needed to use the FHA1 domain as a scaffold for phage display affinity selection. I then introduce ideas for improving the affinity of the pTBD and conclude by discussing strategies for evolving the FHA domain to recognize pSer in peptide ligands.

5.2 The Myc-pTBD structure helps explain prior protein engineering experiments

My work led to solving the crystal structure of an engineered pTBD, complexed with its peptide ligand. The structure provides information as to why certain mutations were necessary for the domain to function as a scaffold in initial phage experiments. When the FHA1 domain was originally selected as a scaffold, it was fused to the minor coat protein III (p3) of the M13 bacteriophage for display on the virus coat. When Dr. Kritika Pershad evaluated recombinant virions, she did not observe any interaction of the displayed domain for its peptide ligand. After confirming that the FHA1 was being displayed on the virus, Dr. Pershad reasoned that the domain's inability to interact with its peptide ligand might be due to misfolding of the domain in the bacteria's periplasm during viral packaging. Examination of the FHA1's crystal structure revealed that the domain contains four cysteine (Cys) residues at positions 34, 38, 74, and 154. Given that the FHA1 domain misfolding may be due to improper disulfide bond formation, Pershad *et al.* [9] replaced either three (3C-3S) or four (4C-4S) cysteine residues with serine. Even though the 3C-3S and the 4C-4S mutants were displayed on recombinant virions, they still failed to fold properly and bind to the peptide ligand. To rescue functionality through directed evolution, a small library ($2x10^4$) of 3C-3S variants was generated through error-prone polymerase chain reaction (epPCR) and affinity selected to isolate a FHA1 domain variant that bound its peptide ligand. DNA sequencing of the D2 variant revealed that it carried the S34F mutation (Fig. 1). In collaboration with Dr. Stefanie Kall, I *in silico* modelled the mutation in the Myc-pTBD structure. In the Myc-pTBD three-dimensional structure (Fig. 2), the Phe34 residue creates an extensive hydrophobic network within the core of the domain, which the Cys34 residue is not able to replace. The increased interactions with the

A.

```
FHA1                1 MENITQPTQQSTQATQRFLIEKFSQEQIGENIVCRVICTTGQIPIRDLSA
FHA1 D2             1 MENITQPTQQSTQATQRFLIEKFSQEQIGENIVFRVISTTGQIPIRDLSA

FHA1               51 DISQVLKEKRSIKKVWTFGRNPACDYHLGNISRLSNKHFQILLGEDGNLL
FHA1 D2            51 DISQVLKEKRSIKKVWTFGRNPACDYHLGNISRLSNKHFQILLGEDGNLL

FHA1              101 LNDISTNGTWLNGQKVEKNSNQLLSQGDEITVGVGVESDILSLVIFINDK
FHA1 D2           101 LNDISTNGTWLNGQKVEKNSNQLLSQGDEITVGVGVESDILSLVIFINDK

FHA1              151 FKQCLEQNKVDRIRSNLKNT
FHA1 D2           151 FKQSLEQNKVDRIRSNLKNT
```

B.

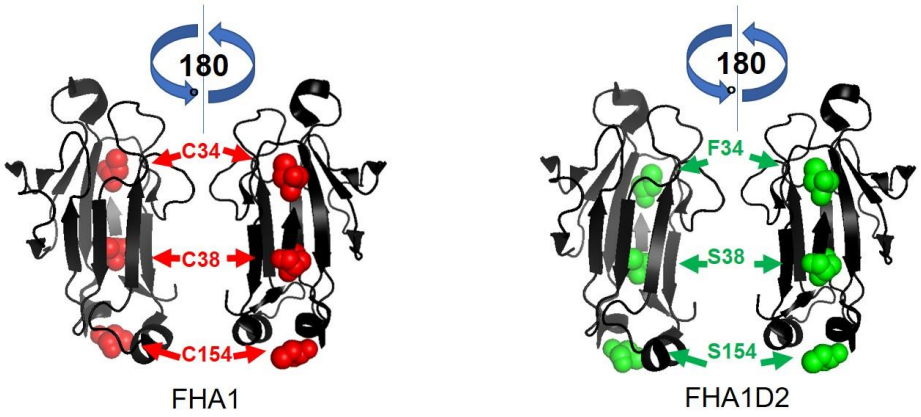

Figure 1. A comparison of the FHA1 and FHA1D2 domains. A. A sequence alignment of the FHA1 and FHA1D2 domains. The three Cys residues of the FHA1 domain are highlighted in red, and amino acid changes in the FHA1D2 mutant are highlighted in green. **B.** The FHA1 domain (PDB 1G6G) is represented in a cartoon format (black), and residues highlighted residues in **A** are represented as spheres. Colors are consistent between the primary and three-dimensional structures. The FHA1 domain is rotated 180° as visualized by showing two copies of the domain. The FHA1 with its native amino acids is on the left while the FHA1D2 with its mutated residues (green) is on the right.

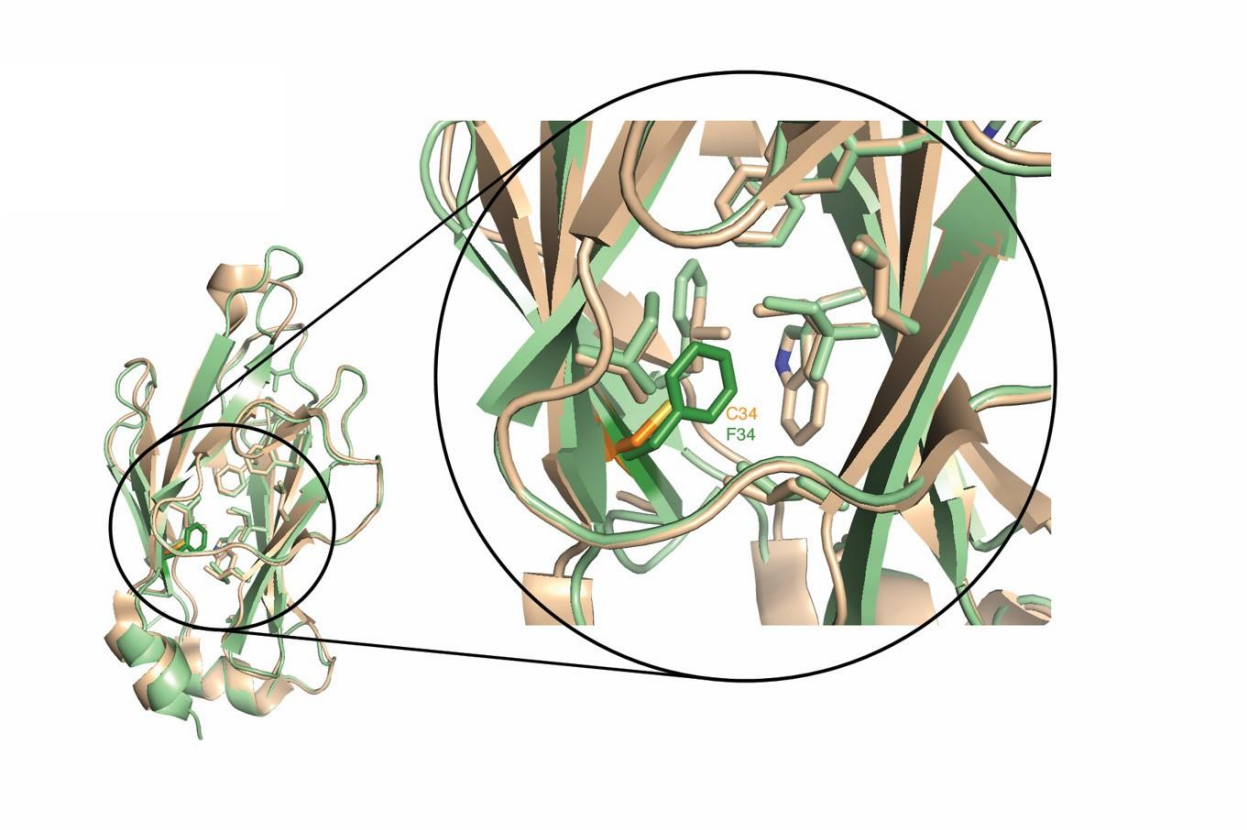

Figure 2. Phe34 creates a hydrophobic network within the core of the pTBD. Cartoon overlay of the three-dimensional structures of FHA1 domain (PDB ID: 1G6G; wheat) and Myc-pTBD (PDB ID: 6C4U; pale green). The FHA1's Cys34 and Myc-pTBD's Phe34 residues are in stick format and represented in orange and forest green colors, respectively. Amino acids within 5 Å of Phe34 are also represented in stick format.

surrounding residues likely improve the domain's stability when displayed on virions. This structural analysis supports observations [9] that only hydrophobic residues at position 34 yield a FHA1 domains that fold properly and are capable of binding the peptide ligand. This analysis does not, however, explain why the domain is unable to properly fold in the periplasm when Cys is present at position 34. One explanation is that there are different protein-folding chaperones in the cytoplasm compared to the periplasm; presumably, the chaperones in the periplasm are able to fold the virus-displayed domain when Cys at position 34 is replaced with Phe.

Improving thermostability was the next step in the directed evolution of the FHA1D2 scaffold. Thermostability is an important attribute because reagents are often used in assays conducted at room or elevated temperatures, thermostable proteins accumulate to a higher degree when overexpressed in *E. coli*, and they remain soluble at higher concentrations [10]. The thermostability profile of FHA1D2 was initially 5°C lower compared to the FHA1 domain [9]. To improve D2's thermostability, Pershad *et. al.*[9], constructed a mutagenic library ($2x10^7$) through epPCR of the D2 coding sequence. To select for thermostable FHA variants, the library was heated to 50ºC and thermostable variants that remain folded and functional were affinity selected. The resulting FHA1G2 variant has a melting temperature (T_m) of 73.8°C, compared to the D2 clone whose T_m is 61.6°C, reflecting a 12°C improvement in thermostability. DNA sequencing revealed three new mutations within the thermostable variant (Fig. 3): T15A, L48F, and N121Y.

To understand how these three amino acid substitutions might contribute to thermostability, I examined the Myc-pTBD's three-dimensional structure. *In silico* modeling provides insight into how the mutated residues interact with other residues in

```
FHA1 D2              1 MENITQPTQQSTQATQRFLIEKFSQEQIGENIVFRVISTTGQIPIRDLSA
FHA1 G2              1 MENITQPTQQSTQAAQRFLIEKFSQEQIGENIVFRVISTTGQIPIRDFSA

FHA1 D2             51 DISQVLKEKRSIKKVWTFGRNPACDYHLGNISRLSNKHFQILLGEDGNLL
FHA1 G2             51 DISQVLKEKRSIKKVWTFGRNPACDYHLGNISRLSNKHFQILLGEDGNLL

FHA1 D2            101 LNDISTNGTWLNGQKVEKNSNQLLSQGDEITVGVGVESDILSLVIFINDK
FHA1 G2            101 LNDISTNGTWLNGQKVEKNSYQLLSQGDEITVGVGVESDILSLVIFINDK

FHA1 D2            151 FKQSLEQNKVDRIRSNLKNT
FHA1 G2            151 FKQSLEQNKVDRIRSNLKNT
```

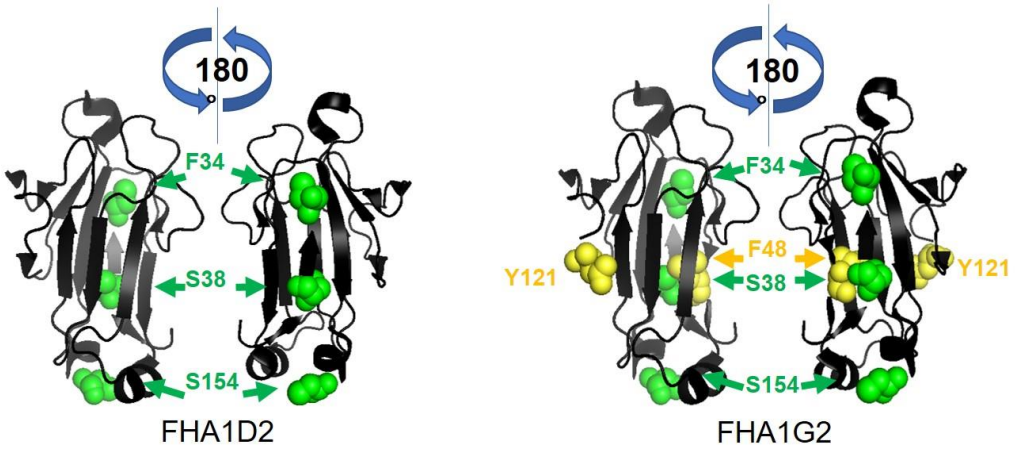

Figure 3. Comparison of the FHA1D2 and FHA1G2 domains. A. Sequence alignment of the FHA1D2 and FHA1G2 variants. The three mutations in FHA1D2 are highlighted in green, and amino acid changes in the FHA1G2 are highlighted in yellow. **B.** The FHA1 domain (PDB 1G6G) is represented as a cartoon (black): highlighted residues in the domains are represented as spheres, and colors in the structure correspond to those in the sequence alignment (**A**). Short arrows point to the amino acid indicated by the text. The domain is rotated 180° (long arrows) to show all highlighted residues. Colors are consistent between the primary and three-dimensional structures. The FHA1 domain is rotated 180° as visualized by showing two copies of the domain. The three-dimensional structure of the FHA1D2 variant, with its native amino acids (green), is shown on the left, while the FHA1G2 variant, with its mutated residues (yellow), is shown on the right.

the domain. One caveat to the analysis is that the T15A mutation is part of the Myc-pTBD's truncated region. As there was no difference in thermostability between the truncated and full-length domains (data not shown), I suspect that the T15A mutation is not solely responsible for the engineered domain's overall improved thermostability. The potential impact of the other two mutations, L48F and N121Y, was assessed *in silico* (Fig. 4). The FHA1G2's L48F mutation positions the Phe48's R-group within 5 Å of the Phe34. The close proximity of the two Phe residues may have led to the G2's improved thermostability, as Budyak, *et al.* [11] observed that pi-pi interactions help stabilize a protein's native state. The N121Y mutation does not appear to contribute to any intramolecular interactions; rather it appears capable of forming a salt bridge with N102 of an adjacent monomer, which is conserved in both constructs. As size exclusion chromatography confirms that the pTBD is monomeric in solution, the observed N102 salt bridge is likely a result of hexamer formation during crystallization. Taken together these data suggest that the improved thermostability is likely due to the L48F mutation, as there is no direct evidence for T15A and N121Y contributing to thermostability. To test this conclusion, one could generate an F48L mutation in the Myc-pTBD and compare its thermostability to FHA1, FHA1D2, and Myc-pTBD in a fluorescence thermal shift assay with the expectation being that the mutated Myc-pTBD will have a similar profile as the FHA1D2 clone.

5.3 Potentially improving the affinity of the pTBD through heterodimeriztion with a recombinant antibody

In Chapter 4, I homodimerized the Myc-pTBD for the purpose of increasing its apparent affinity and probed western blots of either whole cell lysates or c-Myc, which

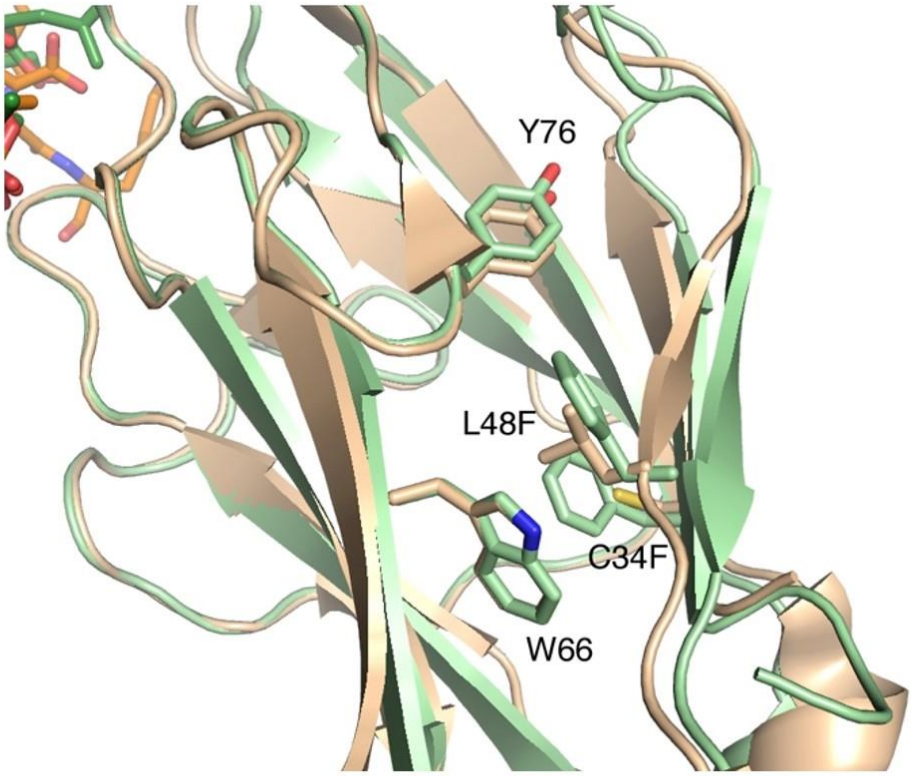

Figure 4. The hydrophobic core of the engineered domain. Cartoon overlay of the published FHA1 domain wild-type structure (PDB ID: 1G6G; wheat) and the Myc-pTBD (PDB ID: 6C4U; pale green). The overlay shows that the C34F mutation within the hydrophobic core of the domain. The R-groups of selected amino acids are represented in the stick format.

had been partially purified through immunoprecipitation (i.e., IP-western). While I was unable to detect Myc-pT58 in either case, two bands were visible in western blots. I interpret the failure to detect the Myc as due to its low abundance in HEK-293 cells engineered to overexpress the protein, even after immunoprecipitation. As with regard to the two reactive protein species observed in the western blots, their sizes (75 and 90 kDa) differ from that of Myc (53 kDa); I suspect that they happen to carry phosphopeptides sequences similar to that of Myc pT308 and they are significantly more abundant than Myc. As no bands are evident on western blots probed with a “dead" pTBD, incapable of binding phosphopeptides, the 75 and 90 kDa protein species likely have the sequence pTxxL. Their ultimate identification will require future experimentation.

One approach to overcome the inability of the pTBD to detect c-Myc on western blots might be to create a heterodimeric, two-site capable affinity reagent. Recently, Gorman *et al.* [12], developed a method, termed Megaprimer Shuffling for Tandem Affinity Reagents (MegaSTAR), that identifies non-competitive binding pairs of affinity reagents through phage display. In this method, two Fibronectin type III (FN3) domains, preselected for binding the target, are tandemly displayed on the phage surface, and tight binders are isolated by affinity selection. The resulting clones carry pairs of FN3 domains that are capable of binding simultaneously to two different sites on the target. These bivalent reagents have an estimated affinity of 2 nM. To generate the two-site capable phosphospecific affinity reagents, a second scaffold capable of interacting with peptide targets would be needed to be identified and chosen for dimerization with the FHA domain. Dr. Michael Kierny previously used an single-chain variable fragment (scFv) phage library to screen for variants against peptides of putative biomarkers of retinal

damage [13], demonstrating that scFvs are a good scaffold for isolating variants against peptide targets. scFvs are single polypeptides that contain two variable regions, a heavy (V_H) and light (V_L) domain, that are linked together through a flexible linker sequence [14]. The V_H and V_L domains come together in an scFv to form a groove that binds peptides [15].

To follow this proposed strategy, one would first build a new vector. The coding regions of the engineered FHA domain and scFv would be cloned into a tandem display vector, as described by Dr. Gorman [16] (Fig. 5). To isolate the two-site capable phosphospecific affinity reagents, three rounds of selection with the FHA and scFv libraries would be performed in parallel. A pThr-containing peptide and a peptide sequence, 20 residues N- or C-terminal to the pThr residue on the protein, would serve as targets for the FHA and scFv libraries, respectively (Fig. 6B). A pool of 500- and 750-nucleotide long FHA and scFv megaprimers, respectively, would be used to prime second strand DNA synthesis and generate millions of pair-wise combinations (Fig. 6C). The resulting pTBD-scFv library could then be affinity selected to yield pairs of two-site capable affinity reagents, composed of one pTBD and one scFv (Fig. 6D).

In a proof of principle experiment, the phosphorylated transcription factor c-Myc is an ideal candidate target because of the lab's familiarity with the protein. It is important to note that this approach is well suited for a protein that is denatured and unfolded on a western blot membrane. The first peptide target in the selection process would be the Myc-pT58 peptide that has been previously used in selection. A second peptide target will be required for selection of the phage-displayed scFv library. This new target should be selected from a region of Myc that is proximal to the pThr58 site. While, it is difficult to

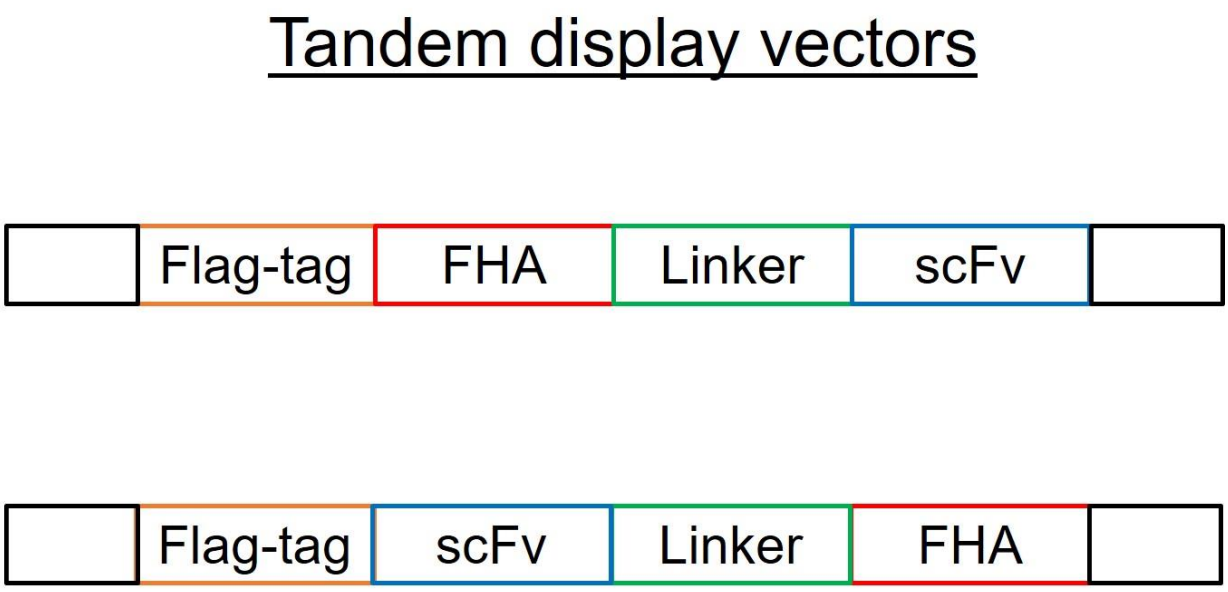

Figure 5. Construction of the tandem display vector. Proposed two tandem display vectors for use in the construction of the MegaSTAR library. The top vector places the FHA at the N-terminus of the protein and the human single-chain Fragment of variable regions (scFv) at the C-terminus, whereas the bottom vector places the scFv at the N-terminus of the protein and the FHA at the C-terminus.

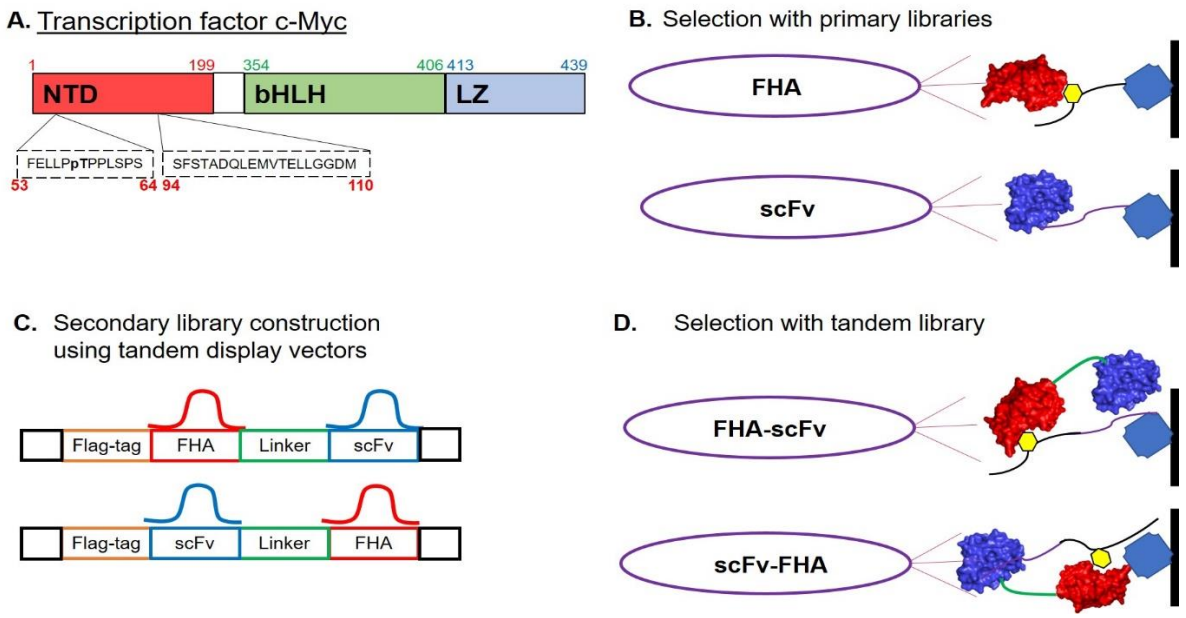

Figure 6. Workflow proposed for isolating phosphospecific two-site capable affinity reagents. The Myc-pTBD (red) and an scFv (PDB: 1P4I; tv blue) are represented as cartoons. The Myc-pT58 (black), Myc-Cterm (purple), and combination of the Myc-pT58 and Myc-Cterm peptides (black and purple) are represented as thin lines. The combination of the Myc-pT58 and Myc-Cterm peptides would allow the tandem displayed domains to simultaneously interact with the target peptide. The phosphate group is represented as a yellow hexagon. All peptides are immobilized using streptavidin (blue box). **A.** Structural domains of transcription factor c-Myc. c-Myc is comprised of the N-terminal domain (NTD, red), a basic helix-loop-helix domain (bHLH, green), and a leucine zipper domain (LZ, blue). The insert of residues 53-64 and 94-110 of the NTD correspond to the peptides proposed in this experiment. The boundaries of each domain are denoted in the color corresponding to the domain type. The figure is adapted from Venegas *et al.* [17]. **B.** Parallel selection of the Myc target peptides using phage libraries displaying FHA or scFv. **C.** Secondary library construction using the tandem display vectors. **D.** Selection of clones from tandem display libraries.

guess what an ideal distance from the pThr58, the new target would be relative to the pThr58 site; one possibility would be to select a region of Myc about 20 amino acids N-terminal to the pThr58 position. One target sequence could be 93-SFSTADQLEMVTELLGGDM-110 of My, which is 35 residues C-terminal to the pThr58 site, which may allow for simultaneous recognition of the FHA and scFv without steric hinderance.

The phosphospecific two-site capable reagents could be used as probes in western blots. After isolation of the two-site capable heterodimeric reagents, I could first test the reagent by probing western blots of activated Myc in the same lysates that I used in Chapter 4. The recombinant Myc variants (WT, S62A, and T58A) would be immunoprecipitated using the anti-HA antibody and probed in the blot with the two-site capable reagent. The pAb anti-Myc-pT58 and anti-HA antibodies would serve as positive controls in the experiment. In this strategy, the IP would enrich the local target concentration on a western blot, possibility yielding positive binding bands.

Alternatively, one could use the FHA domain and scFv to design affinity clamps for probing Myc by western blot. Affinity clamps are recombinant proteins where a primary domain is connected to a secondary domain [18]. The primary domain interacts weakly with a peptide ligand while the secondary domain swings on top of the peptide to “clamp” the peptide between the two domains; such an approach would lead to clamping on both sides of the peptide. The FHA domain would serve to recognize the phosphothreonine and pT+3 position, while the scFv would serve to bind on the opposite side of the peptide ligand.

5.4 Evolving the pTBD to allow for recognition of N-terminal residues

After evolving the FHA1 domain for use as a scaffold in phage display affinity selection, Dr. Pershad and colleagues [9] were able to isolate engineered pTBDs against pThr-containing peptides corresponding to a variety of protein kinases and transcription factors. I continued to use the scaffold to isolate additional pTBDs with the goal of creating a set that could probe all proteins in the ERK signal transduction pathway. In conjugation with Dr. Pershad's early work, and more recently with Ms. Jennifer McGinnis, pTBDs were isolated against a total of 14 out of 17 targets, reflecting an 82% rate of success [9, 19, 20]. A high success rate suggested that the strategy of altering the specificity a domain that naturally recognizes a phosphorylated target to isolate variants against pThr-containing peptides was sound. The next logical step in the project was to characterize a single pTBD and understand the scaffold's limitations.

I established that all engineered pTBDs are both pThr-dependent and specific. I then investigated what factors influence the success rate of isolating a FHA domain variant to a given phosphothreonine-containing peptide. I found that the pT+3 position in the peptide was not only crucial for the protein-peptide interaction, but it was also the major determinant of specificity. These findings led me to conclude that the pT+3 position was a key factor in the selection of pTBDs to pThr-containing peptides.

The crystal structure of the Myc-pTBD revealed the presence of a pocket for the Leu at the pT+3 position in the peptide ligand and demonstrated that the domain can only interact with the R-groups that are capable of filling the pocket. Furthermore, it is also possible that a non-canonical R-group, such as *Norleucine,* could fill the domain's hydrophobic pocket leading to the development of a possible peptidomimetic inhibitor.

The structure of the FHA domain from Tumor necrosis factor-associated factor-interacting protein with a Forkhead-associated domain (TIFA) was recently solved in complex with its peptide ligand (Fig. 7). The structure revealed that the FHA of TIFA recognizes residues N-terminal positions (pT-4 to the pT+1) on its peptide from TIFA (MTSFEDAD**pT**EETVTC) with a dissociation constant (K_d) of 34 μM. The most critical interactions between the domain and the peptide being the residues at the pT-2 and pT-3 positions [21]. Compared to the Myc-pTBD, the FHA of TIFA uses different loop regions to interact with its peptide. The FHA of TIFA uses the β3-β4 and β4-β5 loop regions, whereas the engineered FHA uses the β4-β5 and β10-β11 loops. Another major difference is that there are three critical positions on the FHA of TIFA's peptide: pT-2, pT-3 and pThr positions. These differences suggest an opportunity for improve the specificity of pTBDs.

Based on the TIFA structure, one way to improve the specificity of pTBDs would be to create more contact sites with their peptide ligands. Because the FHA1 domain and its variants already recognize one residue C-terminal to the pThr, including design elements of the TIFA domain might increase its number of contact sites with a peptide ligand and improve its affinity and specificity. As a proof of principle experiment, the Myc-pTBD's β3-β4 loops could be chimerized with the FHA domain of TIFA. (A construct containing Myc-pTBD and TIFA's β3-β4 loops will be referred to as the 'chimeric FHA' (cFHA) for the remainder of this discussion.) The functionality of the cFHA could be evaluated in ELISA with a large set of peptides. For example, the N-terminus of the peptide would contain residues from the FHA of TIFA's peptide (MTSFEDAD**pT**) and the C-terminus would contain residues from the Myc-pTBD's ligand (PPLSPS) to create the chimeric peptide

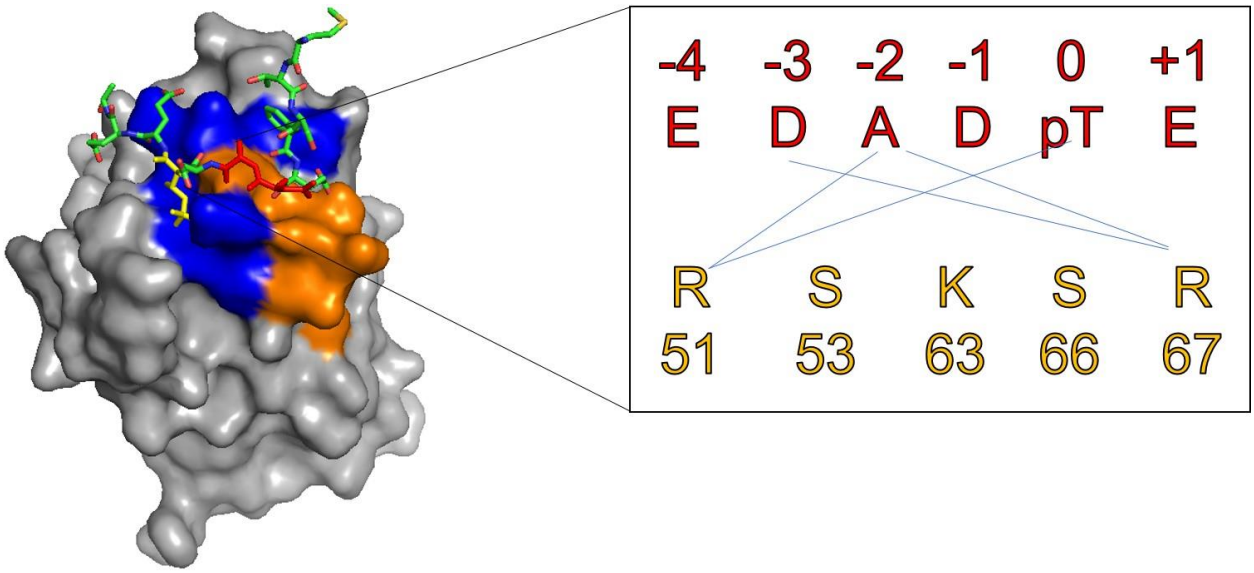

Figure 7. The TIFA-FHA interacting with the TIFA-pT9 peptide. The TIFA-FHA domain (PDB 4ZGI) is represented in the surface view, and the TIFA-pT9 peptide is represented as sticks. The β3-β4 loop is highlighted in orange and the β4-β5 loop is highlighted in blue. The region of the TIFA-pT9 peptide that is critical for binding is highlighted in red. The pThr is highlighted in yellow. Residues in the box that correspond to the peptide and domain are represented in red and orange, respectively. The blue lines indicate which residues on the domain interact with the residues on the peptide. The numbers above the amino acid residues indicate their position on the peptide relative to the pThr moiety. The numbers below the residues from the domain indicate their sequence position. The figure is adapted from [21].

ligand (MTSFEDAD**pT**PPLSPS). If successful, a library of chimeric FHA domain variants could be constructed by randomizing the chimera's β3-β4, β4-β5 and β10-β11 loop regions with NNK codons. The resulting library of cFHA variants could then be used in phage display experiments to select binders to the Myc-pT58 peptide. An alanine scan of the peptide would be an ideal way to confirm that residues N-terminal to the pThr contribute to pTBD binding.

5.5 Evolving the FHA domain to recognize pSer-containing peptides

Protein phosphorylation is a post-translation modification involved in the regulation of signaling networks [22, 23]. Studying signaling networks involves the identification and characterization of phosphosites. Most eukaryotic proteins contain more than one phosphorylatable site (phosphosite), which primarily occurs on serine (89%), threonine (10%), and tyrosine (<1%) residues [24-27]. Probing for phosphoserine (pSer) has been difficult as many antibodies are cross-reactive with pThr residues. Generating a pSer-specific would be a valuable tool for studying protein phosphorylation, and a useful companion to pTBDs.

Early in my Ph.D. thesis research, I tested the hypothesis that the FHA library might contain a variant capable of binding a pSer-containing peptide but was unsuccessful. I interpret this failure to the fact that the FHA's pocket that is responsible for interacting with the pThr's γ-methyl group was unchanged during library construction. Structural analysis of the Myc-pTBD confirmed that the engineered domain uses Arg70, Asn86, Ser85, and Thr106 to interact with the pThr's phosphoryl group. Like the FHA1 [28], the

interaction between the Myc-pTBD and the Thr's γ-methyl group orients the phosphoryl group to interaction with the conserved residues.

With knowledge of the interaction between the pThr and the domain, it might be possible to alter the specificity of the engineered FHA from pThr to pSer. One approach would be to generate single or multiple amino acid replacements in the FHA domain and then affinity selection for binding to peptide carrying a pSer moiety. Modeling the Myc-pTBD *in silico* suggests several candidate positions to change: Arg70, Asn86, Ser85, or Thr106. Thr106 appears to be a promising starting point because it is positioned in such a way as to stabilize Ser's R-group (Fig. 8). Amino acids with long R-groups such as Glutamic acid (Glu) or Lysine (Lys) are good candidates to replace Thr106; modelling suggest that the Glu and Lys R-groups might still interact with the phosphoryl group and the backbone of the peptide (Fig. 8). Such mutations can be easily constructed and tested in ELISA for binding to the Myc-pT58pS peptide variant.

Alternatively, all 20 amino acids could be substituted at any given position with the NNK codon scheme to generate a phage library of pTBD variants. The library would then be used to screen for pTBD variants that interact with pSer and not pThr. The Myc-pTBD can be used as a scaffold. Once a library of Myc-pT variants is constructed, it could be screened with the Myc-pT58pS peptide as a target for affinity selection. To avoid cross-reactive variants that might be isolated, counter selection step would use the Myc-pT58 peptide, to prevent recovery of FHA variants that do not discriminate between pSer and pThr in the peptide ligand. Once a pSer-specific and -dependent domain is isolated and characterized, I could then use such a clone as a template (i.e., scaffold) for constructing

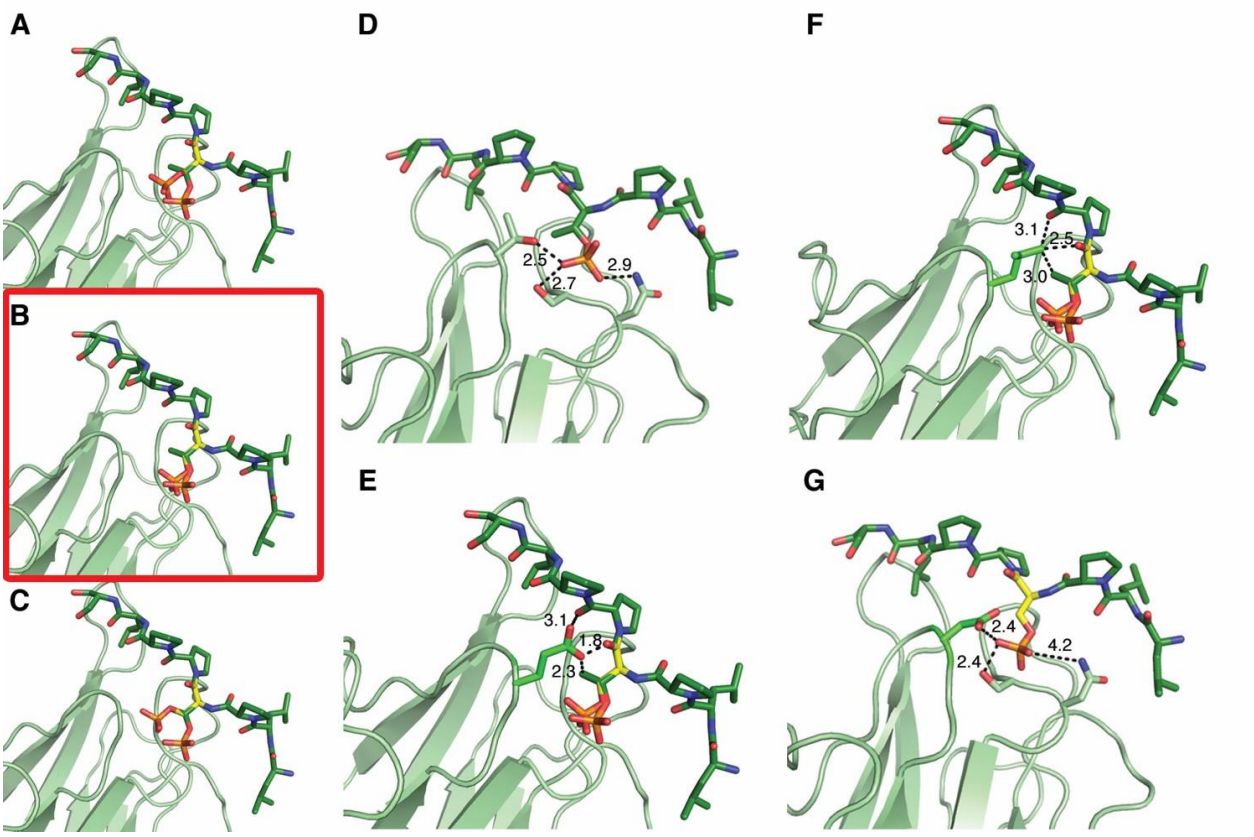

Figure 8. Modeling a pSer-specific FHA domain. A-C. show the three major conformers of pSer (yellow) substituted for the pThr (forest green) position in the Myc-pTBD (PDB ID: 6C4U; pale green). The phosphoryl groups are colored orange. Conformer 2 (red box) most closely mimics the structure. **D.** The residues responsible for orienting the pThr of the Myc-pT58 and the distance in Ångstroms. **E.** A model of the T106E mutation. **F.** The T106L mutation. **G.** A model of the T106D mutation.

affinity reagents to pSer-containing proteins such as Estrogen Receptor alpha-pS118 [29], α-syn-pS129 [30], and tau-pS181 [31].

Having both pSer and pThr specific binding domains would be useful for generating affinity reagents against many phosphorylated proteins. For example, a set of reagents that bind Myc-pS62 and Myc-pT58 could be used in cell-staining assays to determine the localization of each state of Myc.

5.6 Developing the Myc-pTBD as a probe for Myc-pThr58 localization

The next step in evaluating the Myc-pTBD will be to use it to monitor phosphorylation of Myc in cultured cells. Transcription factor c-Myc is phosphorylated in a step-wise dependent manner beginning with the phosphorylation of Ser62 by ERK1/2 (Fig. 9). The Myc-pSer62 conformation prevents it from becoming ubiquitylated by ligases, and, therefore, degraded by the proteasome. When GSK3β kinase phosphorylates Myc at Thr58, there is an additional conformational change [32], which prompts the dephosphorylation of Ser62 by protein phosphatase 2A (PP2A) [33], ubiquitylation by SCF-Fbw7 E3 ligase, and ultimately degradation by the proteasome [34]. Mutations affecting Fbw7's WD40 domain, which contacts the pThr58 in Myc, have been reported in a number of human cancers [35-38]. The biological consequences and subcellular localization of Myc-pThr58 are not currently known. Developing a tool for monitoring the different phosphorylated state of Myc might answer this question.

Gregory, *et al.* [39] observed that when Myc becomes phosphorylated on Thr58 by GSK3β, it translocates to nuclear bodies, which are punctate nuclear structures often

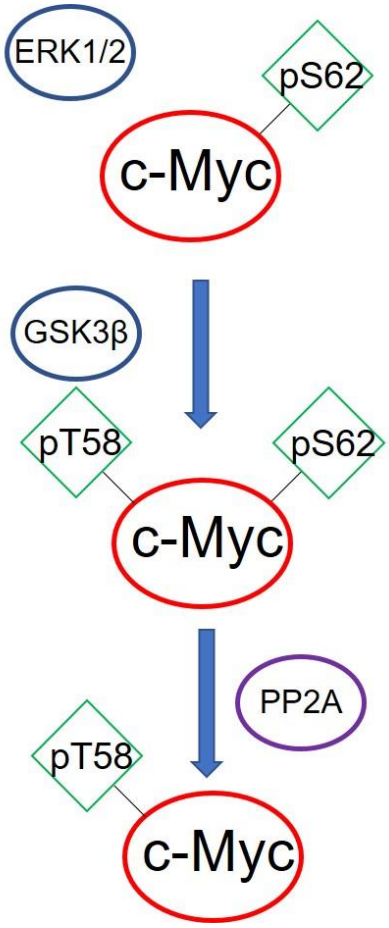

Figure 9. The interdependent-phosphorylation of c-Myc. Myc is phosphorylated at Ser62 by ERK1/2 kinase during growth stimulation. When cell stop receiving growth factor, GSK3β is able to phosphorylate Myc on Thr58 through its interaction with pSer62. Once Myc is dual-phosphorylated, Protein phosphatase 2A (PP2A) will dephosphorylate Ser62, thus leaving Myc phosphorylated on T58. Kinases and phosphatases are presented as blue and purple ovals, respectively.

linked to sites of transcriptional activity. To begin to identify the subcellular location of Myc-pThr58, the African green monkey COS-7 cell line can be transfected with a cytomegalovirus (CMV) promoter-driven murine c-Myc expression plasmid (CMV-Myc) that contains either the HA-tagged WT or the HA-tagged T58A mutant. Separately, the SCF-Fbw7 E3 ligase in transfected COS-7 cells can be knocked out using CRISPR/Cas9 technology. Both the WT and knockout (E3 ligase$^-$) cells would be stained with Myc-pTBD, Myc-pTBD V84A (negative control), and an anti-HA tag antibody. Ki-67 staining would be used to demarcate the nuclear bodies [39]. I would expect a Myc signal in the nuclear bodies of the WT COS-7 cells [39], but not in an E3 ligase-null cell line. As the localization of Myc-pThr58 is not known, there are several possible outcomes to the experiment. One possibility is that the Myc may translocate outside of the nucleus. Cytoplasmic Myc has been reported in ML-1 human myeloblastic leukemia cells [40], but its phosphorylation state and function have not been determined. The cytoplasmic Myc may be phosphorylated at Thr58 and a specific Myc-pTBD could be used as tool to identify phosphorylation state of cytoplasmic Myc.

5.7 Concluding Remarks

Generating phosphospecific affinity reagents is an effective strategy for developing tools to localize and quantify phosphorylation events in cells. In this thesis, I characterized engineered pTBD domains and demonstrated that they are phosphorylation dependent and pThr-specific. Using a variety of biochemical and structural approaches, I was able to identify the molecular determinants in a pTBD that recognizes pT308 of human Myc. My analysis also provide insight into observations previously made by Dr. Pershad. I then determined that dimerizing the Myc-pTBD increased the affinity of the reagent so that it could yield bands on western blots, although they were not the intended Myc target. Future work is needed to improve the utility of pTBD in western blotting.

With the help of Drs. Kall and Lavie, I solved the three-dimensional structure of an engineered FHA domain for the first time. With this structural information in hand, one can now *in silico* model changes in the domain to design a new FHA display library, for the goal of either improving affinity or allowing pSer recognition. Future engineering experiments on the FHA scaffold may contribute to enhanced detection of cell signaling events and biomarkers of disease.

5.8 References

1. Bradbury, A.R., et al., *Beyond natural antibodies: the power of in vitro display technologies.* Nat Biotechnol, 2011. **29**(3): p. 245-54.

2. Lipman, N.S., et al., *Monoclonal versus polyclonal antibodies: distinguishing characteristics, applications, and information resources.* ILAR J, 2005. **46**(3): p. 258-68.

3. Lozano, F., et al., *Low cytoplasmic mRNA levels of immunoglobulin kappa light chain genes containing nonsense codons correlate with inefficient splicing.* EMBO J, 1994. **13**(19): p. 4617-22.

4. Baumann, B., M.J. Potash, and G. Kohler, *Consequences of frameshift mutations at the immunoglobulin heavy chain locus of the mouse.* EMBO J, 1985. **4**(2): p. 351-9.

5. Sroubek, J., et al., *The use of Bcl-2 over-expression to stabilize hybridomas specific to the HERG potassium channel.* J Immunol Methods, 2012. **375**(1-2): p. 215-22.

6. Grimsey, N.L., et al., *Specific detection of CB1 receptors; cannabinoid CB1 receptor antibodies are not all created equal!* J Neurosci Methods, 2008. **171**(1): p. 78-86.

7. Bohmer, T., N. Pfeiffer, and A. Gericke, *Three commercial antibodies against alpha1-adrenergic receptor subtypes lack specificity in paraffin-embedded sections of murine tissues.* Naunyn Schmiedebergs Arch Pharmacol, 2014. **387**(7): p. 703-6.

8. Pradidarcheep, W., et al., *Lack of specificity of commercially available antisera against muscarinergic and adrenergic receptors.* Naunyn Schmiedebergs Arch Pharmacol, 2009. **379**(4): p. 397-402.

9. Pershad, K., K. Wypisniak, and B.K. Kay, *Directed evolution of the forkhead-associated domain to generate anti-phosphospecific reagents by phage display.* J Mol Biol, 2012. **424**(1-2): p. 88-103.

10. Pershad, K. and B.K. Kay, *Generating thermal stable variants of protein domains through phage display.* Methods, 2013. **60**(1): p. 38-45.

11. Budyak, I.L., A. Zhuravleva, and L.M. Gierasch, *The Role of Aromatic-Aromatic Interactions in Strand-Strand Stabilization of beta-Sheets.* J Mol Biol, 2013. **425**(18): p. 3522-35.

12. Gorman, K.T., et al., *Tandem phage-display for the identification of non-overlapping binding pairs of recombinant affinity reagents.* Nucleic Acids Res, 2017. **45**(18): p. e158.

13. Kierny, M.R., et al., *Generating Recombinant Antibodies against Putative Biomarkers of Retinal Injury.* PLoS One, 2015. **10**(4): p. e0124492.

14. Nelson, A.L., *Antibody fragments: hope and hype.* MAbs, 2010. **2**(1): p. 77-83.

15. Bird, R.E., et al., *Single-chain antigen-binding proteins.* Science, 1988. **242**(4877): p. 423-6.

16. Gorman, K.T., Roby, L.C., Giuffre, A., Huang, R., and Kay, B.K., *Tandem phage-display for the identification of non-overlapping binding pairs of recombinant affinity reagents.* Nucleic Acids Res, 2017. **gkx688**.

17. Venegas, L.A., et al., *Generating a recombinant phosphothreonine-binding domain for a phosphopeptide of the human transcription factor, c-Myc.* N Biotechnol, 2018.

18. Koide, S. and J. Huang, *Generation of high-performance binding proteins for peptide motifs by affinity clamping.* Methods Enzymol, 2013. **523**: p. 285-302.

19. Venegas, L.A., et al., *A comparison of phosphospecific affinity reagents reveals the utility of recombinant Forkhead-associated domains in recognizing phosphothreonine-containing peptides.* N Biotechnol, 2016. **33**(5 Pt A): p. 537-43.

20. McGinnis, J. and B.K. Kay, *Generation of recombinant affinity reagents against a two-phosphosite epitope of ATF2.* N Biotechnol, 2017.

21. Weng, J.H., et al., *Uncovering the Mechanism of Forkhead-Associated Domain-Mediated TIFA Oligomerization That Plays a Central Role in Immune Responses.* Biochemistry, 2015. **54**(40): p. 6219-29.

22. Johnson, L.N., *The regulation of protein phosphorylation.* Biochem Soc Trans, 2009. **37**(Pt 4): p. 627-41.

23. Dephoure, N., et al., *Mapping and analysis of phosphorylation sites: a quick guide for cell biologists.* Mol Biol Cell, 2013. **24**(5): p. 535-42.

24. Lin, J., et al., *Understanding protein phosphorylation on a systems level.* Brief Funct Genomics, 2010. **9**(1): p. 32-42.

25. Ubersax, J.A. and J.E. Ferrell, Jr., *Mechanisms of specificity in protein phosphorylation.* Nat Rev Mol Cell Biol, 2007. **8**(7): p. 530-41.

26. Endicott, J.A., M.E. Noble, and L.N. Johnson, *The structural basis for control of eukaryotic protein kinases.* Annu Rev Biochem, 2012. **81**: p. 587-613.

27. Mann, M., et al., *Analysis of protein phosphorylation using mass spectrometry: deciphering the phosphoproteome.* Trends Biotechnol, 2002. **20**(6): p. 261-8.

28. Durocher, D., et al., *The molecular basis of FHA domain:phosphopeptide binding specificity and implications for phospho-dependent signaling mechanisms.* Mol Cell, 2000. **6**(5): p. 1169-82.

29. Murphy, L.C., et al., *Phospho-serine-118 estrogen receptor-alpha expression is associated with better disease outcome in women treated with tamoxifen.* Clin Cancer Res, 2004. **10**(17): p. 5902-6.

30. Oueslati, A., *Implication of Alpha-Synuclein Phosphorylation at S129 in Synucleinopathies: What Have We Learned in the Last Decade?* J Parkinsons Dis, 2016. **6**(1): p. 39-51.

31. Hampel, H., et al., *Total and phosphorylated tau protein as biological markers of Alzheimer's disease.* Exp Gerontol, 2010. **45**(1): p. 30-40.

32. Sears, R., et al., *Multiple Ras-dependent phosphorylation pathways regulate Myc protein stability.* Genes & Development, 2000. **14**(19): p. 2501-2514.

33. Yeh, E., et al., *A signalling pathway controlling c-Myc degradation that impacts oncogenic transformation of human cells.* Nature Cell Biology, 2004. **6**(4): p. 308-318.

34. Wang, X.Y., et al., *Phosphorylation Regulates c-Myc's Oncogenic Activity in the Mammary Gland.* Cancer Research, 2011. **71**(3): p. 925-936.

35. O'Neil, J., et al., *FBW7 mutations in leukemic cells mediate NOTCH pathway activation and resistance to gamma-secretase inhibitors.* Journal of Experimental Medicine, 2007. **204**(8): p. 1813-1824.

36. Welcker, M. and B.E. Clurman, *FBW7 ubiquitin ligase: a tumour suppressor at the crossroads of cell division, growth and differentiation.* Nat Rev Cancer, 2008. **8**(2): p. 83-93.

37. Calhoun, E.S., et al., *BRAF and FBXW7 (CDC4, FBW7, AGO, SEL10) mutations in distinct subsets of pancreatic cancer: potential therapeutic targets.* Am J Pathol, 2003. **163**(4): p. 1255-60.

38. Aifantis, I., E. Raetz, and S. Buonamici, *Molecular pathogenesis of T-cell leukaemia and lymphoma.* Nat Rev Immunol, 2008. **8**(5): p. 380-90.

39. Gregory, M.A., Y. Qi, and S.R. Hann, *Phosphorylation by glycogen synthase kinase-3 controls c-myc proteolysis and subnuclear localization.* J Biol Chem, 2003. **278**(51): p. 51606-12.

40. Craig, R.W., et al., *Altered cytoplasmic/nuclear distribution of the c-myc protein in differentiating ML-1 human myeloid leukemia cells.* Cell Growth Differ, 1993. **4**(5): p. 349-57.

Appendix

6 APPENDIX A: Generating a phosphospecific affinity reagent against phosphorylated Akt using the Forkhead-associated domain

This work was done in collaboration with Ms. Jennifer McGinnis. Ms. McGinnis helped with the characterization and writing.

Introduction

The serine/threonine-protein kinase, Akt is responsible for regulating a range of biochemical pathways involved in cell proliferation and survival. The three isoforms of Akt (i.e., Akt1, Akt2, and Akt3) contain an N-terminal pleckstrin homology (PH) domain, a serine/threonine kinase catalytic domain, and a C-terminal regulatory domain [1]. Activation of Akt is dependent on recruitment of the protein, through its PH domain [2], to the inner side of the plasma membrane, which causes a conformational change [3], allowing PDK1 to phosphorylate threonine 308 (T308) in Akt's catalytic domain and mTORC2 to phosphorylate serine 473 (S473) in Akt's regulatory domain [4, 5]. Once these two residues are phosphorylated, Akt is fully active and phosphorylates a range of intracellular proteins involved in cell survival, growth, proliferation, cell migration and angiogenesis [6].

Given the roles that Akt serves in the cell, biologists are extremely interested in understanding its involvement in cancer. Mass spectrometry and phospho-specific antibodies have been essential tools in pursuing this question by tracking Akt's phosphorylation state and levels in cells and tissues [7, 8]. Such methods have shown a strong link between the hyperactivation of Akt through increased phosphorylation levels

in breast, prostate [9], ovarian [10], and pancreatic cancer [11]. Additionally, studying phosphorylation of specific residues within a protein can provide valuable information as some diseases are marked by the excessive phosphorylation of only one or a few of these residues. For example, the phosphorylation of T308, but not of S473 has been characterized as a marker of lung cancer [12]. Thus, antibodies that recognize specific phospho-residues serve as valuable diagnostic tools to distinguish between diseases caused by Akt deregulation.

Unfortunately, mass spectrometry is limited in its ability to identify these phosphorylation events at a subcellular level, and antibodies are typically unsequenced and not amenable to protein engineering. To circumvent these limitations, current efforts have been focused on generating engineered protein scaffolds that recognize phosphoepitopes. Several protein scaffolds have been engineered to specifically recognize phosphopeptides including the 10^{th} fibronectin type III domain (10FnIII) [13], designed ankyrin repeat proteins (DARPins) [14], the Src Homology 2 domain (SH2) [15], single chain variable fragments (scFv) [16], antigen binding fragments (Fab) [17], and the Forkhead-associated 1 (FHA1) domain [18]. Unlike other scaffolds and most antibodies, FHA domains are selective for pT-containing targets due to a pocket on the domain that interacts with threonine's γ-methyl group [19, 20]. Because of this unique characteristic, a phage library displaying FHA1 variants randomized at residues 82-84 in the β4-β5 loop and residues 133-139 in the β10-β11 loop has been employed to generate affinity reagents to a variety of targets [18, 19, 21]. In this article, we describe the isolation and characterization of Akt1 phosphothreonine 308 (pT308)-binding reagents. We show that

these reagents are pT dependent, bind with high affinity, and recognize the target with comparable or better specificity than commercially made antibodies.

APPENDIX A (continued)

Materials and Methods

Peptides

Peptides were synthesized at University of Illinois at Chicago's Research Resource Center, with >90% purity. All peptides were biotinylated at their N-terminus and amidated at their C-terminus, and included lysine and tyrosine residues to increase peptide solubility and for measuring absorbance, respectively. The phosphopeptide for human Akt1 was KDGATMKpTFCGTPEY (pT308). The peptides KDGATMKTFCGTPEY (T308), KDGATMKpSFCGTPEY (pT308pS), KDGATMKpYFCGTPEY (pT308pY), KDGATMKDFCGTPEY (pT308D), and KDGATMKEFCGTPEY (pT308E) were used in the phosphothreonine substitution study and the peptides KDGATMKTACGTPEY (F309A), KDGATMKTFAGTPEY (C310A), KDGATMKTFCATPEY (G311A), KDGATMKTFCGAPEY (T312A), and KDGAAAAATAAAAAPEY (Ala) were used in the alanine scan study.

Three commercial polyclonal antibodies (pAbs) raised against Akt1-pT308 were compared to the recombinant Akt-pTBD: Cell Signaling Technology, Abcam, and Rockford, and Millipore. The secondary reagent for Akt-pTBD detection was the anti-Flag epitope mAb, M2, which was conjugated to HRP (Sigma–Aldrich).

Cloning and bacterial expression

The phagemid DNA isolated from affinity selection against the pT308 peptide were subcloned into the pKP600ΔIII and expressed and purified as previously described [21]. Protein purity was assessed by sodium dodecyl sulfate-polyacrylamide gel

APPENDIX A (continued)

electrophoresis (SDS-PAGE) and the protein concentration was determined with a NanoDrop A280 spectrophotometer.

Affinity Selections

To isolate FHA variants, the FHA1G2 library was screened against the pT308 target peptide through two rounds of affinity selection using a modified version of a previously described protocol [18]. All the selection steps were performed at room temperature with the KingFisher™ mL Purification System (ThermoFisher Scientific catalog#5400050). The biotinylated peptide (3 ng/µL, 400µL) was immobilized with Dynabeads™ M-270 Streptavidin (ThermoFisher Scientific catalog#65305) and blocked with 2% skim milk in PBS. The phage library containing 2×10^9 members was incubated with the blocked target for 1 hour. Weak or non-binding phage variants were removed by washing the mixture three times with PBST followed by three times with PBS. Virions were eluted from the beads with 40 µg of TPCK-treated trypsin (Sigma-Aldrich), diluted in 400 µL of 50 mM Tris-HCl (pH 8) and 1 mM $CaCl_2$, and used to infect 800 µL of TG1 cells (at mid-logarithmic growth phase) for 1 h at 37°C. The cells were plated on one 15 cm 2×YT/Carbenicillin (CB) agar plate, scraped the next day, and the phage were amplified. Phage particles were precipitated with 24% polyethylene glycol 8000, 3 M NaCl and the phage pellet was resuspended in PBS (0.6 mL). a polyethylene glycol (PEG)/NaCl mixture to concentrate the virions 30-fold. The second and third rounds of selection were performed in a similar manner, however, the pT308 target concentration for rounds two and three were reduced to 1.5 ng/µL and 1 ng/ µL in 400 µL of PBS, respectively. Additionally, the number of washes with PBST and PBS before phage elution were

APPENDIX A (continued)

increased by three, and in the third round of selection, the phage/immobilized target mixture was incubated with free, non-biotinylated pT308 peptide at a 10-fold increase as compared to the immobilized peptide concentration. After the third round of affinity selection, 96 individual clones were propagated as phage, followed by a phage-ELISA to identify functional clones that recognize the peptide target. Positive binding clones were sequenced.

ELISA

Biotinylated peptides diluted in PBS were incubated overnight in 0.5 mM DTT at 4°C. ELISAs were performed as previously described [21] using the peptide targets incubated with DTT at a concentration of 5 ng/µl in100 µl and FHA variants at concentrations varying from 0.01 to 10 µM in PBST. The absorbance was read at 405 nm at 10-min intervals, for a total of 40 min. All experiments were performed in triplicate and repeated three times to confirm reproducibility of the data.

Surface plasmon resonance

The affinity of FHA variants E12 and H11 was measured using Biacore T200 following a similar protocol described in [22]. The pT308 and T308 biotinylated peptides were diluted to 10 µM with PBS followed by immobilization at each channel with 20 µL/min flow rate for 2 min on sensor chip SA. A blank channel without any immobilization was used as a control. The analyte was added in a series of increasing concentration (0.01-5 µM) to all four channels at 25 µL/min flow rate for 180 s of dissociation time.

APPENDIX A (continued)

Results and Discussion

Directed evolution of the FHA1 domain produced variants that recognize an Akt peptide.

Due to the biological significance of Akt phosphorylation, we utilized our FHA library containing $2x10^9$ members to isolate phospho-specific binders able to bind a peptide mimicking a segment from the Akt1 kinase domain to generate reagents that can track Akt phosphorylation in cellular assays. The peptide included a pT residue representing pT308 and the adjacent residues found at positions 302 to 314 (Fig. 1). We performed three rounds of affinity selection against this pT308 peptide, and to increase stringency, we subjected the third round of the immobilized peptide target/phage-bound mixture to free excess peptide target as competitor (Fig. 2a). The weak binding phage were more likely to release from the immobilized target, making them more likely to bind the excess competitor. Thus, our weak binders were washed away with the competitor and only higher-affinity binders remained. Upon elution of these remaining phage, we performed an ELISA to test for clones that bound the Akt1 target peptide (Fig. 2b). Many clones produced a signal anywhere from two times to five times above background levels (data not shown), which demonstrated that we had elicited numerous potential binders.

To further characterize our potential binders, we examined the amino acid sequences of their β4-β5 and β10-β11 loops (Fig. 3a). The sequences revealed that 12 unique clones had been isolated. While this is a relatively large number of clones to be obtained from our library for a given peptide target, the compilation of sequences to generate a logo plot shows that one or two specific amino acids at each loop position appeared approximately

APPENDIX A (continued)

50% of the time (Fig. 3b). The high frequency of specific amino acids at each position suggests that their presence have a positive impact on the FHA/pT308 peptide binding interaction. For example, based on the ELISA experiment, clones E12 and H11 appear to be strong binders, E1 to be an intermediate binder, and B3 to be a weak binder. As expected, we found that 80% of the residues in clone E12's and H11's β4-β5 and β10-β11 loops are amino acids that appear most or second most frequently at each position, while only 50% of E1's residues, and 40% of B3's residues are made of these high frequency amino acids. Additionally, tyrosine is strongly favored at position 83, which is a characteristic of clone E12. This is fitting given that position 83 on the FHA1 domain and other FHA variants are extremely important for their interactions with their phosphopeptide targets [21, 23]. Thus, it appears that a variant's binding strength is dependent on the level of its sequence conservation with other variants, with certain positions being more important than others.

APPENDIX A (continued)

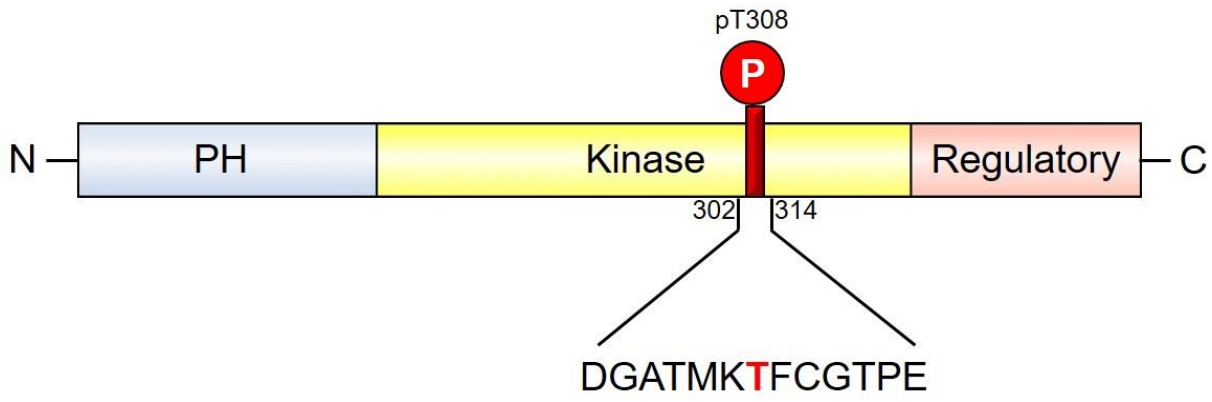

Figure 1. Primary structure of the Akt1. The kinase consists of an N-terminal pleckstrin homology (PH) domain (blue), a serine/threonine kinase catalytic domain (yellow), and a C-terminal regulatory domain (red). The amino acid sequence from residues 301 to 315, including pT308, was mimicked by a peptide target used for affinity selection.

APPENDIX A (continued)

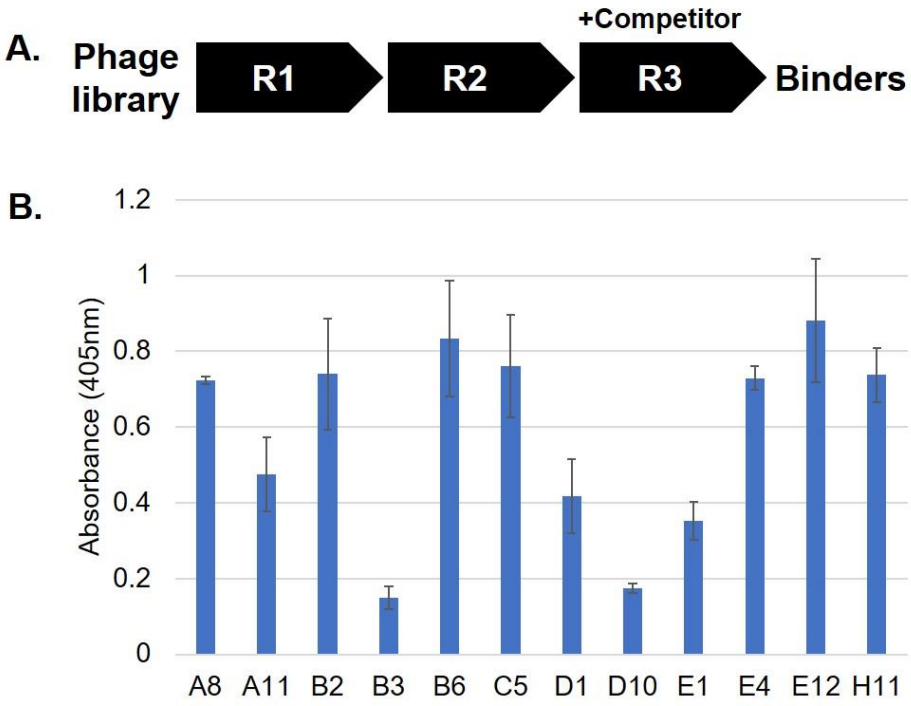

Figure 2. Affinity selection process and ELISA of 10 output clones. A. A phage library displaying variants of a thermostable FHA1 domain was screened through three rounds (R1-R3) of affinity selection, ultimately leading to binding clones. **B.** A phage ELISA of 10 confirmed binding clones. The Akt-pT308 peptide was used as the target in the assay. The phage displaying the FHA variant was detected using the anti-M13-HRP antibody. The experiment was performed in triplicate and the results are an averaged value; error bars reflect the standard deviation of each point.

APPENDIX A (continued)

Clone	β4-β5 Loop	β10-β11 Loop
WT	SRL	GVGVESD
A8	QYY	SMLSVSD
A11	VYR	TPQRPAH
B2	AYV	PSSRTLA
B3	SMI	RQGRESR
B6	TYY	GRTTYGD
C5	SYR	TPQRRDH
D1	RWT	HKNIPGA
D10	SWY	LPLSPTH
E1	VFY	SARHDTH
E4	DYV	RLWTIDQ
E12	AYY	SPHAPSD
H11	SWW	TAHIENA

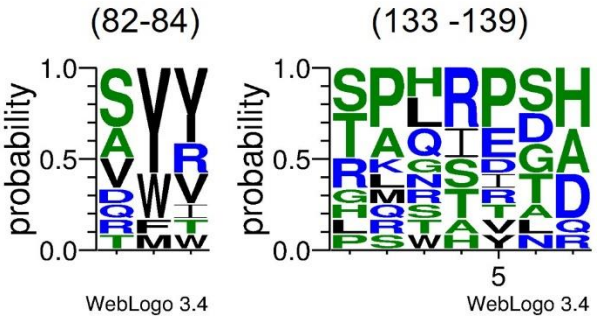

Figure 3. Amino acid sequences of binders in the two regions randomized in the phage-displayed scaffold and pLOGO plots. Left. Primary sequences of the wild-type form of the scaffold and 10 variants that bind the Akt1 phosphopeptide. Either three or 7 residues in the β4-β5 or β10-β11 loops, respectively, were randomized with NNK codons. Residues that differ from the wild-type sequences are show in red. **Right.** Weblogo plots of the frequency of particular residues at each position (82-84 or 133-139). The height of a residue refers to probability of the residue at the given position. Hydrophobic, polar, and charges residues are shown in x, y, and x color, respectively.

APPENDIX A (continued)

Determining the affinity of FHA variants to the AKT target peptide.

To estimate the binding affinity of the FHA clones for the pT308 peptide and confirm our hypothesis relating sequence to binding strength, we performed a competition binding assay. Clones B3, E1, E12, and H11 were selected for comparison (Fig. 4a). IC_{50} values confirmed our previous hypothesis claiming E12 and H11 to be the strongest binders, B3 to be the weakest, and E1 to be an intermediate binder (Fig. 4b). Based on our predictions, it was not surprising that variants E12 and H11 bind strongest to the pT308 peptide. However, unlike FHA variants that have been previously isolated to other pT targets and have IC_{50} values ranging from 1 μM to 1.3 μM [18, 21], the high level of binding was unexpected. We performed surface plasmon resonance (SPR) to confirm these findings and determined the equilibrium dissociation constants (K_D) for E12 and H11 bound to the pT308 to be 162 nM and 178 nM, respectively (Table 1). Again, these numbers illustrated clones E12 and H11 to be much stronger binders than variants we have previously isolated [18].

APPENDIX A (continued)

A.

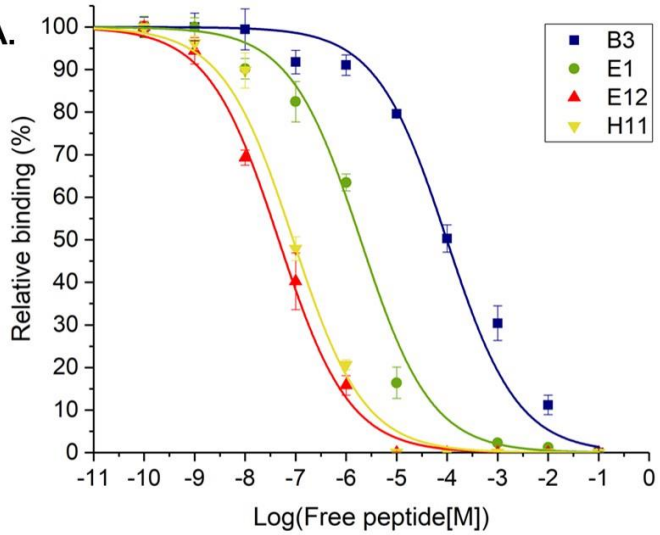

B.

FHA variant	IC_{50}
B3	100 μM
E1	1.95 μM
E12	45 nM
H11	90 nM

Figure 4. Comparing FHA clone affinities. A. Competition binding of clone B3, E1, H11 and E12 to immobilized phosphorylated AKT peptide in the presence of free phosphorylated peptide. Competition binding of clone E12 to immobilized phosphorylated AKT peptide in the presence of free unphosphorylated peptide (black) was used as a control. **B.** IC_{50} binding values for each clone to the AKT phosphorylated peptide.

APPENDIX A (continued)

	FHA Variant					
	E12			H11		
Peptide Target	K_a ($M^{-1}s^{-1}$)	K_d (s^{-1})	K_D (nM)	K_a ($M^{-1}s^{-1}$)	K_d (s^{-1})	K_D (nM)
AKT-pT308	$4.83*10^{4}$	$7.821*10^{-3}$	162±12	$4.157*10^{4}$	$7.401*10^{-3}$	178±8
AKT-T308	2.302	$2.144*10^{-3}$	$9.31*10^{5}$	2.165	$1.01083*10^{-2}$	$5.002*10^{6}$

Table 1. Measure of the Akt-pTBDs' affinities.

APPENDIX A (continued)

Characterization

Due to its high affinity for its target, we chose to further evaluate clone E12's interaction with the pT308 peptide to provide insight into this unusual characteristic. FHA reagents previously generated by our lab are shown to be pT specific. To determine if this is true of clone E12's recognition of the pT308 peptide, the FHA variant was tested for binding to peptides that were substituted with phosphoserine (pS) or phosphotyrosine (pY) at the pT position. Our ELISA result was consistent with previous findings and showed that E12 only recognizes the peptide when position 308 is pT and maintains this same pattern of high specificity that other FHA variants convey as well (Fig. 5a). On the other hand, commercially-made polyclonal antibodies that were generated against the same or a similar Akt1 phosphopeptide varied in their ability to discriminate between pT and the other phosphoresidues. While one antibody (pAb 1) maintained a similar level of specificity as clone E12, another (pAb 2) preferentially bound the unphosphorylated, pS, and pY substituted peptides, and a third antibody did not bind any of the peptides (data not shown). Unlike FHA domains, antibodies bind a variety targets illustrating that they are not the best option for specifically detecting a phosphothreonine residue.

APPENDIX A (continued)

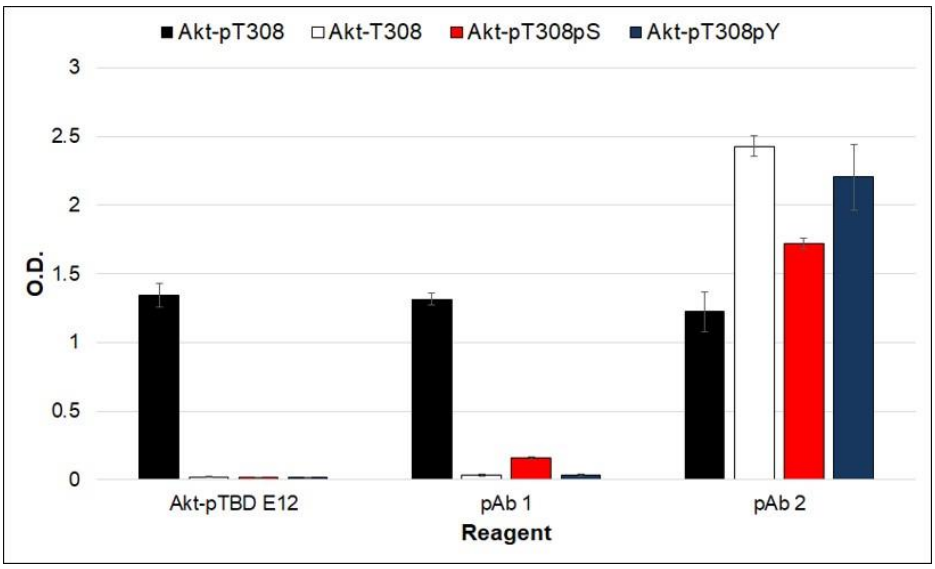

Figure 5. Binding of the Akt1-pTBD to Akt-pT variant peptides. The pThr for each of the cognate peptides was substituted with pSer or pTyr. These phosphopeptide variants, the cognate target, unphosphorylated target, served as targets in the ELISA. Phosphospecific reagents were used to probe targets to test for pThr-specificity. The M2-HRP and goatαrabbit-HRP were used to detect binding of the Akt-pTBD variant or antibody, respectively. Experiments were performed in triplicate and the results are an averaged value; error bars reflect the standard deviation of each point.

APPENDIX A (continued)

References

1. Liu, P., Z. Wang, and W. Wei, *Phosphorylation of Akt at the C-terminal tail triggers Akt Activation.* Cell Cycle, 2014. **13**: p. 2162-2164.

2. Stephens, L., et al., *Protein kinase B kinases that mediate phosphatidylinositol 3,4,5-trisphosphate-dependent activation of protein kinase B.* Science, 1998. **279**: p. 710-714.

3. Huang, B.X. and H.Y. Kim, *Interdomain conformational changes in Akt activation revealed by chemical cross-linking and tandem mass spectrometry.* Mol. Cell Proteomics, 2006. **5**: p. 1045-1053.

4. Sarbassov, D.D., et al., *Phosphorylation and regulation of Akt/PKB by the rictor-mTOR complex.* Science, 2005. **307**: p. 1098-1101.

5. Alessi, D.R., et al., *Mechanism of activation of protein kinase B by insulin and IGF-1.* EMBO J., 1996. **15**: p. 6541–6551.

6. Manning, B.D. and L.C. Cantley, *AKT/PKB Signaling: Navigating Downstream.* Cell, 2007. **129**: p. 1261-1274.

7. Kuo, Y.C., et al., *Regulation of phosphorylation of Thr-308 of Akt, cell proliferation, and survival by the B55alpha regulatory subunit targeting of the protein phosphatase 2A holoenzyme to Akt.* J. Biol. Chem., 2008. **283**: p. 1882-1892.

8. Liu, P., et al., *Cell-cycle-regulated activation of Akt kinase by phosphorylation at its carboxyl terminus.* Nature, 2014. **508**: p. 541–545.

9. Nakatani, K., et al., *Up-regulation of Akt3 in estrogen receptor-deficient breast cancers and androgen-independent prostate cancer lines.* J. Biol. Chem., 1999. **274**: p. 21528-21532.

10. Yuan, Z.Q., et al., *Frequent activation of AKT2 and induction of apoptosis by inhibition of phosphoinositide-3-OH kinase/Akt pathway in human ovarian cancer.* Oncogene, 2000. **19**: p. 2324-2330.

11. Altomare, D.A., et al., *Frequent activation of AKT2 kinase in human pancreatic carcinomas.* J. Cell. Biochem., 2002. **87**: p. 470-476.

12. Vincent, E.E., et al., *Akt phosphorylation on Thr308 but not on Ser473 correlates with Akt protein kinase activity in human non-small cell lung cancer.* Br. J. Cancer, 2011. **104**: p. 1755-1761.

13. Olson, C.A., et al., *mRNA display selection of a high-affinity, modification-specific phospho-IkappaBalpha-binding fibronectin.* ACS Chem. Biol., 2008. **3**: p. 480-485.

14. Kummer, L., et al., *Structural and functional analysis of phosphorylation specific binders of the kinase ERK from designed ankyrin repeat protein libraries.* Proc. Natl. Acad. Sci. U.S.A., 2012. **109**: p. E2248–E2257.

15. Kaneko, T., et al., *Superbinder SH2 domains act as antagonists of cell signaling.* Sci Signal, 2012. **5**: p. ra68.

16. Vielemeyer, O., et al., *Direct selection of monoclonal phosphospecific antibodies without prior phosphoamino acid mapping.* J. Biol. Chem., 2009. **284**: p. 20791-20795.

17. Shih, H.H., et al., *An ultra-specific avian antibody to phosphorylated tau protein reveals a unique mechanism for phosphoepitope recognition.* J. Biol. Chem., 2012. **287**: p. 44425-34.

18. Pershad, K., K. Wypisniak, and B.K. Kay, *Directed evolution of the forkhead-associated domain to generate anti-phosphospecific reagents by phage-display.* J. Mol. Biol., 2012. **424**: p. 88–103.

19. Venegas, L.A., et al., *A comparison of phosphospecific affinity reagents reveals the utility of recombinant Forkhead-associated domains in recognizing phosphothreonine-containing peptides.* N Biotechnol, 2016. **33**: p. 537-543.

20. Huang, Y.M. and C.E. Chang, *Mechanism of PhosphoThreonine/Serine Recognition and Specificity for Modular Domains from All-atom Molecular Dynamics.* BMC Biophys, 2011. **4**: p. 12.

APPENDIX A (continued)

21. McGinnis, J.E. and B.K. Kay, *Generation of recombinant affinity reagents against a two-phosphosite epitope of ATF2.* N Biotechnol, 2017.

22. Lee, H., et al., *Diphosphothreonine-specific interaction between an SQ/TQ cluster and an FHA domain in the Rad53-Dun1 kinase cascade.* Mol Cell, 2008. **30**(6): p. 767-78.

23. Durocher, D., et al., *The molecular basis of FHA domain:phosphopeptide binding specificity and implications for phospho-dependent signaling mechanisms.* Mol. cell, 2000. **6**: p. 1169-1182.

APPENDIX B: GLOBAL JOURNAL PERMISSIONS TO RESUSE PREVIOUSLY PUBLISHED MATERIALS

Journal author rights

In order for Elsevier to publish and disseminate research articles, we need publishing rights. This is determined by a publishing agreement between the author and Elsevier. This agreement deals with the transfer or license of the copyright to Elsevier and authors retain significant rights to use and share their own published articles. Elsevier supports the need for authors to share, disseminate and maximize the impact of their research and these rights, in Elsevier proprietary journals* are defined below:

For subscription articles	For open access articles
Authors transfer copyright to the publisher as part of a journal publishing agreement, but have the right to: • Share their article for Personal Use, Internal Institutional Use and Scholarly Sharing purposes, with a DOI link to the version of record on ScienceDirect (and with the Creative Commons CC-BY-NC- ND license for author manuscript versions) • Retain patent, trademark and other intellectual property rights (including research data). • Proper attribution and credit for the published work.	Authors sign an exclusive license agreement, where authors have copyright but license exclusive rights in their article to the publisher**. In this case authors have the right to: • Share their article in the same ways permitted to third parties under the relevant user license (together with Personal Use rights) so long as it contains a CrossMark logo, the end user license, and a DOI link to the version of record on ScienceDirect. • Retain patent, trademark and other intellectual property rights (including research data). • Proper attribution and credit for the published work.

APPENDIX B (continued)

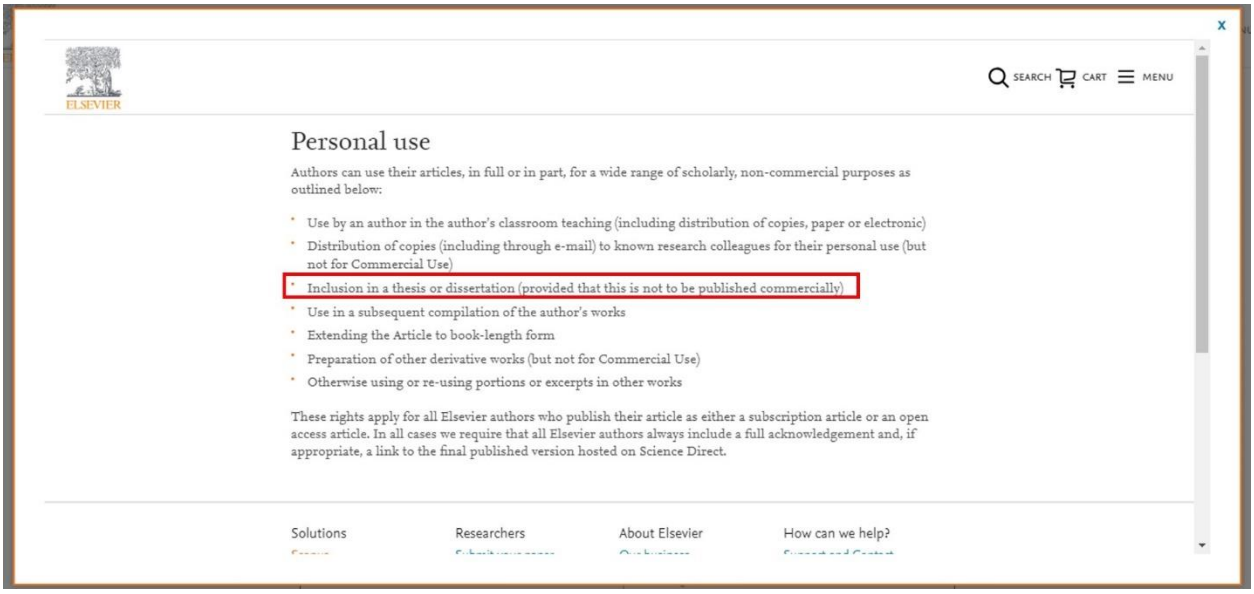

ELSEVIER

SEARCH CART MENU

Personal use

Authors can use their articles, in full or in part, for a wide range of scholarly, non-commercial purposes as outlined below:

- Use by an author in the author's classroom teaching (including distribution of copies, paper or electronic)
- Distribution of copies (including through e-mail) to known research colleagues for their personal use (but not for Commercial Use)
- Inclusion in a thesis or dissertation (provided that this is not to be published commercially)
- Use in a subsequent compilation of the author's works
- Extending the Article to book-length form
- Preparation of other derivative works (but not for Commercial Use)
- Otherwise using or re-using portions or excerpts in other works

These rights apply for all Elsevier authors who publish their article as either a subscription article or an open access article. In all cases we require that all Elsevier authors always include a full acknowledgement and, if appropriate, a link to the final published version hosted on Science Direct.

Solutions Researchers About Elsevier How can we help?

APPENDIX B (continued)

7 Vita

EDUCATION:

University of Illinois at Chicago April 2018
Ph. D. in Molecular, Cellular, and Developmental Biology

St. Edward's University May 2010
B.S. Biology

RESEARCH EXPERIENCE:

University of Illinois at Chicago; Ph. D. Thesis Advisor: Dr. Brian Kay 2012-Present
Graduate Research Assistant

- Re-engineered the forkhead-associated domain using techniques in protein engineering
- Performed phage display selections of affinity reagent libraries to generate reagents for phosphoprotein detection
- Constructed secondary libraries to improve reagent affinity and specificity
- Optimized high throughput assay to characterize FHA variant panels
- Solved the crystal structure of a phosphospecific affinity reagent

University of Texas at El Paso; Lab of Dr. June Kan-Mitchell 2010-2012
Research Assistant II

- Generated specific CD8+ T-cells against conserved regions of HIV and Rift Valley fever virus
- Characterized specific CD8+ T-cells using multi-parametric flow cytometry
- Maintained mammalian cell lines

PUBLICATIONS:

- **Venegas LA**, Kall S, Bankole O, Lavie A, Kay BK. Generating a phosphospecific affinity reagent against transcription factor c-Myc using the Forkhead-associated domain. *New Biotechnology.* doi: 10.1016/j.nbt.2018.05.001.

- **Venegas LA**, Zhao Q, Weiner MP, Kay BK. Reagents for detecting phosphosites within proteins. *J Bioinform, Genomics, Proteomics* 2(3): 1022.

- **Venegas LA**, Pershad K, Bankole O, Shah N, Kay BK. A comparison of phosphospecific affinity reagents reveals the utility of recombinant Forkhead-associated 1 domains in recognizing phosphothreonine-containing peptides. *New Biotechnology*. doi:10.1016/j.nbt.2015.12.006, 2016.

- Xu W, Watts DM, Costanzo MC, Tang X, **Venegas LA**, Jiao F, Sette A, Sidney J, Sewell AK, Wooldridge L, Makino S, Morrill JC, Peters CJ, Kan-Mitchell J. The nucleocapsid protein of Rift Valley fever virus is a potent human CD8+ T cell antigen and elicits memory responses. *PLoS One* 8: e59210. doi: 10.1371/journal.pone.0059210, 2013.

PRESENTATIONS: 2010-2018

- EMBO Workshop on the modularity of signaling proteins and networks Seefeld, Austria
- GEMSSA Research Symposium Chicago, IL
- US HUPO Next Generation Proteomics Tempe, AZ.
- Gordon Research Conference for Chemistry and Biology of Peptides Ventura Beach, CA.
- University of Texas at El Paso Symposium on Infectious Diseases and Health Disparities in a Changing World, El Paso, TX.

AWARDS: 2010-2018

- Best oral presentation (2nd Place) GEMMSA Research Symposium
- UIC Department of Biology Graduate Student Research Award
- USDA HIS Education Grant Program NIFA Award 2010-38422-21223

- Carl Storm Underrepresented Minority Fellowship
- Diversity Supplement-National Institute of Allergy and Infectious Diseases (NIAID)